TECHNIQUES FOR MODELING RESERVOIR SALINITY

By

John Hendrick

August 1973

HYDROLOGY PAPERS
COLORADO STATE UNIVERSITY
Fort Collins, Colorado

62

TECHNIQUES FOR MODELING RESERVOIR SALINITY

By
John Hendrick

HYDROLOGY PAPERS
COLORADO STATE UNIVERSITY
FORT COLLINS, COLORADO 80521

August 1973

No. 62

TABLE OF CONTENTS

LIST OF SYMBOLS

Symbol	Definition
A	Fourier coefficient
A_j	Gain function of a periodic input, tons per acre-foot per thousand tons per month
A_r	Fourier coefficient of the rth harmonic
B	Fourier coefficient bank storage change, thousands of acre-feet per month
B	Salt mass in bank storage change, thousand tons per month
B_r	Fourier coefficient of the rth harmonic
C	$(2n - 1)\pi/2L$
C	Fourier coefficient
C_b	Accumulated bank storage, thousands of acre-feet
C_j	Fourier coefficient of the jth harmonic
C_s	Concentration of inorganic dissolved solids, tons per acre-foot
C_{si}	Concentration of inorganic dissolved solids in inflowing water, tons per acre-foot
C_{so}	Concentration of inorganic dissolved solids in outflowing water, tons per acre-foot
C_v	Coefficient of compression for water, unit volume per atmosphere
$C^2_{xy}(f)$	Coherence function
D_h	Monthly elevation change, feet
D_τ	Value of a periodic function at time τ
D_v	Monthly change in reservoir volume, thousands of acre-feet
E	Evaporation, acre-feet per month
$E[\cdot]$	Expected value
$E_p(Y)$	Annual pan evaporation, inches
$E_r(Y,M)$	Reservoir evaporation depth in year Y and month M, inches
E_t	Value of a random variable at time t
$F(t)$	Water surface elevation at time t, feet
$F'(t)$	$F(t + i + 1) - F(t + i)$
$G(f)$	Calculated spectral density function
H	Water surface elevation, feet
$H(f)$	Fourier transform of h(t), or gain function
$\|H(f)\|$	Magnitude of gain function, tons per acre-foot per thousand tons of salt load per month
I_j	Periodic function with the jth harmonic
$I(k)$	Discrete input at time k
I_m	Main stem water inflow, thousands of acre-feet per month
I_m	Main stem salt inflow, thousands of tons per month
I_p	Precipitation, thousands of acre-feet per month
I_t	Tributary water inflow, thousands of acre-feet per month
I_t	Tributary salt inflow, thousands of tons per month
I_u	Unmeasured water inflow, thousands of acre-feet per month
I_u	Unmeasured salt inflow, thousands of tons per month
K	Specific electrical conductance of water, micromhos per centimeter at 25° C
L	Length
L	Aquifer width, feet
L_1	Salt load, thousands of tons per month
L_2	Salt load, thousands of tons per month
M	Mass of salt, thousands of tons
N	Number of discrete points in time T
O	Water outflow, thousands of acre-feet per month
O	Salt outflow, thousands of tons per month
$O(i)$	Discrete output at time i
P	Pressure, atmospheres
P_k	Pan evaporation coefficient
P_{sw}	Percent of sediment by weight
$P(x,t)$	Unit step response function
Q	Average flow through a reservoir, thousands of acre-feet per month
$Q(t)$	Aquifer discharge, thousands of acre-feet per month
$Q_i(t)$	Reservoir inflow, thousands of acre-feet per month
$Q_o(t)$	Reservoir outflow, thousands of acre-feet per month
R	Aquifer perimeter, feet

LIST OF SYMBOLS (Cont.)

Symbol	Definition
R	Water budget residual, thousands of acre-feet per month
R_i	Fourier coefficient of ith harmonic
R(M)	Residual evaporation depth in month M, inches
S	Reservoir contents, thousands of acre-feet
S	Aquifer storage coefficient, dimensionless
S	Reservoir salt storage, thousands of tons
S(f)	Smoothed spectral estimator
T	Aquifer transmissivity, L^2T^{-1}, gallons per day per foot
T	Time
T	Temperature, degree Centigrade
T	Duration of one cycle of a periodic process
T	Tons
TDS	Total inorganic dissolved solids concentration, tons per acre-foot
T_1	Sum of dissolved solids concentration, tons per acre-foot
T_2	Sum of dissolved solids concentration, tons per acre-foot
U(i)	Discrete response function of a linear system
U(t)	Indicator function
U(x,t)	Instantaneous unit impulse response function
V	Reservoir contents, thousands of acre-feet
V	Volume, L^3
V_o	Initial volume, L^3
W	Random variable
W	Specific weight of water containing suspended sediment, pounds per cubic foot
W(t)	Load of a dissolved material, MT^{-1}
W(t)	Salt load, thousands of tons per month
X(f)	Fourier transform of x(t)
$X_{i,i=1,4}$	Random variables
Y	Random variable
Y(f)	Fourier transform of y(t)
Z	Random variable
Z_t	Random variable at time t

Symbol	Definition
a_j	jth autoregressive coefficient
a_n	Fourier coefficient
b	Linear trend
b	Aquifer thickness, feet
b_n	Fourier coefficient
c	Constant coefficient
c_i	Coefficient of variation of variable i
$c_{xy}(f)$	Cospectrum
f	Frequency, cycles per time or cycles per month (cpm)
g(f)	Spectral density
$g_{xy}(f)$	Cross-spectral density
g(f)	Estimated spectral density
h	Piezometric head, feet
h(t)	Kernel function
h(x,t)	Ground-water level, feet
i	Subscript or index
j	Subscript or index
k	Decay coefficient of a non-conservative substance, T^{-1}
k	Permeability, LT^{-1}, gallons per day per square foot
k	Subscript or index
K(τ)	Kernel function at time τ
m	Subscript or index
m	Number of points calculated in a discrete correlogram
m'	Index of summation
m_i	Mean of ith variable
m_τ	Mean of time τ
n	Subscript or index
$q_{xy}(f)$	Quadrature spectrum
r	Subscript or index
r	Correlation coefficient
r_{ij}	Correlation coefficient
r_k	Auto-correlation coefficient at lag k

LIST OF SYMBOLS (Cont.)

Symbol	Definition
$r_{xy}(k)$	Cross-correlation between x and y at lag k
r_1	First serial correlation coefficient
s	Dissolved solids concentration, tons per acre-foot
s_i	Standard deviation of ith variable
s_c	Initial concentration, tons per acre-foot
s_τ	Standard deviation at time τ
s(t)	Dissolved solids concentration in a thoroughly mixed reservoir at time t
t	Time
x	Distance from aquifer boundary, feet
$\bar{x}$	Average salt load, thousands of tons per month
x_i	Random variable at time i
x_t	Random variable at time t
$x(\tau)$	Input to a linear system at time τ
y_i	Random variable at time i
y(t)	Output of a linear system at time t
Δ	Finite increment
$\sum$	Summation
α	Aquifer diffusivity, L^2T^{-1}, gallons per day per foot
α	Tolerance level

Symbol	Definition
α_m	Fourier coefficient
β_m	Fourier coefficient
$\gamma(f)$	Population spectral density
θ_j	Phase of jth harmonic
μ_τ	Mean at time τ
μ_x	Mean of x
ν	Degrees of freedom
ξ_t	Random variable at time t
ξ_x	Residual from x
ξ_y	Residual from y
π	3.14159
ρ_k	kth autocorrelation coefficient
ρ_T	Density at temperature, T
ρ_{xy}	Cross-correlation coefficient
σ_τ	Standard deviation at time τ
τ	Time
ϕ	Phase, degrees, or radians
$\phi(f)$	Phase function
χ_ν	Statistic from the chi-squared distribution
ω_j	Period of the jth harmonic
∞	Infinity

ACKNOWLEDGMENTS

This paper is based on research performed by J. Hendrick during studies toward a Doctor of Philosophy degree at Colorado State University. Sincere thanks are extended to Dr. Vujica Yevjevich of the Civil Engineering Department for his advice, insight, and constructive criticism.

The author would like to thank the U. S. Bureau of Reclamation and especially Mr. Albert Gibbs of the Water Utilization Section for encouraging this research. Without this cooperation and financial support the study could not have been completed.

ABSTRACT

The movement of dissolved solids (in the text also called "salinity") through a reservoir was investigated and modeled in this study. It is shown that for a reservoir with a detention time greater than one year, the concentration of dissolved solids in the outflow can be modeled by a straightforward linear salt-mix model.

A review of the thermal stratification pattern of a monomictic reservoir was made to provide an understanding of the mixing and movements of water in storage. Mathematical models which attempt to reflect this pattern are reviewed to ascertain their potential for use in a basin simulation model. Unfortunately, their complexity and data requirements make them too cumbersome for the numerous calculations required in a basin study using the data generation method.

Lake Mead, on the Colorado River, was chosen as an example for comparing various techniques of simplifying the relationship between quality of inflows, storage and outflows of a reservoir. Water and salt budgets were used to verify that inputs and outputs of water and salt had been accounted for during the 1935 through 1968 historic data period. An attempt was made to model water movement into bank storage by multiple regression analysis. The elevation of the reservoir surface was found more significant than reservoir storage for estimating bank storage. The convolution method was used to solve equations representing ground-water movement adjacent to the reservoir. Successful application was hindered by a lack of information about properties of the aquifer. However, the general pattern of ground-water movement was satisfactorily reflected.

Multiple regression analysis was used to find a relationship between the salt concentration of the outflow and inflowing salt load and reservoir storage. The results of this approach could predict outflow concentration satisfactorily. However, since regression coefficients are unique for each specific case, the method is dependent upon having a set of data for parameter estimation.

Spectral analysis of the inflowing salt load and outflowing dissolved solids concentration was used to identify the smoothing effect of storage. The gain function between the inputs and outputs closely approximated that expected for a completely mixed reservoir. Time series analysis methods were used to isolate periodic, time-dependent Markovian, and random components of inputs and outputs of the reservoir system. The resulting residual series were inspected by the cross-correlogram and coherence function and were shown to be random processes independent of each other.

For the objective of finding a model which reflects the system well, yet requires minimal numerical calculation, the simple mass balance approach is recommended. This model is acceptable since the gain function between inputs and outputs indicates the system is completely mixed, and the concentrations predicted by the linear mix model compare very well with historic data.

FOREWORD

Water quality problems have been compounded in recent decades, primarily as the result of increased pressure on the environment by various human activities and by population growth. Larger and larger communities pour more and more waste water into rivers and other bodies of water, increasing the concentration of dissolved matter in water with time, even when primary and secondary water waste treatments have been used. An increase of water consumption in producing various industrial products results in more and more chemicals, heavy metals, and particularly poisonous substances reaching the rivers and other bodies of water. Modern technological processes connot be conceived without the use of large quantities of water. An increase in industrial production is usually associated with an increase of salinity concentration in water, even after various water waste treatments have been undertaken. Modern agriculture continuously increases the use of

various chemicals which partly migrate into the natural bodies of water. Mining, tourism, transportation, timber harvesting, and other human activities add their load of dissolved matters by increasing the salinity of natural waters. The two major components of social developments, namely population growth and the increase in standard of living demand larger and larger water quantities to be used, with more and more waste returning into the rivers.

The removal of suspended, floating and bottom carried materials in water wastes, is relatively economical and is widely practiced. The biological pollutants can be treated in one or another conventional manner. However, the removal of excessive dissolved solids from water needs yet to find an economical solution in most cases, especially for those users who cannot absorb a high unit price of water. Therefore, the control of water pollution resulting from increased salinity concentrations is attractive only if done by less expensive means in comparison with the direct removal of dissolved solids from the water (tertiary treatment of waste water). Natural river flows fluctuate highly in time, especially from season to season, and from year to year. In contrast, the fluctuations of the total quantity of dissolved solids oscillate in a much narrower range either from season to season or from year to year. As a consequence, the dry season river flows are usually under the heaviest pollution pressure of salinity concentration.

While the average concentration of dissolved solids in the total water flow of a longer period is usually low and acceptable for most users, the case is different for the prolonged seasons of low flows. A standard threshold for dissolved solids concentration often makes the water use unacceptable to many users for months. As a consequence, the flow regulation by reservoirs and by other bodies of water represents an attractive and economical approach for solving water quality problems by control of salinity concentration. This is particularly true in case of multiple-purpose reservoirs with the sharing of reservoir costs by all participants in the benefits of this type of reservoirs. The reservoir solutions to high salinity problems are attractive when the water of high and low inflows into reservoirs are sufficiently mixed before it leaves the reservoir. In general, the higher the ratio between the average reservoir water volume and the average annual water inflow, and the smaller the ratio between the highest and the lowest inflows, the more evenly the concentration of dissolved solids in reservoir outflows is distributed through the year.

Problems related to effects of storage reservoirs on quality of outflowing water, and to distributions of salinity concentration inside the reservoir at any time, are inherent to any systematic approach to decreasing the concentration of dissolved matters in water. This is true at present, and will be more so in the future. Attempts have been made and approaches developed to study these problems by using theories of diffusion, density currents, convective vertical movements, water exchange between the underground and surface parts of the reservoir, evaporation, and similar processes of hydraulics and hydrology, in order to explain and/or to predict the water salinity concentration downstream of reservoirs. While the classical principles of fluid mechanics and hydraulics have been successful in explaining various processes occurring in reservoirs, they have been less effective in predicting the water quality of reservoir outflows over periods of several years.

The Ph.D. dissertation by Dr. John Hendrick, presented in this hydrology paper, shows how systems analysis in the form of input-response-output approach can be used to investigate the quality of outflows from reservoirs, particularly for predictive purposes. Because the Lake Mead on the Colorado River was well observed for many years for both water quantity and water quality of inflows and outflows, it has been used as an example of the methodology developed, based on a system analysis approach. The potentials of classical approaches for modelling salinity concentration of reservoir outflows have also been investigated in this thesis.

It is logical to expect that a complex problem, like the effects of reservoirs in general and their type of operation in particular, on salinity of outflows cannot be solved uniquely by using any simple approach of fluid mechanics. Neither the use of black-box or gray-box approaches of systems analysis may be effective in accurately predicting the effects of new reservoirs on water quality, before they have been built and operated for sometime. It seems that only the combined approach, by using the classical deterministic hydraulic laws of water mixing and moving processes in lakes and reservoirs and the input-response-output systems analysis, applied to a sufficiently large number of existing reservoirs, can lead to methods which could reliably predict the effects of new reservoirs on water quality. Because most new reservoirs have multi-purpose objectives to serve, the computation of the smoothing of salinity concentration of reservoir outflows should be of such an accuracy that an equitable allocation of costs and a compromised reservoir operation method can be reliably determined. Any advanced method of computing these effects and introducing the results of this method into the benefit-cost analysis of a new reservoir as well as the development of operational rules or optimization techniques, represents a welcome contribution.

The results of the thesis work by Dr. John Hendrick should be viewed as a contribution in a long process of improvements bit by bit in techinques to be available for predicting the water quality of reservoir outflows, and in using the reservoirs for the abatement of water pollution in case of a high concentration of dissolved solids in low river flows.

The research presented in this paper is a combined effort by U. S. Bureau of Reclamation, which supported Dr. Hendrick's work for a year, and Colorado State University, by supporting Dr. Hendrick for two years as a Ph.D. graduate research assistant and by providing advice and guidance, both through the National Science Foundation grants "Stochastic Processes in Hydrology", No. GR-11444 and "Stochastic Processes in Water Resources", No. GR-31512X.

Vujica Yevjevich
Civil Engineering Department
Colorado State University
Fort Collins, Colorado

September, 1973

Albert E. Gibbs
Division of Planning Coordination
U. S. Bureau of Reclamation
Denver Federal Center
Denver, Colorado

CHAPTER I

INTRODUCTION

1.1 Background

Water quality behavior in reservoirs has received increased attention in recent years. This resulted from several factors including current environmental concern, quality degeneration by greater water usage, and earlier neglect of water planners to evaluate the impact of development and use on water quality. Of the numerous indicators of the materials present in water, salinity is of primary concern in the southwestern United States and is the major concern of this study. In moist climates such as those of the Pacific Northwest or eastern United States a good water supply and low evaporation rates do not create serious salinity problems. In the arid and semi-arid southwestern states of lesser rainfall, virtually all the water supply is in demand. High evaporation rates, consumptive irrigation use, and salts leached by irrigation collectively create a major water quality problem. The Environmental Protection Agency (19:1)[1] in a report of the Colorado River Basin Water Quality Control Project states that "Salinity is one of the most serious water quality problems in the Colorado River Basin." This E.P.A. report also discusses specific alternatives for managing dissolved solids in the Colorado River Basin to alleviate the adverse effects of high salinity. To properly evaluate salinity changes resulting from future land and water use patterns, reservoir operation management, irrigation management, salt load reduction, and programs for water supply augmentation, planners need tools for accurately estimating the quality of water in a basin under a wide variety of conditions.

1.2 Need for Reservoir Salinity Models

As indicated by Kriss and Loucks (31), abundant literature is already available related to analyzing water resources systems. The traditional river basin analysis has been based upon water quantity until interest provoked development of techniques for evaluating costs and benefits of water quality. However, when water quality is included as an important system parameter, the availability of analysis techniques decreases. This is unfortunate since the Federal Water Quality Act of 1965 encourages water quality consideration in river basin planning by authorizing grants when this aspect is included.

One problem of water quality modeling is evaluating the response of the system for given initial states and input conditions. Although much effort has been expended on elaborate models of dissolved oxygen and temperature systems, salinity has been assumed conservative and modeled by a mass budget. In general, this approach is acceptable since it is intuitively appealing, fits many real situations well, and is fairly simple.

One important facet of a basin salinity model is the movement of dissolved solids through a reservoir. Refined models are needed which can predict the effect of storage on downstream quality as inflows to the reservoir and operation of the system vary. Hopefully, this study provides insight and technical tools for modeling salinity in a water resources system.

1.3 Objectives and Scope

The broad goals of this study are to investigate the general behavior of reservoir salinity and compare several methods of quantitatively modeling this phenomenon. The research was planned to provide immediately usable methods for predicting the concentration of dissolved solids in reservoir outflows based only on characteristics of the inflow of the state and the system. It was desired to develop a reservoir salinity model which would require minimal computer storage and time for inclusion in multi-year simulation studies of basins comprised of several reservoirs.

The study was limited to conservative dissolved materials in water such as total dissolved solids, salinity, salt, and inorganic dissolved solids passing through a reservoir which has a single annual overturn. Data on a monthly time basis was used for model parameter estimation and validation. The modeling techniques applied include regression, time series analysis, convolution, and mass balance.

---

[1] Numbers in parentheses refer to entries in the bibliography.

CHAPTER II

GENERAL MODEL FOR SIMULATING SALINITY THROUGH A RESERVOIR

2.1 Introductory Remarks

This section describes the overall system modeled, discusses criteria the model must meet, and provides a perspective for judging various system formulations. The models investigated in this study are largely judged on their ability to form an integral part of an entire basin simulation. The need for using simulation-type models is quite clear to planners who are asked to describe a system whose states and inputs are largely stochastic processes measured only for a relatively short duration or with limited data. This sample trace of input history may no longer be considered adequate for evaluating future system outputs. The simulation (sample generation, or Monte Carlo) approach attempts to represent the statistical properties as estimated by analysis of the historic data. Once the structure of the time series is uncovered and mathematically described, the planner has a new tool for extending his alternative inputs beyond the narrow sample of the historic data. He also may vary the model parameters to objectively inspect the behavior of the system under new conditions.

The discussion above can be clarified by application to the reservoir system sketched in Fig. 2.1. For this formulation the time series such as flows, salinity loads, sediment loads, evaporation, and salt gains and losses provide inputs to the reservoir body proper. This system can be broken into input time series and the reservoir itself. All inputs to the system may be represented as stochastic, deterministic, or deterministic-stochastic processes. They may be structured from historic data or modeled to reflect future conditions such as increased water diversions and usage, changes in salt loading patterns, flow augmentation, and weather modification. The reservoir itself encompasses the processes of storage of water and dissolved salts, their movements, and the internal mixing from the location of measured inputs to a sampling point below the outlet. Modeling the response and output from the reservoir is the main topic of the present study.

Several subjective criteria should be considered before a model is constructed. Simplicity is one of the most important. It is not difficult to envision the advantages of a simple model. Consider a water resources system involving several reservoirs. Analysis of this system could require updating the outflow quality of each reservoir at every time increment. A basin with five reservoirs run for a simulation period of 50 years on a monthly time step would require 3,000 calculations of reservoir quality. A planner using the data generation method would undoubtedly like to perform several of these 50-year simulations for each set of basin plans. The cost of running such a model will obviously become exorbitant if the calculation time for one time step is on the order of even one minute. The advantage of a very simple model should be clear.

The time and space scales of the problem being modeled are also important. For example, a model constructed to provide information on a yearly basis would not require detailed analysis of seasonal, monthly, or daily events. On the other hand, a model might be required to reflect events which change significantly in minutes or hours. One model would not be satisfactory for both cases. The time interval of the model should match the need for information required to solve the problem. Since the monthly time step is frequently chosen for basin simulation models, it will be used in this study.

Spatial variations of a quantity also play a major role in model appraisal. Problems such as determining the distribution of a waste near a sewage outfall or the temperature profile near a reservoir outlet require "near-field" models utilizing short distance increments. "Far-field" problems are those which require modeling the variation of a quantity over a long distance such as several miles. The change in salinity of a river as it flows from its headwaters to its mouth hundreds of miles away would typify this spatial scale. The models resulting from this study will be required to reflect the change in water quality over the entire length of a reservoir. They will not be expected to produce information over short spatial distances. The importance of these criteria will become evident as the study progresses.

The next section introduces the structure of the input time series in more detail, while the last section discusses specific methods of attacking the problem of transferring salinity through the reservoir.

2.2 Time Series Representation of Inputs

The general structure of the hydrologic and water quality time series comprising the various inputs to a reservoir can be represented by a sum of deterministic (periodic) and stochastic components. These terms can be expressed as

$$x_t = m_\tau + s_\tau \cdot \varepsilon_t \qquad 2.1$$

in which m_τ may be a periodic mean and s_τ a periodic standard deviation. Both may be a sum of sinusoidal terms taking the general form

$$D_\tau = \sum_{j=1}^{m} C_j \cos(\omega_j \tau + \theta_j). \qquad 2.2$$

The stochastic component, ε_t, may be either completely random or a sum of autoregressive and random terms. It can be represented by a k^{th} order linear Markov model.

$$\varepsilon_t = \sum_{j=1}^{k} a_j \varepsilon_{t-j} + \xi_t \qquad 2.3$$

with a_j the autoregressive coefficients and ξ_t an independent stochastic component. The first-order Markov model often provides a good measure of dependence in hydrologic processes. Equation 2.1 then becomes

$$x_t = m_\tau + s_\tau \left[r_1 \left(\frac{x_{t-1} - m_{\tau-1}}{s_{\tau-1}} \right) + \xi_t \sqrt{1 - r_1^2} \right] \qquad 2.4$$

with r_1 the first serial correlation coefficient. The model selected for final use depends upon the structure of the data set and results of tests for significance of the various components.

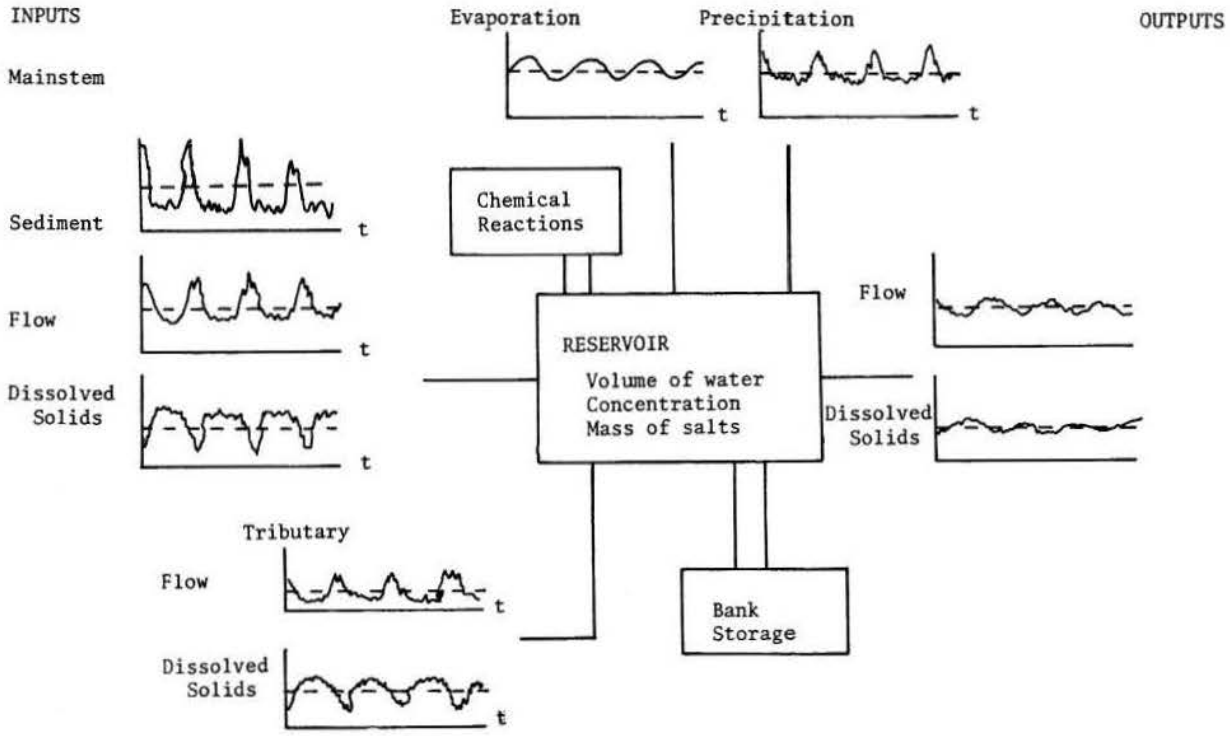

Fig. 2.1 Schematic representation of a reservoir system.

This model theoretically can duplicate any historic data set by incorporating an unlimited number of the parameters, C_j , ω_j , θ_j , and a_j. However, its main value is in economizing on the number of parameters required to maintain the properties of the historic sample. Once the structure is ascertained and model parameters estimated, the planner has the power to generate an infinite number of sequences of a given size representing potential events.

Some very valuable aspects of the model of Eq. 2.1 should be mentioned. First, the effect of controls or management can be easily added. If, for example, a flow augmentation program is anticipated, the change could be simulated by increasing the mean or amplitudes of periodic components of the original flow and operating the basin model under projected conditions. A salinity reduction program could be evaluated by reducing means or altering amplitudes of the dissolved solids component. The manipulation of the input structure is limited only by the anticipation of new conditions and the desires of the user.

The second asset of the simulation method is that by investigating the system response to an array of input traces instead of only one historic sequence, a wider range of events and sequences can be sampled. This provides the modeler with a broader base of results to aid him in decision making. It should not be construed that this method is able to "predict the future." It does not. It does give the user the power to inspect the distribution of possible outcomes resulting from assumed future conditions.

2.3 Methods of Modeling Salinity Transport

As will be shown later, even though the stochastic time series analysis does not have a long history of practical hydrologic applications, the methods and theory are available in the literature for immediate use. However, a reservoir salinity model has not been adequately developed and applied for simulation purposes.

The problem centers around finding mathematical relations between the system states and inputs such that outputs can be reliably estimated. A system model capable of transforming the inputs into the outputs without knowledge of the internal workings is conceived as a "black box." This approach has the advantage of relatively uncomplicated mathematical structure and may offer savings in computer time and storage. The development and application of the model may depend on historic data for parameter estimation. Since any model is only an abstraction of a physical process, selection of its form is largely up to the experience, knowledge, judgment, and criteria of the modeler.

A second direction of modeling is to explore the system properties and internal mechanisms and describe them by differential equation. This requires intimate knowledge of hydrodynamic movements and diffusion processes as well as methods and data for estimating the parameters relating the model to specific situations. Many investigators find this approach satisfactory since it gives the impression of explaining the physical process more completely and provides an intuitive sense of security. The feeling alluded to is that the basic principles of physics and chemistry when appropriately applied are infallible and are, at least, better than the nebulous black box type of model.

Determining which approach to follow was one of the major dilemmas encountered in this study. The problem was attacked by reviewing reservoir quality models and general techniques of analyzing water resources systems. The first step, covered in Chapter 3 , was to investigate the mechanism of reservoir stratification and circulation to provide a basis for judging potential model formulations.

CHAPTER III

RESERVOIR STRATIFICATION AND MIXING

When approaching a new problem with limited knowledge about the phenomenon under consideration, building up understanding of the system behavior is a valuable beginning. If the basic mechanism is understood, models can be selected to reflect the salient aspects and represent better the input to output transfer. This chapter presents a qualitative description of the internal mechanism of reservoir mixing, stratification, and circulation. Although some fundamental aspects are first reviewed, the results are essential for understanding the more complex processes described later. Knowledge of the system's behavior will also provide insight into the credibility and limitations as well as advantages of various model forms.

3.1 Density of Water

The main factor controlling stratification in a body of water is density. A discussion of the parameters involved is prerequisite to understanding water movement in a reservoir or lake. The effects of four parameters--temperature, dissolved solids concentration, suspended material, and compressibility of water --are summarized below.

1. Temperature. Temperature has a nonlinear effect on density. Maximum density occurs at approximately 39°F (4°C). The change in density per unit of temperature varies with temperature. Water becomes less dense not only with an increase in temperature above 39°F (4°C) but also with a decrease below 39°F. The following equation from Tilton and Taylor (55) may be used to calculate density (ρ_T, g/cc) as a function of temperature (T, °C).

$$\rho_T = 1 - \{[\frac{(T - 3.9863)^2}{508929.2}] \frac{(T + 288.9414)}{(T + 68.12963)}\} \qquad 3.1$$

2. Dissolved Solids - Conductance. Water of a consistent makeup of ionic constituents usually displays a high degree of linear dependence between total dissolved solids concentration (C_s) and specific electrical conductance (K). The slope and intercept of the relationship are not the same for every reservoir or stream. From chemical analysis data on Lake Mead, for example, a least squares estimate of parameters gave the relationship

$$C_s = 17.48 + 0.684\ K \qquad 3.2$$

Since specific ions have different atomic mass units, the sum of dissolved solids obtained from a conductivity relationship does not define the dissolved material adequately to exactly determine density. Even if the exact ionic composition were known, density could not be easily determined since the molecular structure of dissolved materials in a solution of several ions is difficult to quantify.

An empirical curve published in a report by Leifeste and Popkin (34) indicates a gain of approximately 0.0008 g/cc in density for 1,000 mg/l dissolved solids. This is fairly consistent with published densities of similar solutions (7). The relationship $\Delta\rho_{C_s} = 8.0 \times 10^{-7} \times C_s$ was adopted for use in this illustration.

3. Silt or suspended load. Density of water containing undissolved but suspended sediment material can be computed quite easily assuming a sediment specific gravity of 2.65. The equation used was given by Davis and Wark (11)

$$W = \frac{10021.8}{160.6 - P_{sw}} \left[\frac{\text{lbs.}}{\text{ft}^3}\right] \qquad 3.3$$

with W the specific weight, and P_{sw} the percent of sediment by weight in the water-sediment mixture. From this, density may be calculated by dividing the specific weight by 62.4.

4. Compressibility. As water descends it is subject to increasing hydrostatic pressure and increases in density due to compressibility. The coefficient of volumetric contraction (7) is 50.0×10^{-6} (unit volume/atmosphere) at 10°C (50°F).

By the definition of density,

$$\rho = \frac{\text{mass}}{\text{volume}} . \qquad 3.4$$

Using a volume of 1 cubic centimeter initially, the volume at any pressure (in atmospheres) is

$$V = V_o - P \cdot C_V \qquad 3.5$$

where P is the pressure in atmospheres, C_V is the coefficient of compression, and V_o is one cubic centimeter.

When these parameters are put into Eq. 28 with unit mass, the expression for density becomes

$$\rho = \frac{1}{1 - P \cdot C_V} \qquad 3.6$$

Since one atmosphere equals 33.9 feet of water depth, a relationship between depth and densith can be found.

Density was plotted in Fig. 3.1 for all four of the above factors over the range anticipated in reservoir environments. Figure 3.1 clearly indicates that the effects of compression and dissolved solids (or conductance) are minor compared to the percent of silt and to temperature. For water with less than 0.1 percent silt, temperature is the predominating factor. Suspended silt could outweigh the effect of temperature only under conditions of concentration higher than those found in the main portions of a lake or reservoir. Warm water overlying cooler water is less dense and tends to retain its position.

3.2 Stratification in Monomictic Reservoir

A deep lake or reservoir in a climate where minimum water temperatures do not fall below 4°C provides a general case for discussion of stratification. Prior to spring, the reservoir is uniformly mixed at its minimum temperature. As solar radiation warms the upper layers, they become less dense and a thermal gradient develops. Mixing from wind action and lower surface temperatures due to evaporation and nocturnal cooling transports heat downward, warming the water below the surface. As this progresses, the typical stratified pattern emerges.

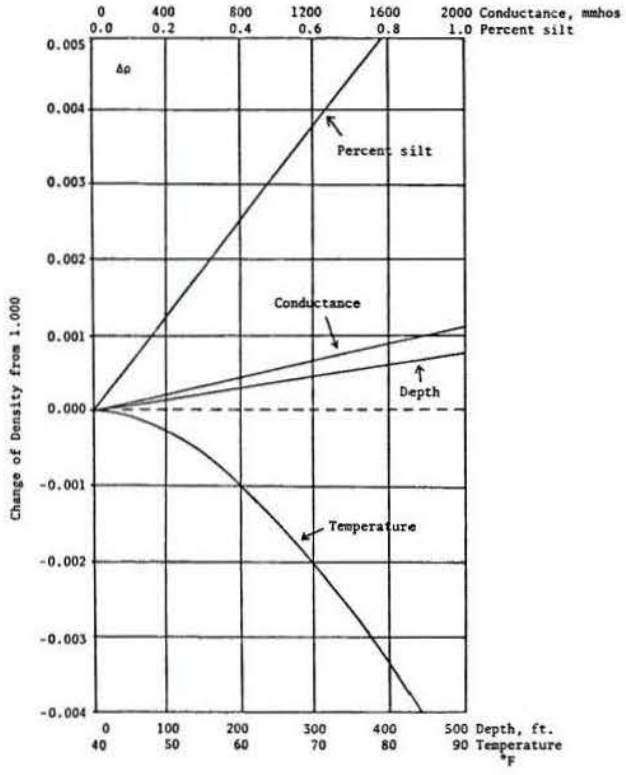

Fig. 3.1 Effect of silt, conductance, hydrostatic pressure (depth) and temperature on the density of water.

The upper layer or epilimnion is distinguished by fairly well-mixed warmer temperatures and daily circulation whereas the lower layer, or hypolimnion, is colder and fairly undisturbed. The two zones are separated by a region of rapid temperature change called the thermocline and defined by Hutchinson (23:428) as, "...the plane of maximum rate of decrease in temperature..." The region (as opposed to plane) between the hypolimnion and epilimnion is termed the metalimnion. If in a relatively shallow lake the wind-induced currents are sufficient to completely mix the entire body, the water mass is termed homiothermal and can be considered an epilimnion. In a deep lake the thermal stratification pattern further develops during the summer, reaching its most pronounced pattern in early fall. Cooler air reduces the temperature of surface water during the fall. It then becomes denser and sinks until a depth of similar density is reached. The process continues through late fall and winter until the minimum surface temperatures and maximum densities have been reached and the turnover is complete. This mixing will include water near the bottom of the reservoir only if the winter surface temperatures are sufficiently low to make the descending water dense enough to penetrate the lower hypolimnion. As spring approaches, the reservoir begins another stratification cycle. Figure 3.2 illustrates this seasonal pattern.

The above discussion is applicable to water bodies whose minimum temperature is above 4°C. If colder temperatures are produced, the body may be dimictic or experience two overturns, one in the fall and one in the spring. In this instance the winter stratification is inverse, with colder (but less dense, since it is less than 4°C) water near the surface. This phenomenon generally occurs in western North

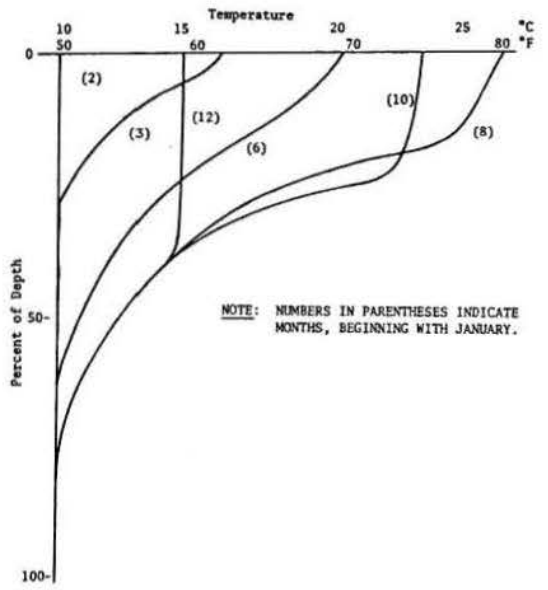

Fig. 3.2 Typical monomictic reservoir stratification pattern showing changes in profiles of water temperature.

American lakes farther north than about 40°N. latitude. South of this latitude dimictic lakes are less likely and would be expected only at high altitudes. Here the monomictic type is most common. Because of randomness of climatic variables, the same lake in a transitional region may display monomictic properties one year and dimictic properties in another.

3.3 Circulation in a Large Monomictic Water Body

The following discussion typifies the movement of water in a large monomictic reservoir where the maximum stream temperature is similar to the maximum reservoir surface temperature, and the minimum stream temperature is the same or less than the minimum reservoir temperature. The pattern of inflows and circulation illustrated in Fig. 3.3 shows the movement of dissolved materials through the reservoir.

After completion of the fall turnover, the reservoir water is mixed more than at any other period. Relatively uniform horizontal and vertical temperature and salinity gradients typify this state. During this period the major water movement is vertical rather than horizontal. In the winter period shown in Fig. 3.3, the inflow rate is low and contains a high dissolved solids concentration. This inflow accumulates with the water of high concentration from the fall and slowly migrates towards the outlet. As spring approaches, runoff becomes greater from snowmelt and spring precipitation and reaches its lowest salt concentration of the year. This is also the period of greatest load entering the reservoir due to high flows as shown during May and June in Fig. 3.3. Water traveling in a stream in springtime responds more rapidly to solar heating than the larger mass of the reservoir and becomes less dense than most of the reservoir water. Wunderlich (65) termed this flow regime overflow. Its occurrence was also detected in Lake Mead by Anderson and Pritchard (1). This mass of water is identified by a low dissolved solids concentration and can be traced in Fig. 3.3 as it moves towards the outlet. This relatively homogeneous water may travel

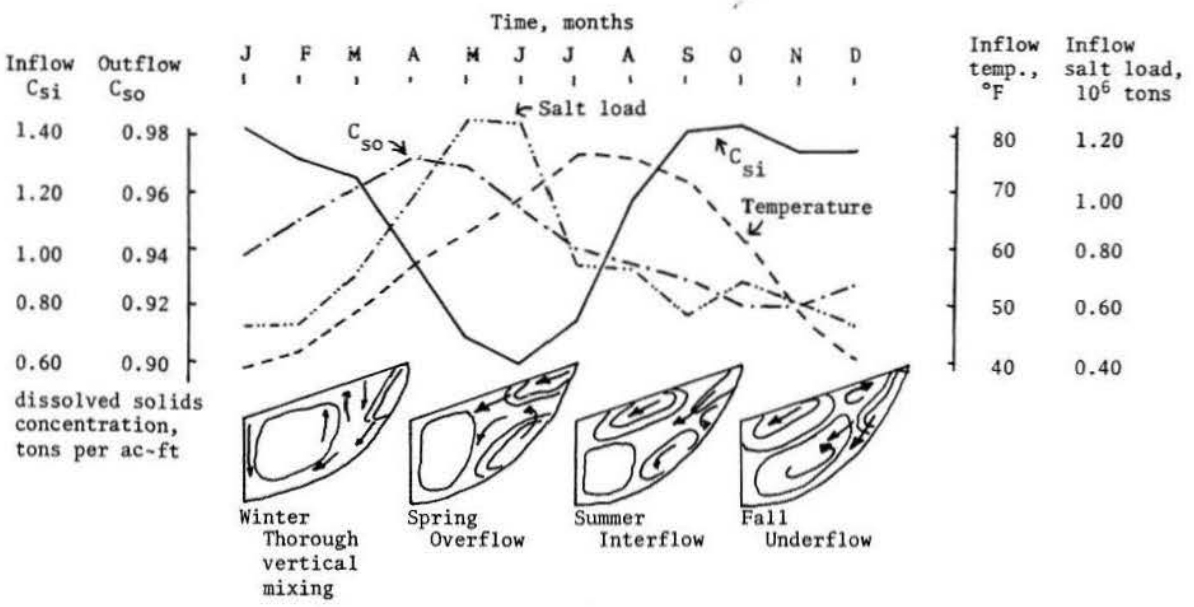

Fig. 3.3 Seasonal pattern of mixing and movement of water in a large monomictic reservoir.

rapidly on the surface of the reservoir and reach the outlet much sooner than the average reservoir detention time would indicate. When the fall turnover occurs before the cell reaches the outlet, it becomes well-mixed with water in the reservoir and loses its identity. It is also possible for the spring inflow to go directly to the outlet and retain some of its original characteristics. Secondary currents may develop and partially mix the spring inflow with the water of higher concentration at lower levels.

During the summer the temperature of inflowing water is similar to that in the upper layers of the reservoir. Due to its higher salinity, the streamflow water may be denser than surface reservoir water and less dense than water at low depths. The flow then enters somewhere between the surface and the bottom and is appropriately designated an interflow. Secondary mixing currents may be formed above and below the interflow layer. Figure 3.3 shows the higher concentration and warm temperatures of the inflow in this season.

As fall approaches, water in the stream responds more rapidly to cool temperatures and attains a density found at lower reservoir depths. During this low-flow period, the highly saline inflow descends even deeper as it seeks layers of compatible density. With the minimum streamflow temperatures of winter at or below those on the bottom of the reservoir, the entering flow descends to the reservoir floor and is termed an underflow. This pattern can be seen in the sketch of fall conditions in Fig. 3.3.

As discussed in the previous section, the fall overturn vertically mixes water from the surface to the lower depths of the reservoir. This event is largely responsible for the loss of identity of the spring inflow which was of higher-than average quality. By the time an inflow volume of water reaches the outlet, it has been subjected to the fall turnover as well as the effects of secondary currents throughout the year. Although the plot of outflow concentration C_{so}, of Fig. 3.3 indicates a large annual change, the range is much smaller than that for inflow concentration. In fact, compared to the inflow, the outflow concentration is nearly a constant.

How the various inflows mix before reaching the outlet in a particular reservoir depends on reservoir storage, shape, and detention time. In a reservoir with an effective volume[1] much greater than the average annual inflow or outflow, it may take several years for incoming water to reach the outlet. When this occurs, the inflow could be subject to more than one fall overturn and experience a prolonged opportunity for mixing. Conversely, a reservoir with a relatively small volume and high flow rates could have detention time on the order of a few weeks. The underflow-interflow-overflow pattern is applicable in each case. However, the degree of mixing and the lag time between input and output create an extremely complex system of flow patterns.

3.4 Models of Reservoir Stratification

In the last five years numerous efforts have been aimed at modeling the thermal stratification phenomenon just described. The purpose of reviewing these models is twofold. First, they may provide viable alternatives to the black-box approach to some problems. Second, the review illustrates the complexity and difficulty of modeling some of the more sophisticated concepts. Since all the models of stratification have a large common foundation, the similar aspects of the group from several publications (2, 24, 38, 45, 47, and 64) will be described with comments on specific merits of individual models as needed.

The basis for these models is water buoyancy due to density differences induced soley by temperature. It is often assumed that density is a linear function of temperature, in contrast to the known relationship illustrated in Fig. 3.1. The reservoir is broken into horizontal layers of uniform properties, as illustrated in Fig. 3.4.

[1] The term "effective volume" is used to represent the water which must be displaced for inflow to reach the outlet.

Each layer is identified by its temperature, elevation, and volume. Vertical mixing is modeled by an approximate diffusion equation in which the time rate of transport is proportional to the spatial gradient. This equation can be quite complex, such as those used by Jaske (24), Orlob (38), and Ryan and Harleman (47), or extremely simplified as the one used by Beard and Willey (2). During periods of surface cooling, water is mixed downward until its temperature is equal to or greater than the next lower layer. This is a fairly good approximation of the physical process occurring in the fall turnover of the monomictic reservoir described in Section 3.2. Inflows enter at the surface and descend until a layer of similar temperature is reached. The models of Beard and Willey (2) and Ryan and Harleman (47) provide for heat exchange as the inflow descends.

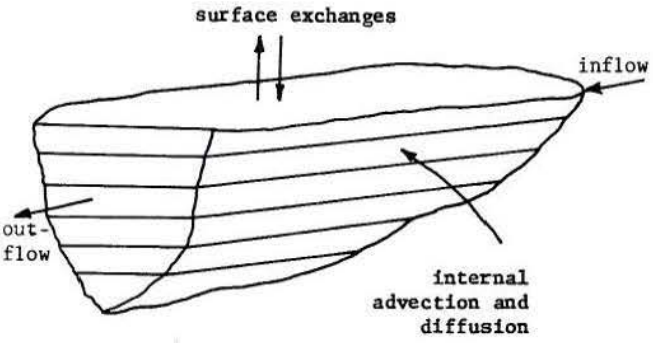

Fig. 3.4 Finite layer approach to modeling a stratified reservoir.

A variety of methods for removing water near the outlet have been tried. Beard and Willey (2) have taken the simplest approach by removing a volume of water from the layer nearest the outlet and lowering above layers to fill the empties space. Other models (24, 38, 45, 47, 63, and 64) incorporate a variety of schemes to approximate the velocity profile and withdrawal layer thickness. Several theoretical formulations and field and laboratory models of this type of flow have been investigated and are reported in the literature (5, 9, 12, 17, 27, and 29).

All models require some form of heat budget to model heat exchange and temperature of the water mass. The data requirements for this facet of the model vary widely, ranging from only air temperatures, solar radiation, evaporation, and precipitation in the model of Beard and Willey (2) to more elaborate data needs such as wet and dry bulb temperatures, atmosphere pressure, wind speed, and cloud cover required for the Water Resources Engineers Model (45, 63, and 64). The rate of heat movement by "eddy diffusion" is controlled in all models by a mixing or diffusion coefficient. The value of this coefficient has been a problem in all models and several methods of estimating it have been tried with limited success. This transfer coefficient controls vertical mixing of reservoir layers and establishment of the thermocline.

Spatial variation has been modeled by dividing the reservoir into individual segments or cells. Water Resources Engineers personnel have developed a segmented version of the stratified model, and Jaske (24) has applied a three-dimensional cellular type structure to Lake Roosevelt. One major problem of this method is modeling the advective transfer between cells. This depends upon the hydrodynamic movement of reservoir currents and requires extensive field measurement for model calibration and verification. It does provide a method of representing major horizontal currents as well as secondary currents and vertical advective motion.

In summary, several models are currently available which represent stratification and mixing by simplifying the internal structure and behavior of the reservoir. They have the advantage of providing an estimate of the distribution of quality throughout the entire volume. Their operation often requires computer storage of large arrays and solutions of differential equations. Also, time series of several meteorological variables may be required for very sophisticated models. To the author's knowledge, salinity has not been added and tested in these models for long term simulation purposes.

CHAPTER IV

INVESTIGATION OF MATHEMATICAL TECHNIQUES FOR ANALYSING WATER QUANTITY AND WATER QUALITY SYSTEMS

There are a variety of tools one can choose from when attempting to model any type of input-output system as a black-box. It is necessary to review the available techniques and select the most appropriate one for the problem at hand. This section reviews several such methods and provides background information for understanding the applications reviewed in Sections 4.2 and 4.3.

4.1 Black-Box and Time Series Analysis Techniques

A wide range of model complexity is available, beginning with the simplest formulation which is linear, time invariant, and has a single input and a single output, to the most complex which is nonlinear, time variant, and has multidimensional inputs and outputs. In most instances, the time invariant, linear, single input, single output formulation has been most successful. There are many possible ways to attack the problem by identifying the mathematical operations which change inputs to outputs. System identification is the first step. The problem is to postulate or discover the general form of the system transfer function, which is the mathematical operator on the inputs which produces the outputs. Parameter estimation follows when the general form of the system transfer function has been ascertained. For both system identification and parameter estimation, some criteria such as least squares comparison of observed and predicted output may be used. Unless knowledge about the system is available which permits one to postulate a set of differential equations or a mathematical description of the physical processes of the system, identification and parameter estimation must both be approached by goodness-of-fit criteria.

One example of a system function well known to hydrologists is the unit hydrograph. Output ordinates resulting from any inputs are summed to produce the total response. The title "instantaneous unit hydrograph" has been given to the kernel function, or the system response function of a watershed transposing instantaneous rainfall input into runoff. The output of the system results from convoluting the input with the kernel. The general form is given by

$$y(t) = \int_{o}^{t} h(t-\tau)x(\tau)d\tau, \qquad 4.1$$

where $y(t)$ is the output at time t, $h(t-\tau)$ is the kernel at time $t-\tau$, and $x(\tau)$ is the input at time τ.

An alternative to convolution in the time lag domain by summing products of inputs and weighting functions is provided by transforming inputs and outputs into the frequency domain.

The output at time t can be expressed by an infinite Fourier expansion

$$y(t) = \sum_{r=0}^{\infty} A_r \cos r \frac{2\pi\tau}{T} + \sum_{r=1}^{\infty} B_r \sin r \frac{2\pi t}{T} \qquad 4.2$$

with T the duration of the longest periodic component. The input $x(\tau)$ and the kernel function $h(t-\tau)$ can also be similarly expressed by

$$x(\tau) = \sum_{n=0}^{\infty} a_n \cos n \frac{2\pi\tau}{T} + \sum_{n=1}^{\infty} b_n \sin n \frac{2\pi\tau}{T} \qquad 4.3$$

and

$$h(t-\tau) = \sum_{m=0}^{\infty} \alpha_m \cos m \frac{2\pi(t-\tau)}{T} + \sum_{m=1}^{\infty} \beta_m \sin m \frac{2\pi(t-\tau)}{T}. \qquad 4.4$$

After substituting the Fourier expansions into the convolution integral, $y(t)=\int_{t-T}^{t} x(t)h(t-\tau)d\tau$, O'Donnell (37) found integrals whose sums were zero when m was different from n. When m equals n, the coefficients of the harmonics of the output can be found as

$$A_o = Ta_o\alpha_o \qquad 4.5$$

$$A_n = \frac{T}{2}(a_n\alpha_n - b_n\beta_n) \text{ for } n \geq 1 \qquad 4.6$$

and

$$B_n = \frac{T}{2}(a_n\beta_n + b_n\alpha_n). \qquad 4.7$$

These three equations may be used to solve for the coefficients of the kernel so that

$$\alpha_o = \frac{1}{T}\frac{A_o}{a_o} \qquad 4.8$$

$$\alpha_n = \frac{2}{T}\frac{a_nA_n + b_nB_n}{a_n^2 + b_n^2}, \qquad 4.9$$

and

$$\beta_n = \frac{2}{T}\frac{a_nB_n - b_nA_n}{a_n^2 + b_n^2}. \qquad 4.10$$

Given the input and output, one could fit a harmonic series to them and obtain the coefficients of the kernel. However, using a finite number of harmonic coefficients introduces some errors into the estimation of the kernel. Also, errors in the input and output data will lead to errors in estimating the harmonic coefficients. O'Donnell (37) does not indicate how to handle the residual inputs remaining after a finite number of harmonic terms are removed. He does suggest using large numbers of data points to improve estimates of coefficients.

Phillippee and Wiggert (40) applied O'Donnell's method to rainfall and runoff with only moderate success. The main problem they encountered was separating base flow from surface runoff. They also found

that predicted runoff duration and hydrograph ordinates varied from the observed data depending on the type of storm used to derive the kernel. The events they studied were selected to include only smooth single peaked hydrographs.

Knisel (28) applied this technique to analyze karst aquifer responses to rainfall and found the response function to vary in a smooth curve around 1.00.

Two extensions of the harmonic analysis approach are first to break inputs and outputs up into cosine terms for all significant harmonics and an error term, namely

$$y(t) = \bar{y} + \sum_{i=1}^{m} a_i \cos \omega_i + \xi_y \qquad 4.11$$

and

$$x(t) = \bar{x} + \sum_{j=1}^{m} b_j \cos \omega_j t + \xi_x \qquad 4.12$$

Taking coefficients corresponding to a given cycle in input and output,

$$b_j = k_i a_i \qquad 4.13$$

and

$$w_j = w_i + \phi_i \qquad 4.14$$

Thus, input is attenuated or amplified and shifted in phase at every significant frequency. When these signals are removed from both the input and output, the input will be a nonperiodic residual series, but the output may have additional significant harmonics. This will indicate amplification added by the system and can be modeled as a filter.

The harmonic analysis of periodic data has been used to describe time series from a variety of systems. A discussion of hydrologic applications can be found in Roesner and Yevjevich (46) and Yevjevich (67). Chow (8) applied this technique to represent precipitation, watershed storage, and evaporation in a general hydrologic system model. When the actual operation of the system is not of interest, this type of model can be used to simulate output time series directly as a combination of deterministic and random components. Yevjevich (68) describes the structure of hydrologic system inputs and outputs and provides a compact discussion of the periodic-stochastic modeling process. Matalas (35) provides a general description of time series analysis techniques as well as the autoregressive model.

The second more sophisticated approach to harmonic analysis is to use Fourier transforms applied to convolution. In the frequency domain, the convolution is transformed into multiplication, yielding

$$Y(f) = H(f)X(f), \qquad 4.15$$

where Y(f), H(f), and X(f) are Fourier transforms of y(t), h(t), and x(t), respectively. The ensuing review of fundamental spectral analysis techniques elaborates on the advantages of this approach.

Spectral analysis is a statistical tool receiving current attention and increased use in engineering application. The basic principle of spectral analysis is to break a time series up into periodic components and inspect the distribution of variance densities over frequency. The fundamental methods of spectral analysis will be briefly explained in this section, and examples of applications given in Section 4.3.

Beginning with time series, x(t), of length T, specified at N discrete times of equal spacing, the finite Fourier series may be constructed to approximate it as given by the classical equation

$$x(t) = A_o + 2 \sum_{m=1}^{n-1} [A_m \cos 2\pi m f_1 t + B_m \sin 2\pi m f_1 t] + A_n \cos 2\pi n f_1 t \qquad 4.16$$

where f, equals the fundamental frequency selected for the analysis. If n is taken equal to N/2, each value of the Fourier series will coincide with the original set. The highest frequency attainable from the discrete set corresponds to a period of two time steps and equals $1/2\Delta t$, or 0.5 cycles per time interval. It is sometimes advantageous to express Eq. 4.16 in the form

$$x(t) = R_o + \sum_{m=1}^{n-1} R_m \cos (2\pi m f_1 t + \theta_m) + R_n \cos (2\pi m f_1 t), \qquad 4.17$$

where

$$R_m = A_m^2 + B_m^2, \qquad 4.18$$

with

$$\theta_m = \arctan \frac{B_m}{A_m}, \qquad 4.19$$

$$A_m = R_m \cos \theta_m, \qquad 4.20$$

and

$$B_m = -R_m \sin \theta_m. \qquad 4.21$$

R_m is the amplitude and θ_m the phase of the m-th harmonic.

The mean square value of the fluctuation about the mean, the variance can be expressed as

$$\sigma^2 = 2 \sum_{m=1}^{n-1} R_m^2 + R_n^2. \qquad 4.22$$

The Fourier line spectrum is produced when the squared amplitudes are plotted against frequency. The variance density spectrum results when the variance over a small interval of frequency is divided by the interval width and this width is reduced to zero in the limit. Conceptually, the variance density spectrum is a display of the distribution of the total variance over the frequency range from 0.0 to 0.5 cycles per time interval. If the series is standardized to have the variance equal to 1.0, the area under the spectrum is also 1.0. This operation is especially helpful for comparing two dissimilar time series on an equal basis. Another approach to the variance density spectrum is through either the autocorrelation function of the autocovariance function by using the Wiener-Khintchine equations. The autocovariance function is a measure of the average variance of a series with its values at lag k apart. The autocorrelation function is the autocovariance function standardized by the variance of the series. Expressed mathematically, the covariance function is

$$\text{Cov}\,[x(t),\, x(t+k)] = E\,[(x(t) - \mu_x)\,(x(t+k) - \mu_x)] \quad 4.23$$

where E( ) is expected value. The autocorrelation function, ρ_k, is given by

$$\rho_k = \frac{\text{Cov}\,[x(t),\, x(t+k)]}{\sqrt{\text{Var}\; x(t) \cdot \text{Var}\; x(t+k)}} \quad 4.24$$

where Var x(t) is the variance of the x(t) series.

For a discrete series, Yevjevich (67) uses the following equation for estimating ρ_k.

$$r_k^2 = \frac{\frac{1}{N-k}\sum_{i=1}^{N-k} x_i x_{i+k} - \frac{1}{(N-k)^2}\left[\sum_{i=1}^{N-k} x_i\right]\left[\sum_{i=1}^{N-k} x_{i+k}\right]}{\left\{\frac{1}{N-k}\sum_{i=1}^{N-k} x_i^2 - \frac{1}{(N-k)^2}\left[\sum_{i=1}^{N-k} x_i\right]^2\right\}^{1/2}\left\{\frac{1}{N-k}\sum_{i=1}^{N-k} x_{i+k}^2 - \frac{1}{(N-k)^2}\left[\sum_{i=1}^{N-k} x_{i+1}\right]^2\right\}^{1/2}} \quad 4.25$$

Given that the autocorrelation and covariance functions are even functions, the area under the spectral density function is unity, and the frequency range varies from 0 to 0.5, the spectral density function can be expressed as (67:92)

$$\gamma(f) = 2\left[1 + 2\sum_{k=1}^{\infty} \rho_k \cos 2\pi f k\right]. \quad 4.26$$

Unfortunately, this leads to a biased and inefficient estimate. To overcome this, a variety of schemes involving smoothing either the autocorrelation function before taking the cosine transform or the smoothed spectral estimators can be used. Details of this procedure may be found in texts on spectral analysis such as those of Jenkens and Watts (25), or Blackman and Tukey (4). The smoothing function used in this study is called "Hanning" and is applied to the spectral estimators, g(f), resulting in the smoothed estimator

$$S(f_j) = 0.25\, g(f_{j-1}) + 0.50\, g(f_j) + 0.25\, g(f_{j+1}). \quad 4.27$$

One important specific spectrum is that of a first-order linear autoregressive process which follows the model

$$x_i = \rho\, x_{i-1} + \xi_i\,. \quad 4.28$$

The spectrum of x is (67:113)

$$\gamma_x(f) = \frac{2(1-\rho^2)}{1 - 2\cos 2\pi f + \rho^2} \quad 4.29$$

for ξ_i an independent series with $E[\gamma(f)] = 2$. The general shape of the correlogram and variance density spectrum is sketched in Fig. 4.1 (67:114).

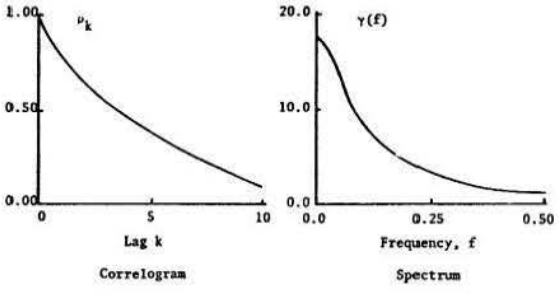

Fig. 4.1 Shape of the correlogram and spectrum of a first-order autoregressive process.

When investigating the structure of time series by spectral techniques, some idea is needed of the variation in the estimated values for testing their significance. The derivation of tolerance limits is available in the literature for all the common smoothing functions. In general for $\hat{g}(f)$ the estimated spectral density and $\gamma(f)$ the population value, Jenkens and Watts (25:252) show that the random variable $\nu\hat{g}(f)/\gamma(f)$ is distributed as chi-squared with ν degrees of freedom. Yevjevich (67) suggests using the equivalent degrees of freedom equal to 8N/3m or 2N/m for normal and non-normal variables, respectively. N is the total number of observations and m is the number of lags in the correlogram. Thus, a $100(1-\alpha)\%$ tolerance interval for $\gamma(f)$ may be calculated as

$$\frac{\nu\,\hat{g}(f)}{X_\nu(1 - \alpha/2)} \le \gamma(f) \le \frac{\nu\,\hat{g}(f)}{X_\nu\,(\alpha/2)} \quad 4.30$$

Fig. 3.10 of Jenkens and Watts (25:82) may be used to obtain values of $\nu/X_\nu(\alpha/2)$ and $\nu/X\,(1-\alpha/2)$.

Further exploration of spectral density provides an estimate of the effects of a linear system on transforming inputs into outputs. For example, consider the linear system which has the form of the physically realizable convolution integral

$$y(t) = \int_0^{\infty} h(\tau)x(t-\tau)\, d\tau, \quad 4.31$$

where y(t) is the system output, s(t) is the input, and $h(\tau)$ is a kernel or weighing function. If the input is a periodic function,

$$x(t) = a \sin(2\pi f t + \theta) \quad 4.32$$

the output can be shown to equal

$$y(t) = a\,|H(f)|\,\sin[2\pi f t + \theta + \phi(f)] \quad 4.33$$

The factor $|H(f)|$ at the same frequency of the input scales the amplitude and is called the gain, while $\phi(f)$ is the phase shift of periodic inputs moving through the system. The gain and phase functions can be more fully understood by a discussion of cross-spectral analysis. In addition to the covariance or autocorrelation functions already discussed, the cross correlation or cross-covariance function will be required. In general the cross-correlation function,

$$\rho_{xy} = \frac{\text{Cov}\; xy}{\sigma_x \sigma_y} \quad 4.34$$

and can be estimated by Eq. 4.25 replacing x(i+k) by y(i+k). The cross-spectral density function of the two discrete series x(t) and y(t) is defined by

$$\gamma_{xy}(f) = 2\sum_{k=0}^{\infty} \rho_{xy}(k) e^{-2i\pi fk}, \quad 4.35$$

where i is $\sqrt{-1}$. The complex expression above may be written

$$g_{xy}(f) = c_{xy}(f) - iq_{xy}(f). \quad 4.36$$

The real part, $c_{xy}(f)$ is called the cospectrum and measures the in-phase covariance of x(t) and y(t) at frequency f. The imaginary term, $q_{xy}(f)$, is called the quadrature spectrum and measures the contributions to covariance at different frequencies when the harmonics of x_t series are delayed by 90 degrees. If

$g_{xy}(f)$ is expressed in the polar form

$$g_{xy}(f) = |g_{xy}(f)|\, e^{-i\theta_{xy}(f)} \qquad 4.37$$

then $$|g_{xy}(f)| = \sqrt{c^2_{xy}(f) + q^2_{xy}(f)} \qquad 4.38$$

is the cross-amplitude function

and $$\theta_{xy}(f) = \tan^{-1}\left[\frac{q_{xy}(f)}{c_{xy}(f)}\right] \qquad 4.39$$

is the phase function. The gain function of y_t from Eq. 4.33 becomes

$$|H(f)| = \frac{|g_{xy}(f)|}{g_x(f)} \qquad 4.40$$

and the phase function $\phi(f)$ from Eq. 4.33 is equivalent to $\theta_{xy}(f)$.

The linear correlation between two series at any frequency can be estimated by the coherence. It is defined by

$$C^2_{xy}(f) = \frac{c^2(f) + q^2(f)}{\gamma_x(f) \cdot \gamma_y(f)} . \qquad 4.41$$

Similar to the coefficient of determination, coherence varies between 0 and 1.0. According to Jenkens and Watts (25) a spurious correlation may result when the series show a high cross correlation at a lag other than zero.

It should be noticed that the above discussion is for linear, time-invariant systems. Rodriguez-Iturbe (43) points out that to model a nonlinear time-varying system, the weighing function $h(\tau)$ would be a function of the input, $x(t)$, and also vary with time, $h(\tau,t)$.

4.2 Application of the Convolution Sum to a Ground-water System

Application of the convolution of inputs by a weighing function for a ground-water system will be required later as the problem of modeling bank storage is approached. The formulation is begun by considering the one-dimensional diffusion equation

$$\frac{\partial^2 h}{\partial x^2} = \frac{S}{T}\,\frac{\partial h}{\partial t} , \qquad 4.42$$

where h is the piezometric head above a zero datum, x is the horizontal distance from the water-aquifer boundary, S is the aquifer storage coefficient, T is the aquifer transmissivity equivalent to Kb, with K the permeability, b the aquifer thickness, and t the time.

Several investigators have used convolution as a method of solving this equation for a variety of aquifer properties and boundary conditions. Cooper and Rorabaugh (10) provided an elegant mathematical treatment of bank storage and ground-water movement due to varying stream stages. The convolution relation was used for an analytical solution derived from Eq. 4.42. They presented graphical results which represented a wide range of aquifer properties. Moench and Kisiel (36) used stream hydrographs and ground-water level data along an ephemeral stream in Arizona to illustrate the application of the convolution approach. Hall and Moench (20) briefly reviewed previous use of the convolution relation and presented expressions in discrete form for solving the diffusion equation. They applied the results to a hypothetical aquifer with a stage hydrograph as the input. Figure 4.2 illustrates two fundamental aquifer configurations commonly used in the derivation of equations for water table elevation and aquifer discharge. The semi-infinite case results from assuming the aquifer boundary extends to infinity, whereas in the finite case the aquifer is limited to the width, L .

Hall and Moench (20) gave general relationships for both water table elevation and discharge. For either case

$$h(x,t) = \int_0^t F'(\tau)\, P(x, t-\tau)\, d\tau, \qquad 4.43$$

or $$h(x,t) = \int_0^t F'(\tau)\, U(x,t-\tau)\, d\tau, \qquad 4.44$$

and $$Q(t) = T \int_0^t F'(\tau)\, \frac{\partial P(0, t-\tau)}{\partial x}\, d\tau, \qquad 4.45$$

where $h(x,t)$ is the water table elevation at distance x and at time t, $F'(t)$ is the time derivative of system input, $F(t)$ is the system input at time t, $P(x,t)$ is the unit step response function, and $U(x,t)$ is the instantaneous unit impulse response function.

The equations for the impulse response, unit step response and its time derivative were given for both the semi-infinite and finite cases. For the semi-infinite aquifer

$$U(x,t) = \frac{x}{(4\pi\alpha)^{1/2} t^{3/2}} \exp - \left(\frac{x^2}{4\alpha t}\right), \qquad 4.46$$

$$P(x,t) = \operatorname{erfc} \frac{x}{(4\alpha t)^{1/2}} , \qquad 4.47$$

and

$$\frac{dP(0,t)}{dx} = - \frac{1}{(\pi\alpha t)^{1/2}} . \qquad 4.48$$

For the finite aquifer

$$U(x,t) = \frac{\pi\alpha}{L^2} \sum_{n=1}^{\infty} (2n-1) \exp(-C^2\alpha t) \sin(Cx), \qquad 4.49$$

$$P(x,t) = 1 - \frac{4}{\pi} \sum_{n=1}^{\infty} \frac{\sin(Cx) \exp(-C^2\alpha t)}{(2n-1)} , \qquad 4.50$$

and

$$\frac{dP(0,t)}{dx} = - \frac{2}{L} \sum_{n=1}^{\infty} \exp(-C^2\alpha t). \qquad 4.51$$

In both cases α is the aquifer diffusivity, T/S ; π is 3.1416; exp represents exponentiation; erfc is the complimentary error function; C is $(2n-1)\pi/2L$; and L is the aquifer width.

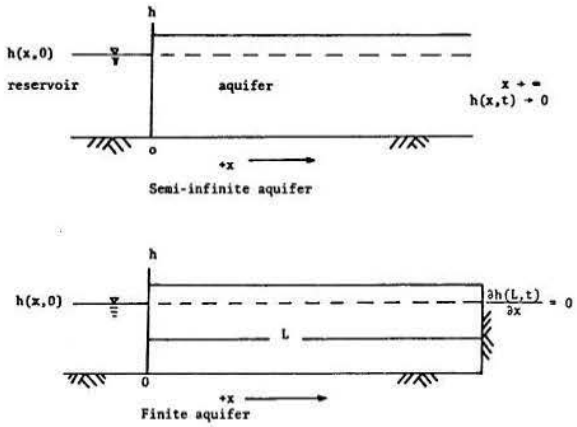

Fig. 4.2 Geometric properties of semi-infinite and finite aquifer models.

Derivation of the above equations is simplified by the fact that the instantaneous unit impulse response function is the time derivative of the unit step response. That is,

$$U(x,t) = \frac{dP(x,t)}{dt} . \qquad 4.52$$

The general Eqs. 4.43, 4.44, and 4.45 for elevation and discharge can be expressed in the discrete form

$$O(i) = \sum_{k=1}^{i} I(k)U(i-k+1)\,\Delta k \qquad 4.53$$

with O(i) the output, I(k) the input, U(i-k+1) the response function or system kernel, i the output time step, and Δk the time interval.

This is the general discrete form of the convolution relation and can be applied to any system if the input and response function are known. In practical application, the response function is terminated when either the number of terms becomes cumbersome or the ordinates are relatively insignificant.

4.3 Applications of Time Series Analysis Techniques to Water Quality Variables

The Fourier series representation of a periodic water quality parameter has been used by numerous investigators. Several will be cited to indicate the wide applicability of this technique. Ward (60) used a sine curve to represent the annual temperature of 38 Arkansas streams. He found very little variation in the parameters of the sine function and the mean temperature from year to year. He also concluded that the daily temperature could be well modeled by a sine curve estimated from monthly average data. Generally, over 95 percent of the variance in the original series was explained by a single sine curve. Thomann (53) applied Fourier series and used power spectra to analyze hourly temperature and dissolved oxygen data of the Delaware River. He found the annual harmonic most significant. This reference also gives background information on the techniques used. Kartchner et al. (26) applied a similar analysis to model diurnal fluctuations in temperature and dissolved oxygen of Little Bear River in Utah. They found the periodic model explained 90 percent of the variance in hourly dissolved oxygen and 75 percent in temperature. Dixon et al. (16) made wide use of the Fourier technique in representing temperature, biological oxygen demand, and dissolved oxygen seasonally and hourly in the development of quality model for a simulation of the Little Bear River study area in Utah. The final example of Fourier analysis modeling of periodicity in water temperature is Kothandaraman's (30) applications to a large Illinois river. He found periodic components explaining about 95 percent of the temperature variance. Sharp (48) described several time-variant components of water chemistry time series and a variety of tests for their existence. The main behavior modes discussed were trend, cyclic, and oscillatory. He proposed using correlogram analysis to indicate the pattern reflected by the data.

The several above examples illustrate the wide use of Fourier analysis for modeling periodic water quality variations. More sophisticated investigations of time series using spectral analysis techniques are also abundant in the literature. Again a few outstanding examples will be cited. Rodriguez (43) provided an extensive discussion of spectral analysis techniques and the validity of their application to hydrological data. He used results of cross-spectral analysis to investigate relationships between temperature, precipitation, atmospheric pressure, and runoff in the Pacific Coast area of the United States. Rodriguez and Nordin (44) applied spectral analysis to monthly series of sediment and discharge data of the Rio Grande River in New Mexico. They generally found significant peaks in the spectra at the annual frequency. The gain function between water and sediment discharge indicated a reduction in amplitude of sediment as the output especially at frequencies over 4 cycles per year. Phase diagrams indicated in some cases the sediment series was leading the runoff series. However, the cross-correlograms, which do not distinguish individual frequencies but rather consider each series as a whole, displayed peaks at a lag of zero. This is one interesting advantage of spectral analysis over the cross-correlogram. The variation of lead or lag of individual cyclic components can be inspected to explore the behavior of the system more thoroughly.

Demayo (13) described the application of power spectra to water quality based on a paper by Wastler (62). Demayo developed methodology and gave computer program listings for calculating spectral analyses. Examples of spectra for temperature, specific conductance, and discharge for a sample station were shown. Thomann (52) applied spectral analysis to biological oxygen demand of waste flows before, during, and after processing in a municipal waste treatment plant. The spectra were useful in detecting 5-day-on-2-day-off periodicity which the raw data did not show. The gain function indicated the primary treatment process resembled plug flow by approximately constant gain. Secondary treatment displayed a higher degree of mixing indicated by a decreasing gain at higher frequencies. A system was formulated and illustrated by a hypothetical example.

Slawson (49) used power spectra to compare concentration of dissolved solids at several locations along the Colorado River. For reaches without storage, there was little or no shift in spectra and a simple translatory model adequately represented the upstream to downstream system behavior. He also briefly investigated the dampening effect of Lake Mead on dissolved solids below Hoover Dam. For reaches involving irrigation return flows, a trend was included and in some cases the semi-annual periodicity became slightly amplified.

4.4 Analysis of Outflow Concentration Assuming That Water is Completely Mixed

The discussion of this section is based upon the assumption that the inflow is instantaneously and thoroughly mixed with water in the reservoir. This also implies that the concentration is the same throughout the reservoir and in the outflow at a given time. Dingman and Johnson (15) have applied this assumption to mixing models of water quality from several New Hampshire lakes. For the completely mixed case, they developed equations expressing the outflow concentration as a function of lake volume, lake concentration, and several other parameters. The analytical results were applied to 23 specific lakes to estimate their residence time and equilibrium concentration for a constant inflow concentration.

Thomann (51) provides a more thorough development of this type of model. For the completely mixed system, he discusses the outflow response to a variety of inflow time series. The sketch below indicates the system under consideration.

Under the assumption of complete mixing in the reservoir, the water in storage may be characterized by a volume, V , and a concentration, s . Also, the concentration of material in the outflowing water is the same as in the reservoir. The mass of a substance entering the reservoir can be represented by a load, W(t) ; the product of inflow and concentration of the dissolved material. The time series of the load input is generally not equal to the load leaving the reservoir since the mass in storage may vary over time. For a reservoir containing a volume, V , of stored water and having a homogeneous concentration, s , the equation expressing a mass balance of any dissolved material is

$$\frac{dM}{dt} = V\frac{ds}{dt} = W(t) - k \cdot s \cdot V - Q \cdot s \qquad 4.54$$

with M the mass of substance in storage, k the decay coefficient of a non-conservative substance, and the other terms as defined above with the exception of the outflow, Q . Although the flow out of a reservoir is generally time varying, this model assumes it, as well as the volume, is constant. This assumption seems quite rigid. However, over a long period, reservoir volume and release are often relatively smooth and their average values characterize them well.

For a general water quality system the substance under consideration might be non-conservative and decay over time. Biological oxygen demand is a typical example. As oxygen is consumed the biological oxygen demand is reduced. The change in mass of such a non-conservative substance is usually modeled by the first-order reaction

$$\left.\frac{dM}{dt}\right|_{\text{reaction}} = -k \cdot s \cdot V \qquad 4.55$$

which results from the differential equation

$$\frac{ds}{dt} = -k \cdot s. \qquad 4.56$$

The following discussion is based upon a conservative water quality parameter such as salinity which does not decay over time. For this case, Eq. 4.54 becomes

$$V\frac{ds}{dt} = W(t) - Q \cdot s \qquad 4.57$$

or

$$V\frac{ds}{dt} + Q \cdot s = W(t) \qquad 4.58$$

The solution of the homogeneous equation,

$$\frac{ds}{dt} + \frac{Qs}{V} = 0 \qquad 4.59$$

with boundary condition $s = s_o$ at $t = 0$ is

$$s = s_o \exp\,[-(Q/V)t]. \qquad 4.60$$

Thus a system with initial concentration s_o will be diluted by inputs containing zero concentration and decay exponentially to zero concentration. Equation 4.60 can be used to predict the flushing time required for a system to reach any fraction of its original concentration after discharge of a pollutant ceases.

The remaining discussion centers about determining the particular solution for various forms of W(t). The final solution is the sum of the homogeneous and particular solutions. The input and output from a step load function of magnitude $\bar{x}$ are sketched below:

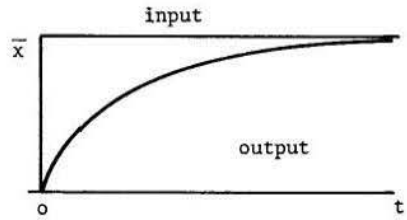

For these conditions

$$V\frac{ds}{dt} + Q \cdot s = \bar{x}\,U(t), \qquad 4.61$$

where U(t) is the indicator equal to zero for t less than 0 and one for t equal to or greater than o and $\bar{x}$ is the magnitude of the dissolved solids load. The solution is

$$s = \frac{\bar{x}}{Q}\,[1 - \exp\,(-Q/V)t]. \qquad 4.62$$

For T equalling V/Q , the detention time,

$$s = \frac{\bar{x}}{Q}\,[1 - \exp\,(-t/T)]. \qquad 4.63$$

As time approaches infinity, exp (-t/T) goes to zero and x equals $\bar{x}/Q$ which is the average load divided by the average flow. This can be used to estimate the steady state result of a step input. For the trend input sketched below, Eq. 4.58 becomes

$$\frac{ds}{dt} + Q \cdot s = b \cdot t \qquad 4.64$$

where b is the increase of load per time unit.

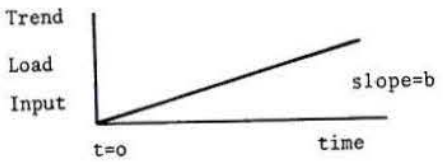

The solution for this case is

$$s = c \exp[-(Q/V)t] + \frac{bt}{Q} - \frac{bV}{Q^2}. \qquad 4.65$$

For the boundary condition $s = s_o$ at $t = 0$

$$s_o = c - \frac{bV}{Q^2} \qquad 4.66$$

so that

$$c = s_o + \frac{bV}{Q^2}, \qquad 4.67$$

and the solution is

$$s = (s_o + \frac{bV}{Q^2}) \exp[-(Q/V)t] + \frac{bt}{Q} - \frac{bV}{Q^2} \qquad 4.68$$

or

$$s = s_o \exp[-(Q/V)t] - \frac{bV}{Q^2}[1 - \exp[-(Q/V)t]] + \frac{b}{Q}t. \qquad 4.69$$

As t becomes large, the outflow concentration rate of change approaches b/Q and concentration becomes infinitely large.

For a periodic loading pattern, the inputs can be expressed as

$$W(t) = \bar{x} + \sum_{j=1}^{n} x_j \sin(\omega_j t - \alpha_j). \qquad 4.70$$

Consider individual terms of periodic inputs such as

$$I_j = x_j \sin(\omega_j t - \alpha_j). \qquad 4.71$$

The differential equation of the process is

$$\frac{ds_{pj}}{dt} + Qs_{pj} = x_j \sin(\omega_j t - \alpha_j) \qquad 4.72$$

and has the solution

$$s_{pj} = x_j A_j \sin(\omega_j t - \alpha_j - \theta_j), \qquad 4.73$$

where A_j is the system gain function given by

$$\left.\begin{aligned} A_j &= \frac{1/V}{[(Q/V)^2 + \omega^2]^{1/2}} \\ \text{or} \quad A_j &= \frac{1}{V[1/T^2 + \omega^2]^{1/2}} \end{aligned}\right\} \qquad 4.74$$

with θ_j the system phase function equal to arctan $(T\omega)$ which goes to $\pi/2$ as ω becomes large.

For first order autoregressive inputs with noise, ξ_t

$$\frac{ds}{dt} + Qs = \rho_1 Z_{t-1} + \xi_t \qquad 4.75$$

The input $\rho_1 Z_{t-1} + \xi_t$ can be considered a square pulse input, $Y(t)$. This pulse can be represented by two step functions, one positive, beginning at time t, and the other negative, beginning at time $t + \Delta t$, as sketched below.

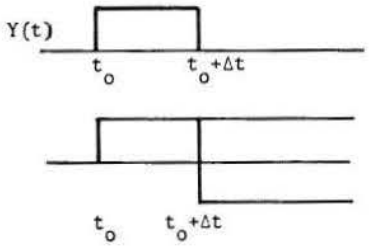

The output from $Y(t)$ at time $t = t_o$ is

$$\left.\begin{aligned} s_y &= \frac{Y(t)}{Q}[1 - e^{-t/T}] \\ \text{or} \quad s_y &= \frac{Y(t)}{Q}[1 - e^{\frac{-Q}{V}t}] \end{aligned}\right\} \qquad 4.76$$

The output from $-Y(t)$ at $t = t_o + \Delta t$ is

$$\begin{aligned} s_{-y} &= 0 \text{ for } t < t + \Delta t \\ &= \frac{-Y(t)}{Q}[1 - e^{-(t - \Delta t)/T}] \end{aligned} \qquad 4.77$$

The total response from the single pulse input

$$\left.\begin{aligned} s_A &= s_Y + s_{-Y} \\ \text{or} \quad s_A &= \frac{Y(t)}{Q}(1 - e^{-t/T}) \quad \text{for } t_o < t \leq t_o + \Delta t \\ &= \frac{Y(t)}{Q}(1 - e^{-t/T}) - \frac{Y(t)}{Q}(1 - e^{-(t-\Delta t)/T}) \\ &\qquad \text{for } t \geq t_o + \Delta t \end{aligned}\right\} \qquad 4.78$$

or finally,

$$s_A = \frac{Y(t)}{Q}[e^{-(t-\Delta t)/T} - e^{-t/T}] \quad \text{for } t \geq t_o + \Delta t \qquad 4.79$$

Consider a series of many pulses similar to those just described.

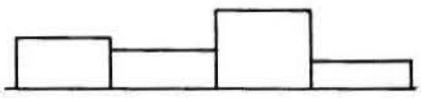

The system output at any time t, will be the integral (or sum) of the responses from past pulse inputs which may be dependent via the Markov model,

$$s_t + \sum_{j=1}^{t} Y(j)\, K(t-j+1) \qquad 4.80$$

where Y(j) is input at time j and K(t) is the response function given by

$$K(t) = \frac{1}{Q}\left[e^{-(t-\Delta t)/T} - e^{-t/T}\right]. \qquad 4.81$$

Eq. 4.80 then becomes

$$s_t = \sum_{j=1}^{t} (\rho_1 z_{j-1} + \xi_j)\, K\,(t-j+1). \qquad 4.82$$

This is the output for a Markovian input. It can be considered as a moving average process applied to the input values. For a simple moving average process Yevjevich (67:48) gives the equation of the correlogram,

$$\rho_k = 1 - \frac{k}{m} \qquad 4.83$$

In this application, m is equivalent to the number of terms in the convolution equation. If t terms are used, $r_k = 1 - \frac{k}{t}$, and approaches 1.0 as t becomes large. For 12 terms, $r_1 = 1 - \frac{1}{12} = 0.92$.

The above discussion has presented methods for operating on various loads entering a completely mixed reservoir to estimate the concentration of the outflow. The model can be formulated to give the outflow concentration s_t, at any time as a function of a mean value, periodic components, autoregressive inputs, and noise in the system not associated with specific detectable inputs.

4.5 Summary of Reservoir Salinity Modeling Techniques

The above review indicated several possible methodologies for modeling the passage of any conservative substances through a reservoir. The stratification approach has the advantage of providing estimates of concentration at any number of points throughout the reservoir. Temperature stratification models are currently being applied which have potential for incorporating salinity as a quality parameter without great difficulty. However, the calibration and verification of this type of model would require salinity information for several depths and over several years' time. This type of data is generally difficult to obtain. Also information describing advective flows and detailed circulation patterns would be required to confidently model large mass movements in the water body. This type of model does have merit for problems requiring a detailed estimate of the vertical salinity distribution, such as designing multiple outlets for selective withdrawal.

The so-called "black box" approach completely ignores the internal mechanisms of the reservoir. This analysis requires only inputs and outputs to evaluate the system transfer function. As the literature indicates, reasonable success for a wide variety of input-output systems has been obtained by using this technique. Time series models fall in this category and show great potential for further water quality system model development. In the role of planning models especially, the economy of using a straightforward input-output relationship is particularly great. Sophisticated models of large water resource systems require substantial computer time and storage space to handle multiple stations, multiple objectives, numerous constraints, short time steps (such as daily, weekly or monthly) and long sequences of multiple runs when a data generation scheme is used. In this type of model, subsystems such as quality movements through a reservoir must give reliable estimates of events with minimum computer storage and calculation time. This type of model requirement was pointed out by Young (69) in comment to the stratification model published by Beard and Willey (2). He suggested coupling the results of fine-grid descriptive models such as those in Section 3.4 with statistical inference techniques. Analysis time would be saved by using simplified least-squared predictive equations to reflect the behavior of the reservoir.

Analysis of outflow concentrations based on the assumption of complete mixing as developed in the previous section has many desirable properties. The model itself is not complicated and does not require extensive computer programming to operate. Computer storage space is nominal, since only a few coefficients or variables must be saved. Also, calculation time is minimal for each time step since the computations are simple. It remains to be seen whether real reservoirs follow the mixing assumption adequately to justify its acceptance.

CHAPTER V

ASSEMBLY OF DATA FROM LAKE MEAD

Chapter IV has introduced several possible techniques for modeling the salinity concentration of water coming out of a reservoir. In this chapter historical data from Lake Mead in Arizona and Nevada, a large monomictic reservoir, is analyzed and refined for the applications forthcoming in Chapter VI.

5.1 Selection of Lake Mead as an Example for Investigation

It was desired to test and compare results of applying the modeling techniques to actual data from a prototype reservoir. Criteria for a field example were established so the results would be generally applicable to reservoirs of similar climate and average detention time. This called for a monomictic reservoir which was stratified in the summer and had enough capacity to store at least a year's inflow. This would produce an average detention time of at least 12 months. To properly evaluate the various models and apply time series analysis techniques, 20 to 30 years of monthly data were desirable. The data set had to contain measurements of inflows, salt concentrations in the inflows, monthly reservoir contents, releases below the reservoir, and the quality of the releases.

An intensive search of USGS Water Supply Papers indicated several reservoirs in the southwestern United States were monitored for the desired parameters. Unfortunately, inspection of the records revealed that a majority of these reservoirs contained data for only a few recent years. During this search for data, Lake Mead on the Colorado River was found to meet all of the requirements above. In addition to this, personnel from the U.S. Bureau of Reclamation were in the process of developing a large-scale simulation model of the entire Colorado River. Since salinity was an integral part of this effort, results of investigating methods of routing salinity through reservoirs would prove very timely. As mentioned in the introductory remarks, salinity levels of the Lower Colorado River are rising to detrimental levels. Since reservoir storage in the Upper Basin of the Colorado affects quality in the lower reaches, investigating the movement of salts through reservoirs such as Lake Mead would be especially useful.

Even though Lake Mead was selected as a single case for investigating the techniques of routing salinity through reservoirs, future applications can be made to other reservoirs in similar climates which also have detention times greater than one year. The assumption of the completely mixed water mass can be verified with a few years of data and the results of this study applied to model the behavior of other reservoirs.

Lake Mead is located near the southern border of Nevada and lies about 40 miles east of Las Vegas. Figure 5.1 shows the entire Colorado River Basin as well as Lake Mead itself. The reservoir began filling in 1935 and received relatively undisturbed inflows until Lake Powell, upstream, started to fill in 1963.

5.2 Data Assembly

In this section the various data sets relevant to Lake Mead are identified and assembled in a form suitable for further incorporation into the models. In some instances, minor refinements were required to make historic information consistent and complete.

In all instances, where available, published records of streamflow were used directly to represent measured inflows to Lake Mead. Table 1 summarizes the period of record for gaged inflows and the magnitude of ungaged tributaries and drainage areas. Where records were available for part of the study period, either correlations were used to estimate flows or the average monthly values were repeated when no satisfactory correlations were found. In this way, monthly flow was assembled for each source from 1935 to 1970 and punched on cards for later use.

Monthly evaporation depth was used as published by the USGS since 1953. For earlier years, monthly values were estimated by computing an annual value based on pan evaporation at Boulder City, Nevada and a monthly distribution following the pattern of the later published data. Table 2 gives an indication of the consistency of annual pan and lake evaporation from 1941 to 1953. Figure 5.2 shows the monthly pattern which results when one-twelfth of the annual total is subtracted from each monthly value. Table 3 was used to further investigate the lake to pan evaporation ratio. Even though the ratio for 1953 through 1969 is 0.73, Kohler, Nordenson, and Fox (21:59) indicate a pan coefficient of 0.70 for annual values from 1941 to 1953. Figure 5.3 shows that in the first years the annual pan evaporation at Boulder City is significantly higher than in later years. This may be due to errors in the first years of data collection or a change in the microclimate surrounding the instrument. However, since the reservoir was just beginning to fill the area was small in 1936 and 1937 compared to later years and further adjustments were not made.

The relationship used to estimate monthly evaporation depth for 1936 to 1952 is represented by

$$E_r\,(Y,M) = \frac{E_p\,(Y)}{12} \cdot P_k + R(M) \qquad 5.1$$

where E_r is the monthly reservoir evaporation depth, E_p the annual pan evaporation, Y indicated the year, M indicates the month, P_k is the pan coefficient, and R(M) is the residual value for month M .

Yearly Boulder City pan evaporation was taken directly from annual summaries of climatological data published by the Weather Bureau (14) and multiplied by a pan coefficient of 0.70. The monthly residuals (variations about 0.0) were the averages from all 17 years of published Lake Mead evaporation and are given in Table 4.

Pan evaporation data were not available at Boulder City prior to 1936. Since the reservoir began storing in February 1935, no appreciable error results in estimating evaporation for that year by the historic monthly averages. The estimated and historic evaporation is plotted in Fig. 5.4.

Whenever possible, dissolved solids concentration, in tons per acre-foot or parts per million, were used directly from published reports. (Note that tons per

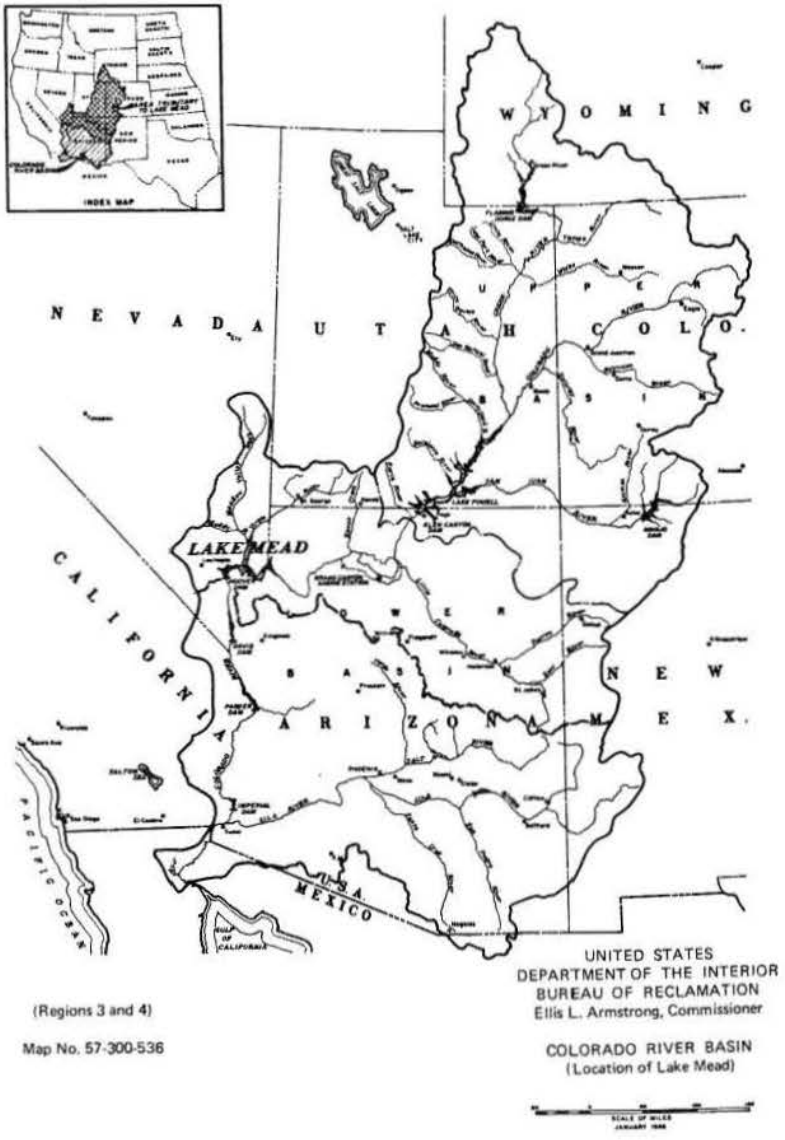

Fig. 5.1 Colorado River Basin

Table 1

Summary of Lake Mead Inflow Sources

Tributary	Drainage (sq mi)	Annual Flow (ac-ft) a/	Period of record	Period estimated
Bright Angel Creek	101	25,650	Oct 1923 to present	None
Kanab Creek	1,085	4,310	Oct 1963 to present	Excluded from study
Tapeats Creek		*58,000	None	1935-1969
Havasu Creek		*47,000	None	1935-1969
Muddy River	6,780	33,760	Feb 1950 to present	1935-1950
Virgin River	5,090	164,500	Oct 1929 to present	None
Las Vegas Wash	2,125	18,260	Feb 1957 to present	1935-1957
Subtotal, excluding Kanab Creek	14,096	347,240		
Colorado River near Grand Canyon	137,800	b/ 9,150,000		
Total	151,896	9,497,240		
Colorado River below Hoover Dam	167,800	9,882,000	Oct 1933 to present	

a/ As published in Water Resources Data for Arizona and Nevada, Part 1, 1970, except those marked by an asterisk (*) which were estimated.

b/ 1922-1962 average was 12,260,000 acre-feet.

Table 2

Ratio of Lake Mead to Boulder City Pan Evaporation a/

Year	Ratio	Year	Ratio
1941	0.71	1948	0.71
1942	0.70	1949	0.69
1943	0.66	1950	0.71
1944	0.68	1951	0.70
1945	0.70	1952	0.72
1946	0.67	1953	0.73
1947	0.68		
		Average	0.70

a/ from (21:59)

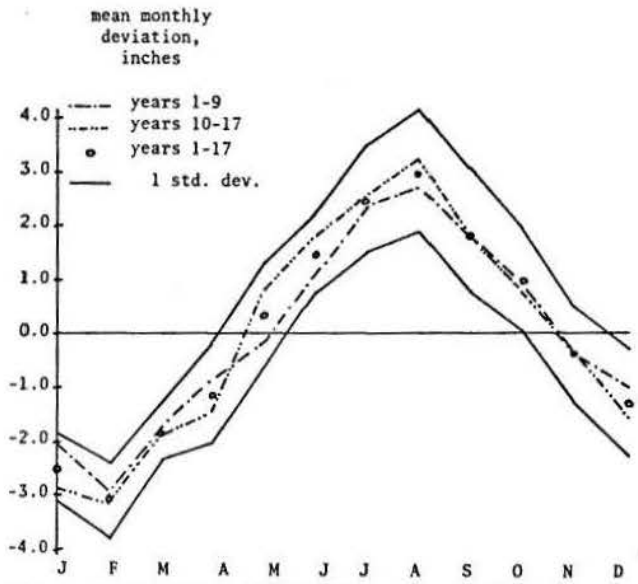

Fig. 5.2 Deviates of monthly evaporation from an average value.

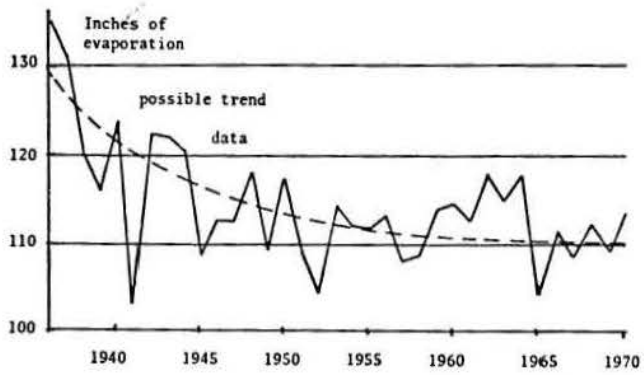

Fig. 5.3 Annual Boulder City pan evaporation.

Table 3

Annual Evaporation Measured From the Boulder City Pan and Estimated For Lake Mead a/

Inches, by Calendar Year

Year	Boulder City pan	Published at Lake Mead	Ratio
1953	114.59	86.2	0.75
1954	112.15	87.3	0.77
1955	111.99	87.3	0.79
1956	113.20	82.3	0.81
1957	108.39	83.2	0.77
1958	109.04	85.6	0.79
1959	114.30	86.1	0.75
1960	114.82	84.4	0.74
1961	113.00	83.4	0.74
1962	118.48	79.7	0.67
1963	115.50	83.0	0.72
1964	118.25	80.2	0.68
1965	104.82	70.9	0.68
1966	112.03	78.9	0.70
1967	109.14	76.9	0.70
1968	112.89	75.5	0.67
1969	109.84	75.2	0.69
			0.73 avg ratio

a/ From (21)

Table 4

Monthly Residuals of Evaporation

M	Month	Residual evap, R(M)
1	January	-2.50
2	February	-3.05
3	March	-1.81
4	April	-1.15
5	May	0.37
6	June	1.48
7	July	2.46
8	August	2.99
9	September	1.81
10	October	1.01
11	November	-0.36
12	December	-1.25
		0.00 average

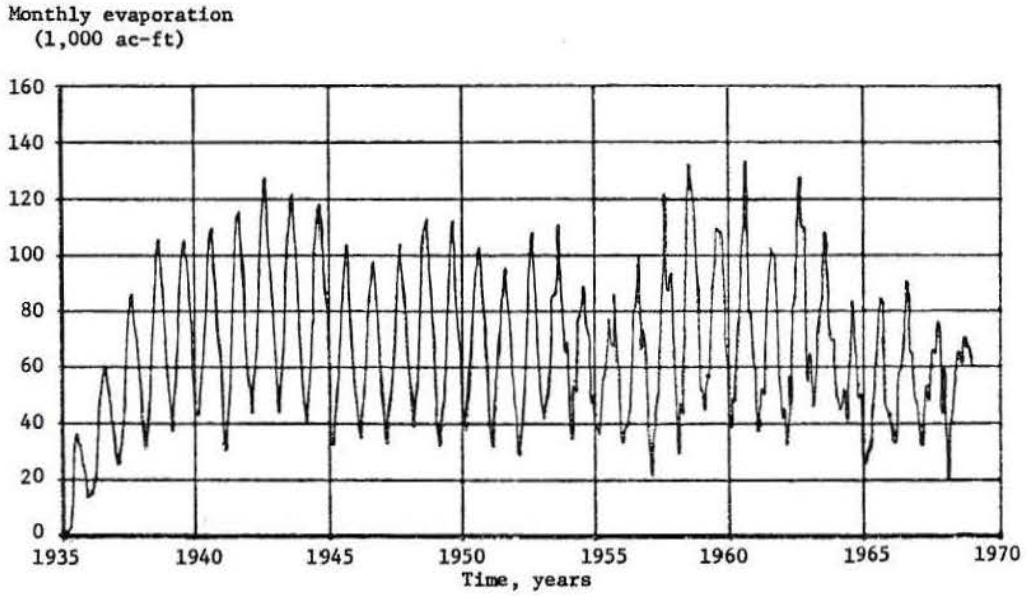

Fig. 5.4 Monthly Lake Mead evaporation, 1935 to 1968.

acre-foot equals parts per million divided by 735.) Monthly concentrations for the Colorado River near Grand Canyon, Arizona; Virgin River at Littlefield, Arizona; and the Colorado River below Hoover Dam, Arizona-Nevada, were taken as published (58). Data prior to 1941 were extracted from an early study of Lake Mead (56). The discussion of dissolved solids concentration of various tributaries of Lake Mead (58) indicated very sparse or no data were available. A search of USGS Water Supply Papers confirmed no long-term quality data were available except at the above three stations. With no better information than rough estimates and spotty samples of water quality, it was decided to estimate dissolved solids concentration of unmeasured tributaries by the estimate of their average concentration relative to the concentration of measured tributaries.

The table below summarizes the estimated average dissolved solids concentration for tributaries of the Lake Mead hydrologic system. The values in this table coincide generally with those given in Appendix A of an EPA report of Colorado River salinity (18).

As Table 5 indicates, the salt load introduced by the six minor tributaries was two orders of magnitude less than contributions from the Colorado River. Even though the 200,000 tons delivered by these sources is less than the Virgin River, their accumulated salt load has a significant effect on a long-term salt budget. It was decided to include the salt contribution of each tributary by assuming a concentration directly proportional to the Virgin River. The proportions of Virgin River dissolved solids concentration from Table 5 were used with slight adjustment to estimate concentration of each tributary.

No attempt was made to adjust or correct published dissolved solids concentration data for this study. Inevitable minor errors due to data collection, the type of analysis, and inconsistencies in the methods of measurement are inherent in the data. The data for the Colorado River near Grand Canyon and below Hoover for 1935 to 1968 are displayed in Fig. 5.5

Table 5

Estimated Average Dissolved Solids Concentration and Discharge of Various Lake Mead Tributaries

Tributary	Annual discharge ac-ft	Concentration tons/ac-ft	Tons of salts/ year	Concentration proportion of Virgin River
Bright Angel Cr.	25,650	0.27	6,930	0.12
Kanab Cr.	4,460	c/ 1.5	6,690	0.65
Havasu Cr.	47,000	c/ 0.5	23,500	0.22
Tapeats Cr.	58,000	c/ 0.2	11,600	0.09
Muddy River	33,830	2	67,660	0.87
Virgin River	164,500	b/ 2.29	376,710	1.00
Las Vegas Wash	18,260	a/ 4.5	82,170	1.97
Colorado River	9,150,000	b/ 0.84	7,686,000	
Total	9,497,240	.87	8,261,260	

a/ Based on chemical quality data since October 1968, and (22).
b/ Based on a long-term record of chemical analysis
c/ From (58:32-33).

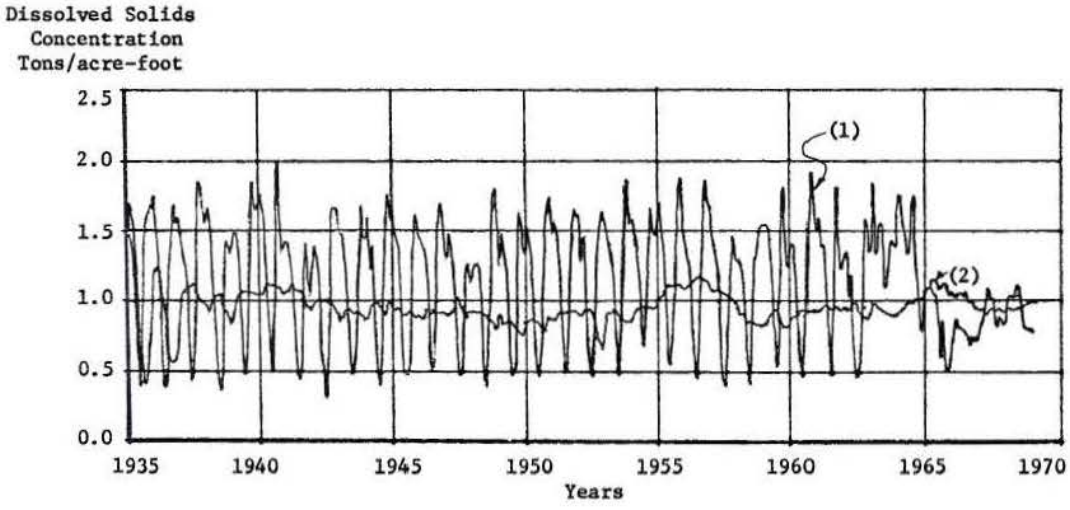

Fig. 5.5 Dissolved solids concentration of (1) Colorado River near Grand Canyon, and (2) Colorado River below Hoover Dam.

During the life of a reservoir, the volume of storage below a given elevation is continually changing due to sediment movement. Generally, sediment is trapped and storage space decreases with time continuously as sediment deposition occurs. Data from surveys of Lake Mead which were made in 1935, 1948 to 1949, and 1963 to 1964 (33) were used to adjust published monthly reservoir contents (USGS Station 9-4210) to include dead storage (water below elevation 895 feet M.S.L.) and the effect of sediment build-up. The sediment accretion each month was calculated as a proportion of the total build-up between survey periods. This monthly proportion was the ratio of the monthly sediment tonnage of the Colorado River near Grand Canyon to the total tonnage during the period between surveys. Figure 5.6 shows the adjusted end-of-month total contents.

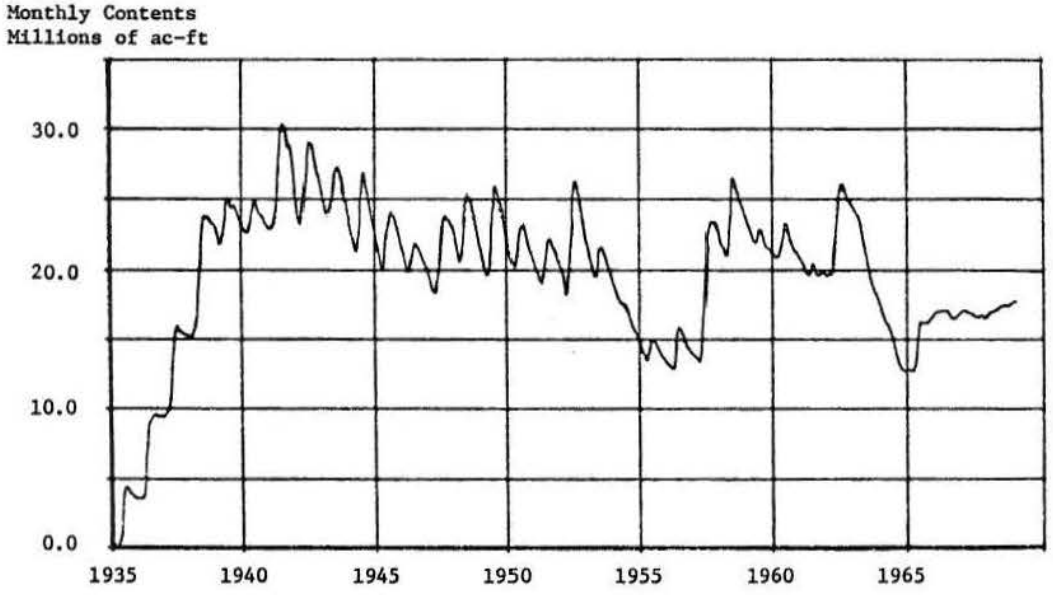

Fig. 5.6 Lake Mead adjusted end-of-the-month contents.

CHAPTER VI

DATA ANALYSIS AND REFINEMENT

In this chapter the data from Lake Mead are analyzed to identify components of the water and salt budgets.

6.1 Water Budget

A water budget for Lake Mead was run using monthly flows as described. The Colorado River near Grand Canyon flow was adjusted for sediment concentration to provide an estimate of the water portion of measured inflow. Lake Mead contents were also adjusted to reflect changes in area-capacity curves and sediment volumes, as described in Section 6.2.4.

A prerequisite to analyzing the system's water quality behavior is accounting for all the water moving through it. The most straightforward approach is a simple accounting of inflows, outflows, and storage change. For the general system of Fig. 2.1, the major system features are main stream inflow, tributary inflow, evaporation, precipitation, bank storage, outflow, and surface storage. All these factors may be combined into one equation by taking a mass balance of water in the system. This yields

$$\Delta S = I_m + I_t + I_p - E - O - B + \xi \qquad 6.1$$

where ΔS is the change in storage from period i to period i+1 ($s_{i+1} - S_i$), I_m the main stream inflow, I_t the tributary inflow, I_p the precipitation on the reservoir, E the evaporation, O is outflow, B is bank storage change (positive into the aquifer), and ξ is an error term resulting from unaccountable quantities and errors in measuring all components.

The water budget then consists of estimating all terms in the budget equation to account for all inflows and outflows of water. When this has been done, a good approximation of the water in storage at any time can be made by applying the budget consecutively in finite step fashion from an initial condition.

Prior attempts to estimate unmeasured inflow and bank storage of Lake Mead have been made by Langbein (32) and by Rechard (41). Langbein's study utilized Virgin River and Bright Angel Creek Tributary inflows which left about 25,000 square miles of drainage unaccounted for. He used an approximation for unmeasured inflow assuming it was directly proportional to Virgin River flow and that bank storage was 0.125 times the surface storage change. The water budget equation was a straightforward accounting procedure given by the following modification of Eq. 6.1.

$$I_m + I_u + I_p - E - O_m = S_{i+1} - S_i + R, \qquad 6.2$$

where I_m is the measured inflow, I_u the unmeasured inflow, I_p is precipitation, E is evaporation, O_m is the measured outflow, S_i the storage at time i, and R is a residual quantity composed of errors in measured and estimated quantities as well as bank storage.

This equation was used directly in the present study, except that precipitation was eliminated and no estimate of unmeasured inflow was initially included. As expected, cumulative bank storage at first rose, then decreased to zero and was negative in 1969, the last year. Knowing a significant input had been neglected, the problem was to estimate the unknown contribution.

As discussed earlier, Langbein accomplished this by making assumptions about bank storage and correlating unmeasured inflow to the Virgin River flow. Rechard (41) analyzed the water budget similarly, but was able to include the measured flows of the Muddy River and Las Vegas Wash which had been gaged since 1950 and 1957, respectively. Rechard rather arbitrarily assumed the unmeasured inflow was related to tributary flow by the equation

$$I_u = 0.75\ (I_B + I_V + I_M + I_L), \qquad 6.3$$

with I_u the unmeasured inflow, I_B the flow of Bright Angel Creek, I_V the flow of the Virgin River, I_M the flow of the Muddy River, and I_L the flow of Las Vegas Wash.

Although Rechard's study supposedly was an improvement in Langbein's, an obvious discrepancy resulted which was not mentioned in prior discussions. This can be seen from the data of Table 4 in his paper (41). In water year 1956, the cumulative residual (bank storage) is shown as 978,000 acre-feet. Inspection of the reservoir stage or storage record shows the 1956 contents were above that measured in 1937. Since the reservoir was filling prior to 1937 and emptying prior to 1956, a larger bank storage would be anticipated in 1956 than 1937. Rechard's report (41) indicates bank storage was 1,981,000 acre-feet at the end of 1937, yet only 978,000 in 1956. In other words, about 1 million acre-feet from 1937 to 1956 had been overlooked.

In the present study a different approach was taken to estimate unmeasured tributary inflow and bank storage. Points in time were selected which showed a similar storage volume and prior history of rise or fall. It was assumed that bank storage would be approximately the same at these two times. The priliminary water budget provided an estimate of bank storage with unmeasured inflow not included. This yielded a deficit in inflow equivalent to the volume required to make bank storage the same at the beginning and end of each period.

Five such periods were found when bank storage should have been equal. The Virgin River and Bright Angel Creek (measured) flows were then totaled for these periods. The extimated inflow deficit and measured tributary inflow were compared and a multiple regression analysis produced the following results:

$$Y = 9.79\ X_1 - 1.07\ X_2 - 225 \qquad r = 0.997 \qquad 6.4$$

$$Y = 4.32\ X_1 - 212 \qquad r = 0.990 \qquad 6.5$$

$$Y = 0.834\ X_2 - 326 \qquad r = 0.980 \qquad 6.6$$

where Y is the unmeasured inflow volume, I_u, estimated from the first budget, X_1 is the volume from Bright Angel Creek, and X_2 the Virgin River volume.

An analysis of the correlation between the Virgin River and Bright Angel Creek annual volumes indicated a high degree of linear dependence (r = 0.997). Thus, one tributary would be as useful as both in the analysis of bank storage.

A second water budget analysis was run including inflow based on the equation above using Bright Angel Creek flows. It should be mentioned that minor depletions and additions due to pumpage to Boulder City and Henderson, Nevada, and precipitation, respectively, were not included.

Results from this budget were quite encouraging and showed a high degree of consistency. Bank storage quantities for the various approaches are illustrated in Fig. 6.1. Annual values were plotted in this figure.

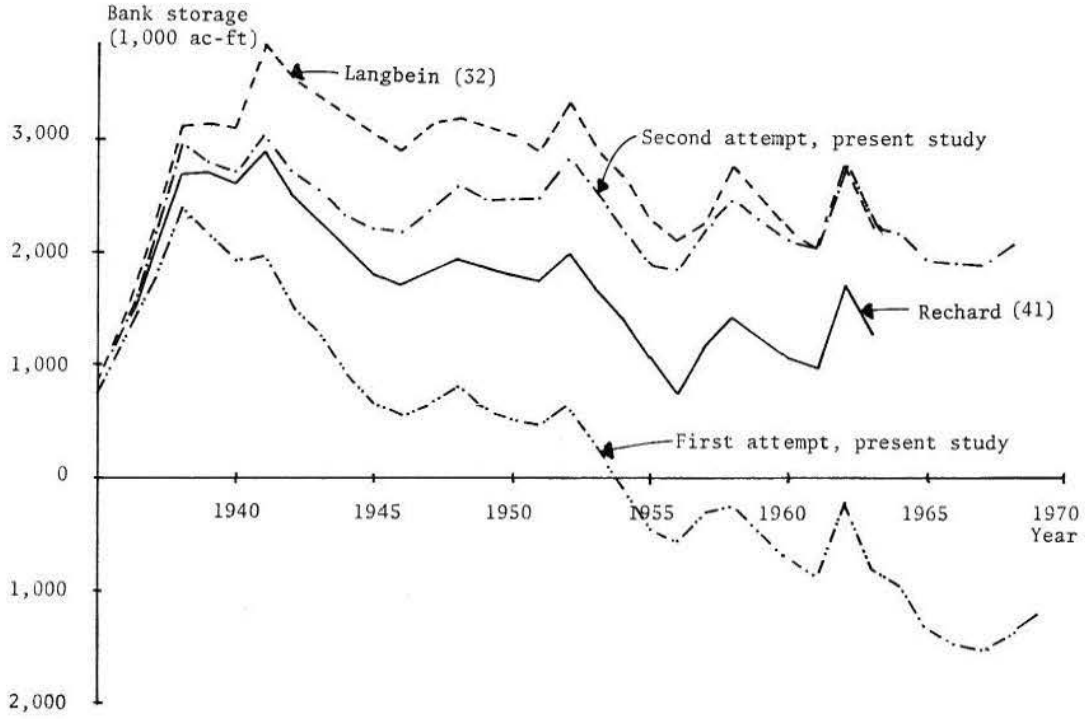

Fig. 6.1 Various estimates of bank storage for Lake Mead.

Although the general level of bank storage appears fairly accurate, many approximations leading to substantial errors in monthly quantities have been included. Monthly errors on the order of 60,000 acre-feet can be expected and should be considered when results from the water budget are being used. Estimated monthly and cumulative bank storage are shown in Fig. 6.2.

The earlier investigations of Lake Mead bank storage were based on annual discharge and storage changes to eliminate or minimize discrepancies resulting from time lags within the system. The possibility of inflow at the Grand Canyon Gage affecting storage over a longer time lag than 1 month was investigated by use of the cross correlogram of Fig. 6.3 between Colorado River monthly flow and monthly reservoir change in contents.

Since there was no cross correlation exceeding that at lag zero, no consistent pattern of lag effect greater than 1 month was detected. Significant r_K values at 12 month were due to the annual period of both series.

Having analyzed the water budget the next step was to determine a relationship between bank storage and surface storage. Even though the change in the monthly bank storage was small compared to the inflow of the Colorado River, the accumulated effect may be quite large. This can be seen in Fig. 6.2 which indicates a total release of about 1 million acre-feet of water from bank storage during the 1963 to 1965 reservoir drawdown.

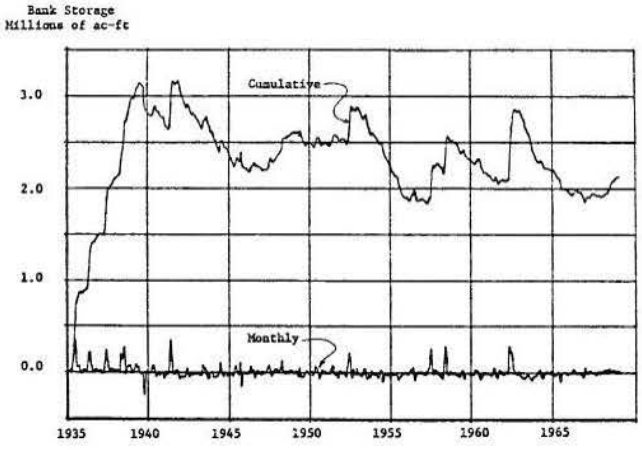

Fig. 6.2 Estimated monthly and cumulative bank storage.

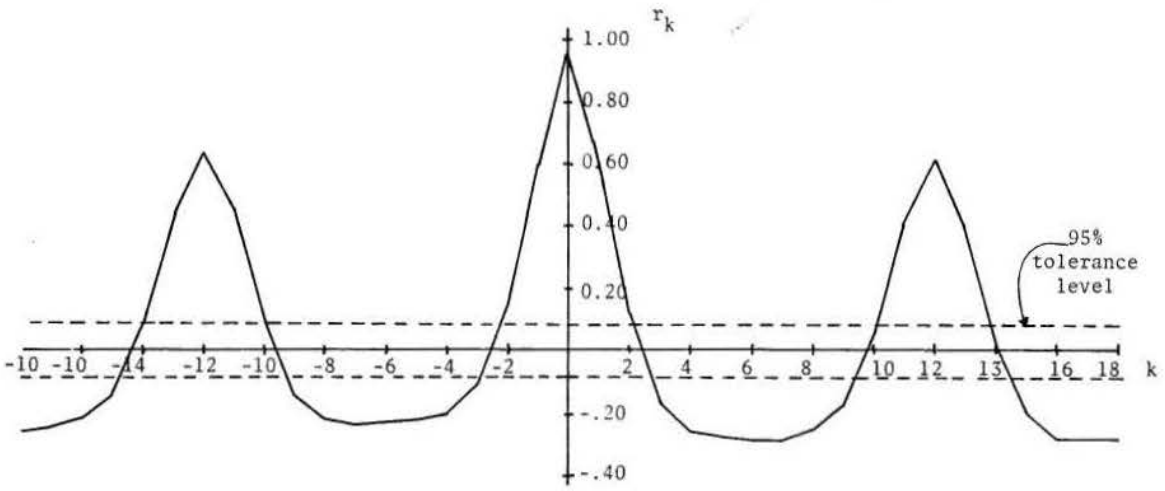

Fig. 6.3 Cross correlogram of Colorado River monthly flow near Grand Canyon and monthly storage change of Lake Mead.

The form of bank storage relationship suggested by Langbein (32) was $R = b\Delta S$, where R is the bank storage, ΔS the annual change in reservoir content, and b is an estimated regression coefficient equal to 0.125. The later work by Rechard (41) indicated b might have been 0.065 for data from 1956 through 1963. Although this formulation is a simplified approach, the results are quite successful. Several factors may influence the bank storage and can be reflected by a more complex model incorporating several variables. The geometric properties of the aquifer and its boundaries can influence the response of bank storage to a change in reservoir surface elevation. If the aquifer extends far from the surface reservoir boundary and the material has a low permeability, several years might pass before the complete effect of a change in water surface elevation would be exerted. Conversely, a narrow aquifer composed of a highly permeable material could respond completely in a very short time. The past history of surface storage might also affect bank storage. Since the hydraulic properties of an aquifer change with the degree of saturation, a reservoir rising during the first filling period will lose more water into bank storage than it will later when the water table of the aquifer is higher. In addition, the hysteresis of ground-water movement could create a time-varying response to storage change.

The above discussion indicates a very complex mathematical model would be required to adequately describe the bank storage response to changes in surface storage. However, the success of the analysis by Langbein's model indicates the potential of a simplistic approach. Two methods of representing bank storage change were investigated in this study. The first was a multiple regression model and the second an application of the convolution sum to the diffusion equation as reviewed in Section 4.2.

The first approach to modeling monthly flows into and out of bank storage was to hypothesize a simple deterministic model, and to use the multiple-regression technique to estimate the coefficients of the postulated relationship. The model investigated was the linear regression of bank storage on the accumulated bank storage in the prior month, the surface storage, the surface storage change since the previous month, the water surface elevation, and the change in water surface elevation from the past month. From inspection of bank storage and reservoir content, the flow in or out of bank storage was largely determined by the reservoir content (or by the elevation of the water surface) and the total bank storage. By relating the change in bank storage to the prior month's bank storage, the past reservoir content was effectively integrated into one quantity.

The possibility of the change in bank storage lagging the change in surface storage was investigated by correlogram of Fig. 6.4. The peaks at 12-month intervals indicate the annual periodicity in both series. This illustrates an immediate response of bank storage to changes in monthly surface storage. It should be noted that there are no significant correlation coefficients which are greater than those at 0 or -1 lag, indicating that for the data of this system, there is no apparent long-delayed response.

With the above quantities, the regression equation was postulated

$$B = f(C_b, V, D_v, H, D_h) \qquad 6.7$$

with B the monthly bank storage change, C_b the accumulated bank storage in the prior month, V the content of the reservoir, D_v the change in reservoir content, H the water surface elevation, and D_h the change of water surface elevation since the past month. The first multiple linear regression of monthly bank storage on the above variables was made with the complete 1935 to 1968 data. The simple correlation matrix indicated the bank storage was most influenced by changes in water surface elevation (r = 0.57) and secondly by surface storage change (r = 0.56). This is not surprising since these two variables are closely related. A summary of the step-wise regression results is given.

			Multiple correlation	
Step	Variable	r	r^2	Increase
1	D_h	0.57	0.33	0.33
2	D^h	0.60	0.37	0.04
3	C_v^v	0.61	0.38	0.01
4	H^b	0.62	0.38	0.00
5	V	0.62	0.38	0.00

The standard error of estimate on Step 1 was 50,000

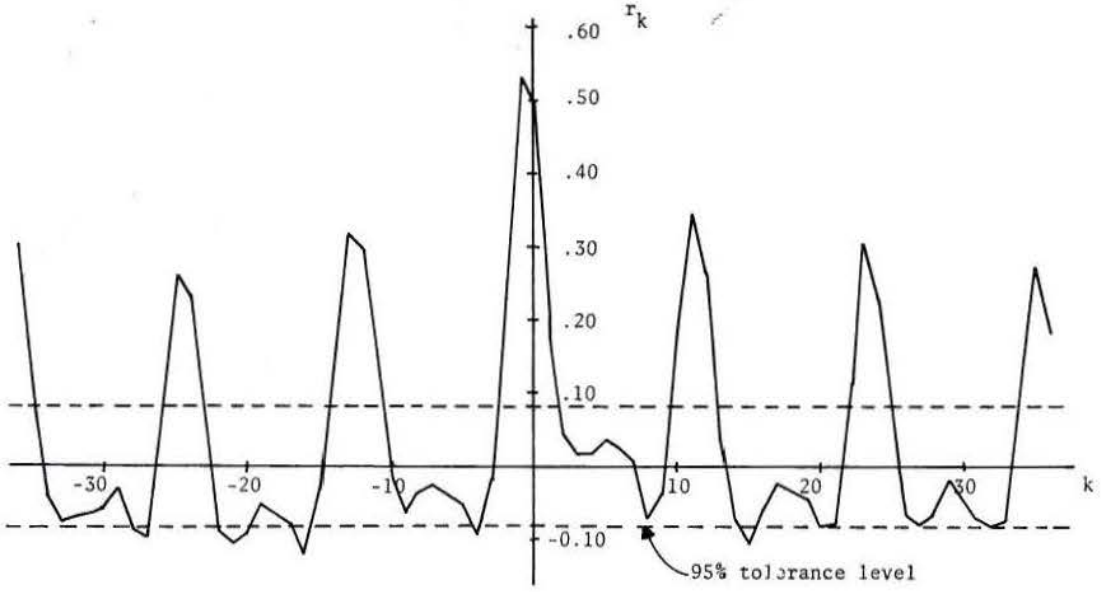

Fig. 6.4 Cross correlogram of monthly storage change and water budget residuals (bank storage).

acre-feet per month compared to 48,000 acre-feet on Step 5, using all variables. It is worthwhile to note that the reservoir content is related to water surface elevation. Similarly, storage change and elevation change are closely related and have a linear correlation coefficient of 0.74. For the data of this analysis, monthly bank storage can be estimated from water surface elevation change alone nearly as well as with the five remaining variables included. The least squares relationship for these data was:

$$B = 1.19 + 3.65\ D_h \qquad 6.8$$

An interesting comparison with previous estimates of bank storage for Lake Mead can be made. Rechard (41) concluded that after the 1954 to 1956 drawdown, the annual bank storage was approximately 6.5 percent of the annual surface storage change. Capacity tables for Lake Mead indicate 90,000 acre-feet of volume between elevation 1100 and 1101, and 112,000 acre-feet between elevation 1151 and 1152, or roughly a 100,000 acre-foot volume change for a 1-foot elevation change under normal operating levels. By using equation 6.8, a 1-foot change in elevation would produce 4,840 acre-feet of bank storage, or approximately 5 percent of the 100,000 acre-foot volume in change. This is very comparable to the percent which Rechard estimated.

The use of elevation change was more appealing than volume change since the hydraulic head on an aquifer is the forcing function causing water movement. A good correlation between the change in surface storage and bank storage resulted since a spurious correlation existed with the third variable, water surface elevation.

Regression analysis was performed on the same variables for several shorter periods between 1935 to 1968 to investigate the effect of different data on this relationship. Results of those analyses are tabulated in Table 6.

The wide range of coefficients and shifting importance of specific variables indicated that the data did not reflect a consistent relationship between the bank storage and the causitive factors.

The 1953 to 1956 period was selected to represent severe drawdown of the reservoir. The low levels of explained variance negate the possibility of formulating any reliable relationships between bank storage change and the reservoir drawdown. For lack of better results, the bank storage Eq. (6.8) for the entire 1935 to 1968 period was accepted as the most representative expression of the bank storage process by the multiple linear regression approach.

The second method of modeling bank storage was the convolution sum approach. Eqs. 4.46, 4.48, 4.49, and 4.51 from Section 4.2 were programmed and convoluted by Eq. 4.53. Terms in Eqs. 4.49 and 4.51 for the finite aquifer were added until the argument in the exponentiation exceeded -120 ($e^{-120} = 7.67 \times 10^{-53}$) or when the ratio of the last term to the sum was less than 0.005.

The mathematical formulation and computer programming for the estimation of bank storage change was clear-cut. The major problem was finding values of aquifer parameters which were representative of a specific reservoir. A range of values for the various parameters is presented in Table 7.

As can be surmised from the table, even an order of magnitude estimate of parameter values for a particular situation was not possible without field tests. A search through publications and personal discussion with several representatives of the USBR and USGS indicated no wells or field test information was available for Lake Mead. The approach taken was to assume values for each of the required parameters, calculate the output using historical water surface elevations, and compare the results with bank storage quantities determined from the water budget. Values of the parameters were adjusted until this comparison did not show any significant improvement. This analysis resulted in parameter values which seemed realistic and also reflected the bank storage quantities of the historical data. Figure 6.5 illustrates the historic and calculated bank storage for one test period. Examples of the kernels for the convolution equation of both cases are illustrated in Fig. 6.6. The finite kernel

Table 6

Multiple Regression Estimates of Bank Storage for Various Periods

Period	Step	Variable	r	Multiple r^2	Increase r^2	Constant	Regression Equation Coefficients D_h	D_v	C_b	H	V	Standard error of estimate (thousands of ac-ft)
1935 to	1	D_v	0.72	0.51	0.51	15.76		0.065				61
	2	D_h	0.75	0.56	0.05	12.21	1.474	0.048				58
1941	3	C_b	0.76	0.58	0.02	41.31	1.051	0.051	-0.013			58
	4	H	0.76	0.59	0.01	-177.77	1.165	0.047	-0.042	0.251		58
	5	V	0.77	0.60	0.91	-215.63	0.996	0.044	-0.109	0.319	0.006	57
1942 to	1	D_h	0.40	0.16	0.16	-0.95	2.85					41
	2	H	0.48	0.23'	0.07	1013.50	3.240			-0.849		40
1952	3	D_v	0.48	0.24	0.01	1023.89	7.576	-0.026		-0.857		40
	4	C_b	0.49	0.24	0.00	945.89	7.593	-0.027	-0.010	-0.771		40
	5	V	0.49	0.24	0.00	4009.19	9.055	-0.035	-0.013	-3.659	0.017	40
1942 to	1	D_v	0.33	0.11	0.11	-5.49		0.015				40
	2	C_b	0.34	0.11	0.00	29.95		0.015	-0.014			40
1956	3	H	0.35	0.12	0.01	-176.84		0.014	-0.029	0.205		40
	4	V	0.38	0.15	0.02	-2865.32		0.015	-0.032	2.799	-0.018	40
	5	D_h	0.39	0.15	0.01	-3042.77	-2.825	0.033	-0.033	2.970	-0.019	40
1953 to	1	H	0.27	0.07	0.07	436.79				-0.397		30
	2	D_v	0.32	0.11	0.04	458.30		-0.010		-0.418		30
1956	3	V	0.37	0.14	0.03	5310.43		-0.012		-5.169	0.037	30
	4	C_b	0.38	0.14	0.00	5293.86		-0.013	-0.017	-5.146	0.039	30
	5	D_h	0.38	0.15	0.01	5609.19	1.585	-0.025	-0.016	-5.453	0.041	30
1958 to	1	D_v	0.61	0.37	0.37	1.11		0.053				42
	2	D_h	0.67	0.45	0.08	1.03	-18.253	0.172				39
1968	3	H	0.68	0.46	0.01	-234.33	-18.455	0.173		0.201		39
	4	C_b	0.69	0.47	0.01	-442.51	-19.024	0.174	-0.033	0.442		39
	5	V	0.69	0.47	0.00	664.44	-18.687	0.170	-0.043	-0.617	0.008	39

Table 7

Estimated or Assumed Aquifer Properties

Symbol	Parameter	Units	Minimum	Maximum	Source
S	Storage coefficient	Dimensionless	0.01	0.20	Chow[d/], Table 13-1, p. 13-4
k	Permeability	gal/day/ft^2	10	100,000	Chow, Table 13-1, p. 13-8
b	Aquifer depth	feet	-	* 500	Depends on reservoir geometry
T	= kb, Transmissivity	gal/day/ft	*5,000	*a/ 20,000	Depends on permeability and aquifer depth
α	$\frac{-kb}{S}$, Diffusivity	gal/day/ft	-	-	Depends on other parameters
L	Aquifer width	feet	10	100,000	No basis. Goes to infinity for semi-infinite case
R	Perimeter	miles	*b/ 150	*c/1200±300	Depends on particular system geometry

* Values with an asterisk are specifically for Lake Mead.
a/ Personal communication, H. M. Babcock, USGS, WRD, Tucson, Arizona.
b/ Based on straight-line estimate of main water body including Overton arm.
c/ Personal communication, M. J. Clinton, USBR, Boulder City, Nevada.
d/ Chow, V. T., Handbook of Applied Hydrology, McGraw-Hill, 1964.

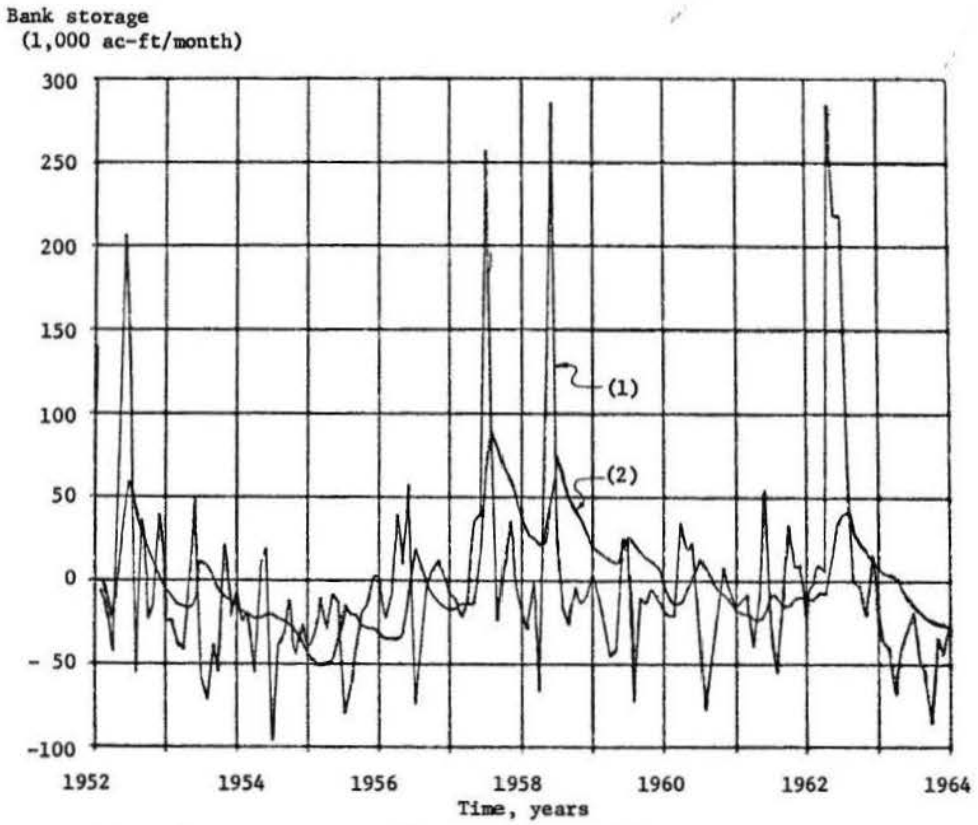

Fig. 6.5 **Bank storage computed by water budget (1), and by the semi-infinite aquifer model (2).**

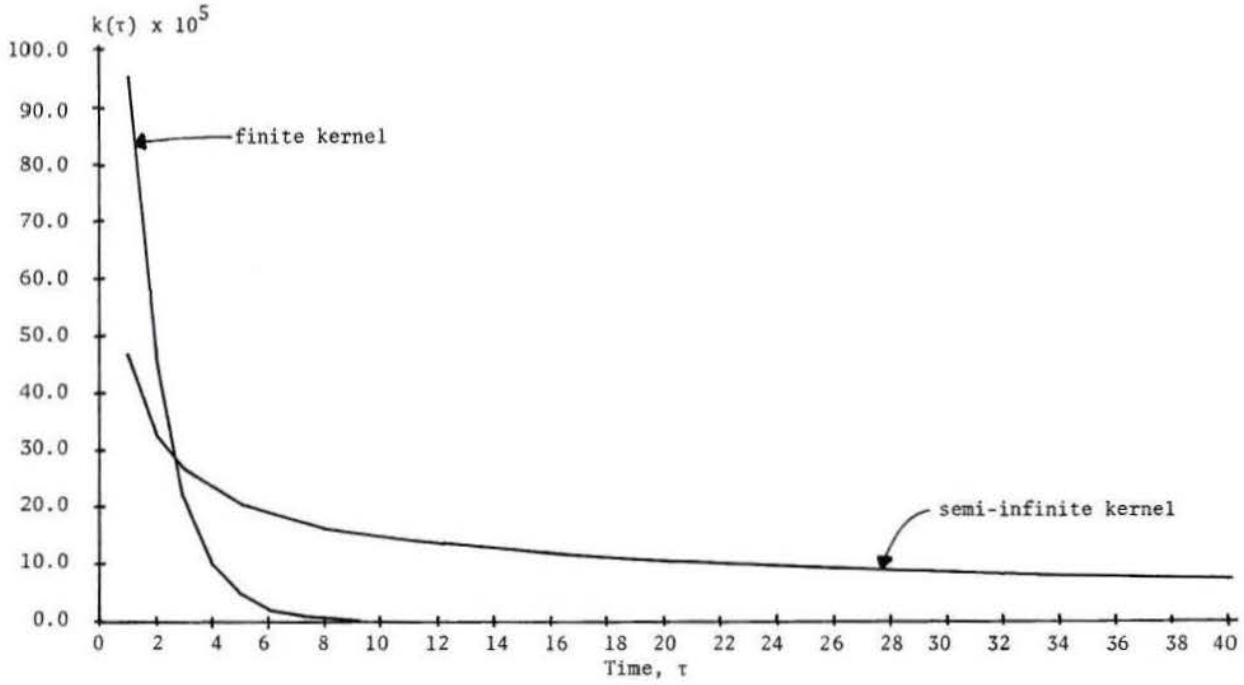

Fig. 6.6 Kernel functions for the ground-water convolution equation.

has high values at short lags, but decays more rapidly than the semi-infinite kernel. Figure 6.7 indicates the effect of truncating the number of terms in the convolution sum for the semi-infinite case. The finite kernel had negligible ordinates after about lag 10.

The correlations between predicted and observed bank storage were generally poor, never exceeding 4 = 0.4. The minimum standard error of estimate was not reduced below 40,000 to 50,000 acre-feet per month, which is on the same order as that found by the multiple linear regression.

Two conclusions can be inferred from this analysis of two approaches to modeling bank storage. First, the data were so contaminated by "noise" that it was nearly impossible to obtain a satisfactory model of

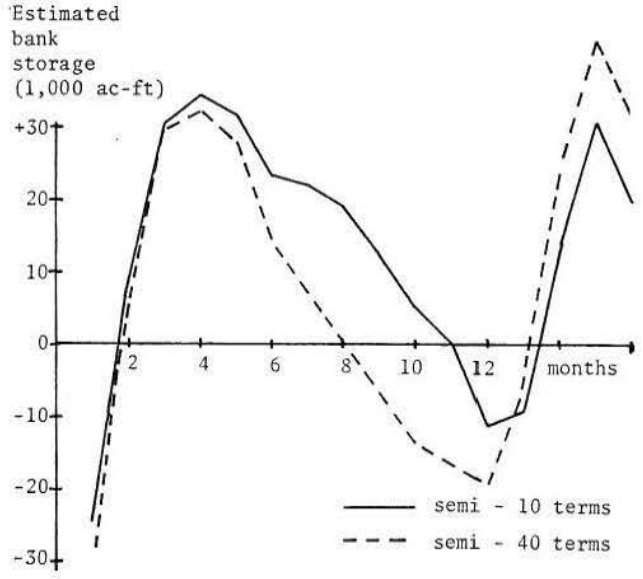

Fig. 6.7 Effect of number of terms in the convolution sum on estimated bank storage for the semi-infinite aquifer.

aquifer response for this system. The quantity of bank storage was estimated by taking sums and differences of several approximated quantities. By this procedure, errors could become quite large. Also, since the variance of a sum of variables includes the variance from each term, plus the non-zero covariance terms, the estimated quantity could have extremely large random fluctuations.

Secondly, based on statistical measures of goodness-of fit such as the coefficient of determination or standard error of estimate, the multiple linear regression approach was just as satisfactory as the convolution approach. However, the convolution model is advantageous since the aquifer properties can be used to produce an estimate of bank storage with no historic data. Application of the regression techniques requires data for parameter estimation. As a general procedure for estimating bank storage, the convolution model with the appropriate aquifer parameter values is recommended.

6.2 Salt Budget

The main purpose of analyzing the salt budget in this study was to confirm that valid estimates of the unmeasured salt quantities had been made. In essence, the salt budget is an exact parallel to the one for water except dissolved solids are accounted for instead of water. Figure 6.8 depicts the major quantities entering into a reservoir salt budget. If the budget can be balanced, it follows that all inputs and outputs have been properly evaluated. This type of budget can be calculated on a monthly basis so the salt mass stored in the reservoir can be traced over time. As this section will illustrate, accurately describing all the inputs and outputs is a very difficult task.

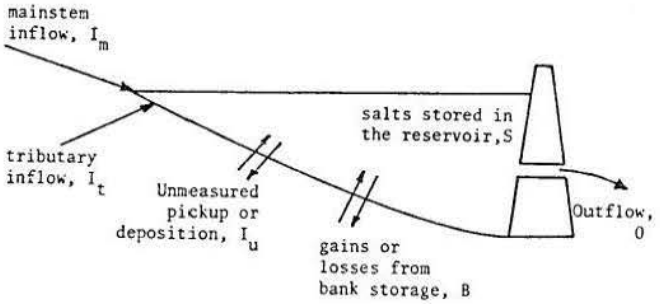

Fig. 6.8 Major components of a reservoir salt budget.

Inputs and outputs of dissolved solids may be balanced by the following budget of salt mass:

$$\Delta S = I_m + I_t + I_u + B - 0 \qquad 6.9$$

with ΔS the change of salt mass stored in the reservoir from period i to period i+1, I_u the unmeasured pickup or deposition, B the bank storage contribution, I_m the measured inflow of Colorado River, I_t the tributary inflow, and 0 the outflow.

The above salt budget describes the main factors for accounting for salt distribution in the reservoir system. The primary source of inflowing salt, I_m, was measured at the Grand Canyon station. Tributary salt inflow was less well defined. However, the main tributary was the Virgin River where salt load measurements have been made since 1941. The salt concentrations of the unmeasured inflows were used as discussed in Section 5.2.

In any reservoir system, there is opportunity for precipitation of salts out of solution, exchange of ions, and dissolution of minerals from sediment and earth of the reservoir bottom. Such a quantity, I_u, cannot be measured and must be estimated indirectly. The salts entering and leaving the reservoir as material dissolved in bank storage water, is another unmeasurable quantity which must be estimated indirectly. Salts leaving in the discharge through the reservoir outlet are readily calculated from the product of flow and concentration. As the reservoir volume changes, there will be a change in the salt mass stored, ΔS. This quantity is not directly measurable and must also be estimated from the salt budget calculation.

If all the unknown factors of the budget are grouped, the salt budget equation becomes:

$$I_m - 0 = \Delta S - B - I_u - I_t. \qquad 6.10$$

The approach used in this study to estimate the unknown quantities was to isolate them and attempt to explain their occurrence. Once a variable is estimated, it can be added on the left-hand side of the

budget equation. It is important, however, that the estimated quantity relates to some known or definable process and has a physical meaning. When all the deterministic quantities have been isolated, some unexplained residuals from a balanced system will undoubtedly remain. These result from processes not included in the model such as chemical reactions, thermal and chemical stratification, short circuiting of flows, or unmeasured salt in flows from tributaries. Hopefully these effects are random and comprise only a small part of the salt budget.

The approach described above was employed using the monthly salt quantities for Lake Mead. The first analysis included the Colorado and Virgin River salt inflows only and the outflows from Hoover Dam for the period 1942 through 1962. This period was selected to eliminate the initial filling period and the drawdown of the mid-1960's when Lake Powell was filling. A tabulation was made of salt inflows, salt outflows, the monthly difference between salt inflow and outflows, and the accumulated sums of these variables.

The overall result of this analysis was that more salt left the reservoir than entered it. In other words, the outflowing salt tonnage exceeded the incoming tonnage. This was anticipated since salts entering in the unmeasured tributaries were not included. Also, salt contributions from material dissolving out of the geologic formations surrounding the reservoir could add substantial tonnage. The accumulated salt defecit from 1942 to 1962 was over 8.8 million tons.

It has been estimated (54) that salt entered Lake Mead from 1935 to 1944 from salt beds flooded by surface storage. The net increase resulting from precipitation of silica and calcium carbonate and solution of calcium sulfate was estimated at around 10 million tons. Results from the salt bud et ran from 1942 indicated an overall excess of salt coming out of the reservoir of about 10 m llion tons by 1945. This reflects three mission components of the model: salts in surface storage, tributary inflows, and additions due to dissolved minerals. From 1945 to 1960, the descrepancy between salt inputs and outputs remained fairly constant, fluctuating between 9 and 13 million tons. However, in 1956 and 1957 when the reservoir was drawn down, the increased salt outflows caused the deficit to exceed 16 million tons. This peak salt deficit follows a period when reservoir storage was reduced by almost 10 million acre-feet and bank storage went down by about a million acre-feet.

The next step of the salt budget analysis was the inclusion of estimated salt inflows from all tributaries as described in Section 5.2. The salt budget equation was revised to

$$I_m + I_t - 0 = \Delta S - B - I_u. \qquad 6.11$$

The budget was run from 1935 to 1968 with tributary salts included as inputs. The difference between salt inflows and outflows was compared to an estimate of salt tonnage in storage computed from the product of reservoir storage (acre-feet) and outflowing salt concentration (tons per acre-foot). This was a fairly representative value since the concentration from 1941 to 1968 averaged 0.94 tons per acre-foot and had a standard deviation of about 0.09, indicating only a minor change.

As expected, the accumulated difference between incoming and outgoing salts rose rapidly to a peak in 1941. Since the reservoir was filling in this period, the estimated stored salts also increased to a maximum in 1941. From the peak in 1941, the difference between accumulated inflowing and outflowing salt decreased between 14 and 17 million tons. A peak in salt difference of over 19 million tons occurred in mid-1952, coinciding with a peak in stored water which had not occurred for the prior three years. From this peak until about March 1957 there was a continual reduction of the accumulated salt difference. This reduction is explainable due to the reservoir storage being the lowest since initial filling. From 1958 through 1961 storage returned to the level of the 1940's, but the salt difference between inf ows and outflows rose above past levels and reached a peak of over 23 million tons by the end of 1962.

Although there were intuitive explanations for changes in differences between salt input and output of the system, quantitizing the unknown salt inflows and outflows was a difficult task. The change in stored salt tonnage was estimated by the product of storage volume and concentration of the outflow. This could be in substantial error since the reservoir is not fully mixed throughout. At this point, the salt budget equation was written as

$$I_m + I_t - 0_m - \Delta S = -B - I_u. \qquad 6.12$$

The problem was to relate the quantities on the right to the residual calculated from the left-hand side. Salt dissolution from the flooded valley would be rapid while the reservoir filled for the first time, and cease either after sediments had covered the sources of salt or the material had been depleted. This suggests a function decaying from an initial value to near-zero such as an exponential. The equation

$$I_u = I_o e^{-kt} \qquad 6.13$$

was tried in the salt budget for several values of I_o and k. When k was chosen such that I_u died out in about 10 years, the outflowing concentration resembled the historic values better. Since this phenomenon occurs only when a reservoir is initially filled, it is not necessary in a long-term simulation model.

Several methods were tried to estimate the salt concentration of water entering and leaving the bank storage with limited success. It was found that a concentration equal to the mean reservoir concentration gave as good a result as more complicated estimates.

CHAPTER VII

MODELING OUTFLOW SALINITY CONCENTRATION

This chapter describes three approaches to modeling the concentration of dissolved solids in reservoir outflows. They are (1) multiple regression, (2) a mixing model, and (3) time series analysis. After each method is applied and discussed, the results are compared to indicate the merits and drawbacks of each method.

7.1 Multiple Regression Approach

Before describing the application of the multiple regression analysis to Lake Mead, the potential for spurious correlation between products or ratios of random variables will be discussed. In analysing data from several measurements such as lengths of body parts of animals or velocities in several directions or locations, it is a common practice to derive dimensionless ratios of variables or mathematical functions of variables and study relationships between them. The degree of the relationship is often measured by the correlation coefficient, r , or the coefficient of determination, r^2 . It is commonly accepted that a high value of r or r^2 indicates an underlying physical basis for the strong correlation. Unfortunately, in many cases, the high correlation does not truly reflect this. Instead, it results from using functions of variables and has been termed "spurious correlation".

The problem has been known for many decades as evidenced by Pearson's (39) early discussion of the correlation induced by using indices for comparing biological quantities and a later paper by Reed (42) giving expressions for spurious correlation of any two functions of variables. Pearson (39) provided the basis for uncovering more recent misinterpretation of correlations among ratios and products as discussed by Chayes (6), Benson (3), and Yevjevich (66). The above three references to spurious correlation are based on Pearson's original work and may be consulted for specific cases of ratios and products not discussed here.

Given four random variables, X_1, X_2, X_3, and X_4 with means, standard deviations, coefficients of variation (standard deviations divided by the mean), and correlation coefficients, m_i, s_i, c_i, and r_{ij} respectively, for i and j from one to four, the general relationship for the correlation between the ratios $Y = X_1/X_2$ and $Z = X_3/X_4$ is

$$r_{yz} = \frac{r_{13}c_1c_3 - r_{14}c_1c_4 - r_{23}c_2c_3 + r_{24}c_2c_4}{(c_1^2 + c_2^2 + 2r_{12}c_1c_2)^{\frac{1}{2}} \; (c_3^2 + c_4^2 - 2r_{34}c_3c_4)^{\frac{1}{2}}} \qquad 7.1$$

This is an approximate relationship which depends on powers of coefficients of variation greater than two being negligible (39:492). When coefficients of variation are large (such that powers and products over two are of magnitude similar to c_i^2 and c_ic_j), the expression above may be in substantial error.

Specific cases of correlations between such quantities as a ratio and its denominator or its numerator and two ratios with the same denominator or numerator have been handily tabulated by Benson(3) . He also gave similar results in tabular form for a variety of combinations of product terms. The relationship for the general case of product correlation (using the above notation with $Y = X_1X_2$ and $Z = X_3X_4$) was

$$r_{yz} = \frac{r_{13}c_1c_3 + r_{14}c_1c_4 + r_{23}c_2c_3 + r_{24}c_2c_4}{(c_1^2 + c_2^2 + 2r_{12}c_1c_2)^{\frac{1}{2}} \; (c_3^2 + c_4^2 + 2r_{34}c_3c_4)^{\frac{1}{2}}} \qquad 7.2$$

The total load, or mass movement of dissolved solids in a water body, is often used in salinity studies. This quantity is formed from the product of concentration and flow. For concentration in units of tons per acre-foot and flow in acre-feet per month, the units for load become tons per month. Spurious correlations result from correlation of the total salt load with streamflow. If X_1 is the dissolved solids concentration and X_2 the flow, then $W = X_1X_2$ is the load and $Z = X_2$ is the flow. The spurious correlation between W^2 and Z is

$$r_{wz} = \frac{r_{12}\,c_1 + c_2}{(c_1^2 + c_2^2 + 2r_{12}\,c_1\,c_2)^{\frac{1}{2}}} \qquad 7.3$$

with r_{12} the correlation between X_1 and X_2 , concentration and flow, $c_1 = s_1/m_1$, the coefficient of variation of concentration, and $c_2 = s_2/m_2$, the coefficient of variation of the flow. For the case of no correlation between concentration, X_1 , and flow, X_2 , r_{12} equals zero and the spurious correlation for $C_2 > C_1$ can be greater than 0.71 as shown by Benson (3:39). When these variables are analyzed, the potential for high correlation values seems obvious. In cases where flow varies more than concentration, i.e. has a greater coefficient of variation, the salt load will follow the flow very closely. Nothing will be learned from correlations of salinity load and flow except the trivial conclusion that high flows carry a greater total mass of salt than low flows.

The potential for high values of correlation coefficients resulting from the use of products or ratios of variables should alert the analyst to closely inspect the variables under study. He should be especially careful to understand that high correlations can result from spurious correlation as well as valid causative relationships.

In this study there is opportunity for correlation coefficients to be effected by combinations of variables. However, the results from regression analysis will not be used to infer a physical relationship between the variables. Also the standard error of estimate will be used to compare various prediction equations as well as the multiple regression coefficient.

Inspection of time series plots of reservoir storage and concentration of outflowing dissolved solids, Figures 5.5 and 5.6, indicates a general inverse relationship between concentration and volume, such as a linear mix model would produce. The mixing approach to estimating concentration is explored in Section 7.2. The approach followed in this section is to

hypothesize which variables bear on the phenomenon under study and use multiple linear regression analysis to determine the best relationship between the selected variables.

The first attempt at estimating outflowing concentration was a correlation with reservoir storage, inflowing concentration of the Colorado River, and monthly change in bank storage. Of these three "independent" variables included, reservoir storage was the most important. The analysis was run from 1944 to 1968 to minimize the effect of initial addition of salts to the reservoir. Table 8 gives the results. The correlation between downstream salt concentration and storage was fairly strong with $r = -0.69$ or $r^2 = 0.48$. Addition of the two remaining variables to the regression equation increased r^2 to 0.51 only. The standard error of estimate using the three variables was 0.06 tons/acre-foot. Evidently the mixing effect of reservoir storage has a greater bearing on outflow concentration than the inflow concentration for this example.

One reason for the low correlation between the upstream and downstream concentrations ($r = -.017$) is the lag and smoothing effect of storage. The cross correlogram of these two time series, Fig. 7.1, indicates a maximum correlation at a 17-month lag. Additional sets of "independent" variables were constructed from the inflow concentration time series by lagging individual values and summing groups of values to reflect the effect of detention in the reservoir.

The next multiple regression analysis included 9 such variables for the 1937 to 1968 and 1949 to 1968 period. The explanation of the variables is included with results in Table 9.

Table 8

Results of Multiple Regression Analysis of Lake Mead Salinity, 1944-1968

	Variable	Mean	Std. Dev.	Units
1.	Outflow TDS	0.940	0.088	Tons/ac-ft
2.	Volume	19872.	3531.	Thousands of ac-ft
3.	Inflow TDS	1.151	0.398	Tons/ac-ft
4.	Bank Storage	-1.45	29.85	Thousands of ac-ft per month

Correlation Matrix

Variable	1	2	3	4
1	1.00	-.69	-.17	-.02
2		1.00	-.01	.19
3			1.00	-.37
4				1.00

Stepwise Summary

Variable	r^2	Std. error of estimate
2	.48	.064
3	.51	.062
4	.51	.062

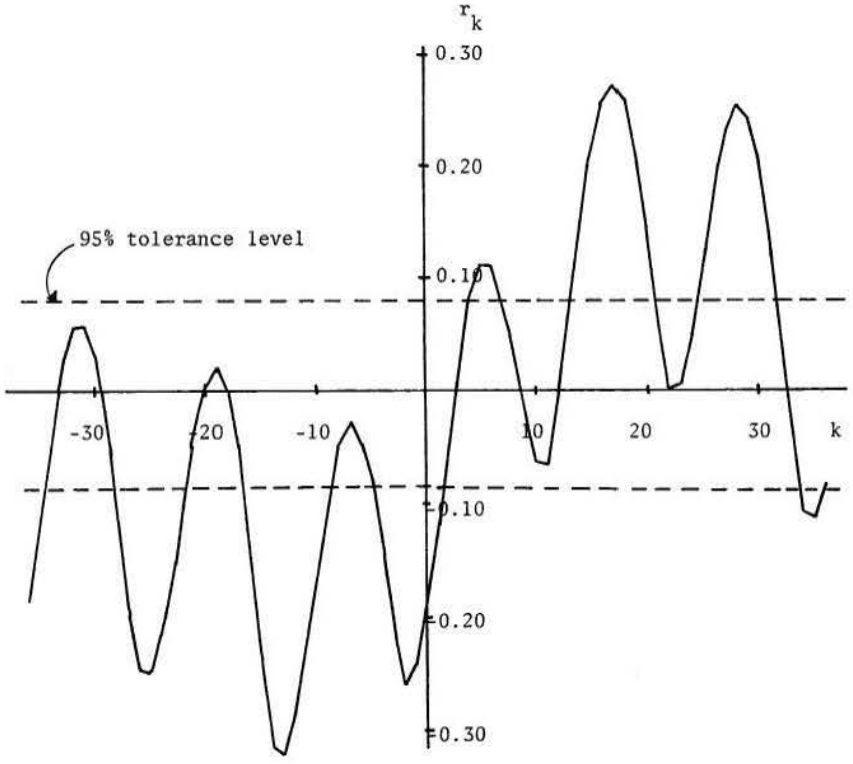

Figure 7.1 Cross correlogram of dissolved solids concentration of Colorado R. near Grand Canyon and below Hoover Dam.

Table 9

Results of Multiple Regression Analysis
of Lake Mead Salinity and Nine Variables, 1937-1968

Variable	Mean	Std. Dev.
1. Outflow concentration (tons/ac-ft)	.955	0.090
2. 17-mo lag inflow concentration	1.178	0.1417
3. Sum of lag 6-11 inflow concentration	7.004	1.589
4. Sum of lag 18-23 inflow concentration	7.054	1.598
5. Sum of lag 16-18 inflow concentration	3.533	1.090
6. Reciprocal of reservoir contents	0.00005	0.00001
7. Water inflow (1,000 ac-ft/mo.)	915.30	951.09
8. Water outflow (1,000 ac-ft/mo.)	855.19	281.36
9. Inflow concentration (tons/ac-ft)	1.159	0.410
10. Tributary salt tonnage (1,000 tons/mo.)	67.516	23.744

Correlation Matrix, 1937 to 1968

Var.	1	2	3	4	5	6	7	8	9	10
1	1.00	.31	.07	.16	.34	.50	.11	-.34	-.16	.15
2		1.00	-.07	.01	.98	.12	.33	.11	-.43	.05
3			1.00	.73	-.05	-.10	.18	-.06	-.05	-.07
4				1.00	.13	-.15	.23	.03	-.16	-.06
5					1.00	.13	.37	.12	-.47	.08
6						1.00	-.20	-.50	.02	.02
7							1.00	.24	-.74	.24
8								1.00	-.08	.06
9									1.00	-.11
10										1.00

Correlation Matrix, 1949 to 1968

Var.	1	2	3	4	5	6	7	8	9	10
1	1.00	.27	.04	.22	.30	.76	.03	-.42	-.15	.03
2		1.00	.01	.10	.98	.13	.29	.23	-.36	-.03
3			1.00	.69	.03	-.02	.14	.02	.03	-.09
4				1.00	.14	-.03	.18	.00	-.12	-.03
5					1.00	.15	.32	.25	-.39	-.01
6						1.00	-.21	-.43	-.01	.05
7							1.00	.30	-.67	.18
8								1.00	-.07	.08
9									1.00	-.06
10										1.00

Stepwise Summary

Variable Added		r^2		Std. error of est.	
'37-'68	'49-'68	'37-'68	'49-'68	'37-'68	'49-'68
6	6	.25	.57	.078	.063
5	4	.32	.63	.074	.059
4	3	.37	.66	.071	.057
8	7	.40	.68	.070	.055
10	8	.42	.70	.069	.053
3	5	.42	.72	.069	.051
7	9	.43	.73	.069	.051
9	10	.43	.73	.069	.051
2	2	.43	.73	.069	.051

The simple correlation matrix indicated the relative importance of each variable to downstream concentration. The reciprocal of reservoir contents had the highest simple correlation coefficient in both sets and was the first variable chosen for multiple regression. It is interesting to note that the standard errors of estimate at this point were 0.078 and 0.063 tons per acre-foot in comparison to the standard deviation of the dependent variable of 0.090. The next variable selected was the sum of concentrations from 16 to 18 lags for 1937 to 1968 and from 18 to 23 lags for 1949 to 1968. This combination was chosen over the 17-month lagged concentration alone in both cases. Although the final coefficient of determination for 1937 to 1968 was $r^2 = 0.48$, the standard error of estimate had not been significantly improved. Also, since several variables were correlated, inclusion of all 9 in a regression equation is not recommended. By dropping off the first 14 years of reservoir operation, the multiple regression relationship was significantly improved. Quite a shift in relative importance of the independent variables also occurred. In both cases the last variable included was the inflow dissolved solids concentration 17 months earlier.

The multiple regression approach was further refined by evaluating the correlation between various combinations of salt loads in thousands of tons from the past with outflow concentration. Six such combinations covering inflow salt lags up to two years were analyzed. The results indicated the load variable including months 15 through 24 in the past was most important whereas shorter groupings of loads were not as significant. This result indicates that inputs to the reservoir measured at the Grand Canyon station have their greatest effect on the output from one to two years in the future. This is consistent with the 17-month lag found in the cross-correlogram of input and output dissolved solids concentration. Figure 7.8 shows a maximum correlation between load input and concentration output at about 17 months. Another attempt at improving the regression model incorporated reservoir contents and input concentration and input load lagged to correspond to maximum values from the cross-correlograms. The multiple regression results again placed most weight on reservoir contents, which alone explained about 23 percent of the outflow concentration variance for 1938 to 1967 data. With all variables included, the multiple correlation coefficient was 0.64, and the standard error of estimate was about 0.07 tons per acre-foot. This indicated little gain from the previous set of lagged variables. Apparently, lagging the inflowing salt load to correspond with the lag of maximum cross-correlation coefficient does not substantially improve the regression relationship.

A final analysis was made using data from 1956 to 1967 and the most important variables from the past runs. The variables used and results are given in Table 10.

The stepwise summary indicated little to be gained by adding more than three variables to the regression equation. Using the most important variables, the equation for predicting salinity in the release is

$$C_s = 0.6485 - 0.0001128 \times L + 0.018205 \times T_1 + 4073.1538 \times V^{-1} \qquad 7.4$$

With C_s the concentration of TDS in the outflow, L_1 the average inflowing load over months 13 to 21 in the past, T_1 the sum of dissolved solids concentration from months 24 to 31 in the past, and v the reservoir contents. With a multiple correlation coefficient of 0.82 and a standard error of 0.054 tons per acre-foot, Eq. 7.4 is recommended as a prediction equation for the concentration of dissolved solids in flows out of Lake Mead.

7.2 Mixing Model Approach

In accordance with the general reservoir circulation pattern described in Chapter III, several attempts were made to model the mixing and time lag of inflows. A study was first made to quantify more precisely the time required for inflows to have an effect on outflow. The cross-correlograms of Figs. 7.1 and 7.8 both indicate an average flow-through time of approximately 17 months. This time depends on the storage volume, and is also a random variable like all other reservoir quantities. As another estimate of this, the end-of-the-month reservoir contents were divided by monthly flow for the 1935 to 1968 period. The average was 41 months, or just under 3-1/2 years. Each monthly detention time estimate was then adjusted by the factor 17/41, or 0.41, to produce an average of 17 months. The resulting distribution of time lags was very interesting. As Fig. 7.2 shows, at least a third of the lags were less than one year and almost a fifth were less than six months. This indicates that the largest flows in the spring could possibly reach the outlet in only two or three months. The smallest inflows, on the other hand, might not affect the outflow for over two years.

This result was used to formulate a mixing model that reflected the movement and mixing of water entering the system. The mechanics of mixing and the time to reach the outlet were varied monthly depending on the inflow rate. This was accomplished by accumulating past inflows until a volume equivalent to the effective volume of the reservoir had entered the system. The effective volume was taken as 40 percent of the actual contents, equivalent to the ratio 17/41 from the lag time study. Inflowing loads prior to this time were then added and mixed until a volume equivalent to the effective volume was included. The outflowing concentration was then equal to that of this mixture, or the load divided by the effective volume. Since outflow concentration data indicated the spring inflow reached the outlet the following November, the concentration for November was calculated by the above procedure. Through the winter and spring months the mixture for November was mixed with the entire volume of reservoir water in an attempt to model the winter turnover. This process was reflected by weighing various linear combinations of salt loads and water masses of past inputs with the quantities calculated for November. For the summer months it was assumed that the outflow concentration would be a mixture of inflows over a year's time beginning 6 to 8 months in the past. Several other similar methods of representing this lag were tried.

The results of many attempts to incorporate the missing pattern into a quantative model gave poor results. The correlation coefficients between predicted and observed concentrations were only around $r = 0.55$ and the standard errors of estimate were about 0.16 tons per acre-foot.

In view of the limited success of these attempts to reproduce the behavior of mixing in the reservoir by a complex model, a simpler approach was tried. A straightforward mass balance on salts in the reservoir

TABLE 10

Results of Multiple Regression Analysis of
Lake Mead Salinity, 1956-1967

Variable	Mean	Std. Dev.	Units
1. Average of lag 13-21 inflow salt load	730.083	251.246	10^3 Tons/mo.
2. Sum of lag 13-20 inflow concentration	9.390	1.897	Tons/ac-ft
3. Sum of lag 24-31 inflow concentration	9.739	1.648	Tons/ac-ft
4. Reciprocal of reservoir contents	5.473×10^{-5}	1.146×10^{-5}	$(10^3$ ac-ft$)^{-1}$
5. Sum of lag 16-18 inflow concentration	3.537	1.081	Tons/ac-ft
6. Monthly reservoir release	727.001		10^3 ac-ft
7. Concentration of TDS in release	0.966	0.093	Tons/ac-ft

Correlation Matrix

Variable	1	2	3	4	5	6	7
1	1.00	-.527	-0.018	-0.525	-0.399	0.048	-0.574
2		1.00	0.415	0.231	0.831	0.217	0.447
3			1.00	0.167	0.414	0.155	0.412
4				1.00	0.171	-0.339	0.716
5					1.00	0.289	0.355
6						1.00	-0.194
7							1.00

Stepwise Summary

Variable added	r^2	Std. error of Estimate
4	0.51	0.065
3	0.60	0.059
1	0.67	0.054
6	0.67	0.054
2	0.68	0.054
5	0.68	0.054

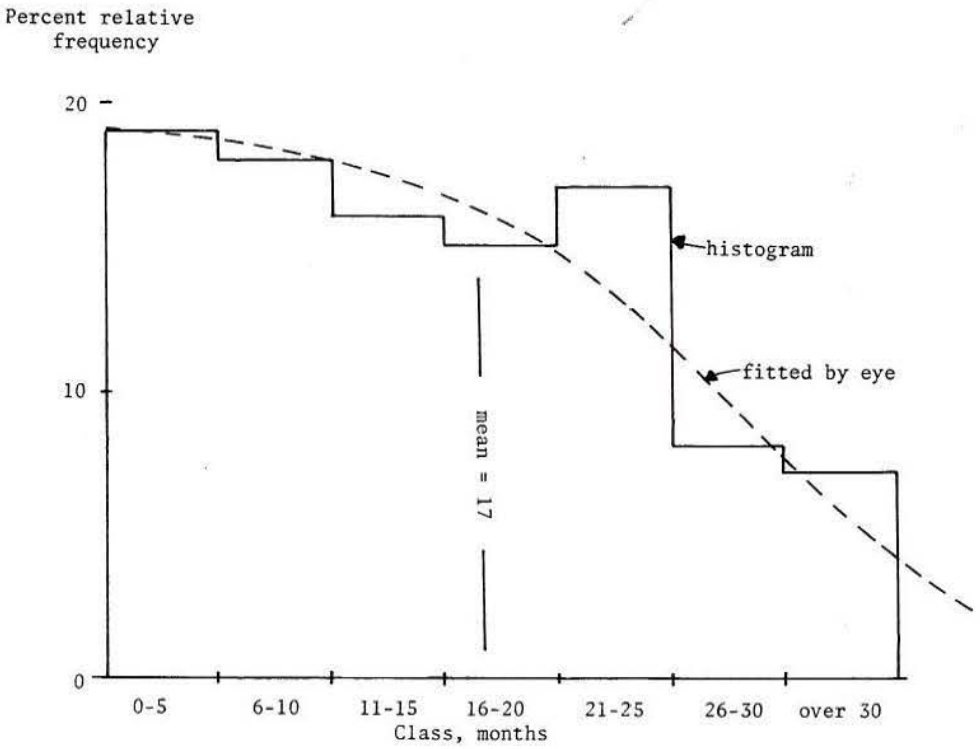

Fig. 7.2 Distribution of adjusted detention times for Lake Mead inflows.

was used to estimate the tonnage in storage in any month. This tonnage was the accumulation of salt entering minus the salt leaving. The outflow concentration was the ratio of the tons of salt in the system divided by the monthly reservoir contents. Salts leaving the system were calculated as the product of discharge and estimated concentration. Since the actual reservoir content was used as the diluting volume, evaporation was indirectly accounted for. The results of this analysis were very good. For the 1935 to 1968 period, the mean salinity was predicted at 0.962 tons per acre-foot compared to a value of 0.952 calculated from the data. The correlation between predicted and historic concentration values was r = 0.78, and the standard error of estimate was 0.081 tons per acre-foot. The model followed the extreme changes such as the 1955-1956 and 1965-1966 rises in concentration quite well as Fig. 7.3 shows. Although this model is simple, the main factors and processes governing reservoir behavior are incorporated in its structure. It also has an implicit self-correcting property. When outflow concentration is overestimated, salt output is also overestimated, bringing subsequent approximations back to the proper level.

7.3 Time Series Analysis

In this section, Fourier and spectral analysis are used to investigate the periodic structure of inputs, outputs, and system behavior. The first part presents results obtained from analyzing annual periodic components of salinity load inputs and concentration outputs. Spectral analysis is employed later in this section to investigate the system structure over the frequency range from zero to 0.5 cycles per month. The use of the gain function is explored and results are shown for two sets of data.

Analysis of cyclic components for seven different time periods during 1941 to 1968 was used to compare historical results with the theoretical mixing model predictions based on the completely mixed model structure of Section 4.4. These seven periods were selected to represent stable conditions over short time spans as well as average conditions over many years. Fourier analysis of the salinity input load at Grand Canyon and the dissolved solids concentration of outflows are presented in Tables 11 and 12. The 12-month harmonic was isolated for these calculations since it was the most significant for all the periods used. The columns of the tables follow the Fourier analysis coefficients of the equations

$$x(t) = \bar{x} + A \cos \omega t + B \sin \omega t, \qquad 7.5$$

$$x(t) = \bar{x} + C \cos (\omega t + \phi), \qquad 7.6$$

$$C = \sqrt{A^2 + B^2}, \qquad 7.7$$

$$\phi = \tan^{-1} (B/A). \qquad 7.8$$

Although the explained variances of the inflowing salt load indicate the annual period is not significant for most cases, some periodicity is definitely apparent in certain years. The annual cycle in the 1961 to 1963 period is least significant. This is due to the closure of Lake Powell upstream. In the other periods, the annual cycle explains from 25.5 to 62.2 percent of the original variance. Thus, the cyclic model can be used to reflect a large portion of the structure of the inflowing salt load. The annual component of the concentration of dissolved solids in the outflow is not significant for any of the time periods studied. Again, this component varies in magnitude for different periods. For the 1941 to 1968 data, it is essentially non-existent. However, in other periods it explains up to 48.7 percent of the original variance.

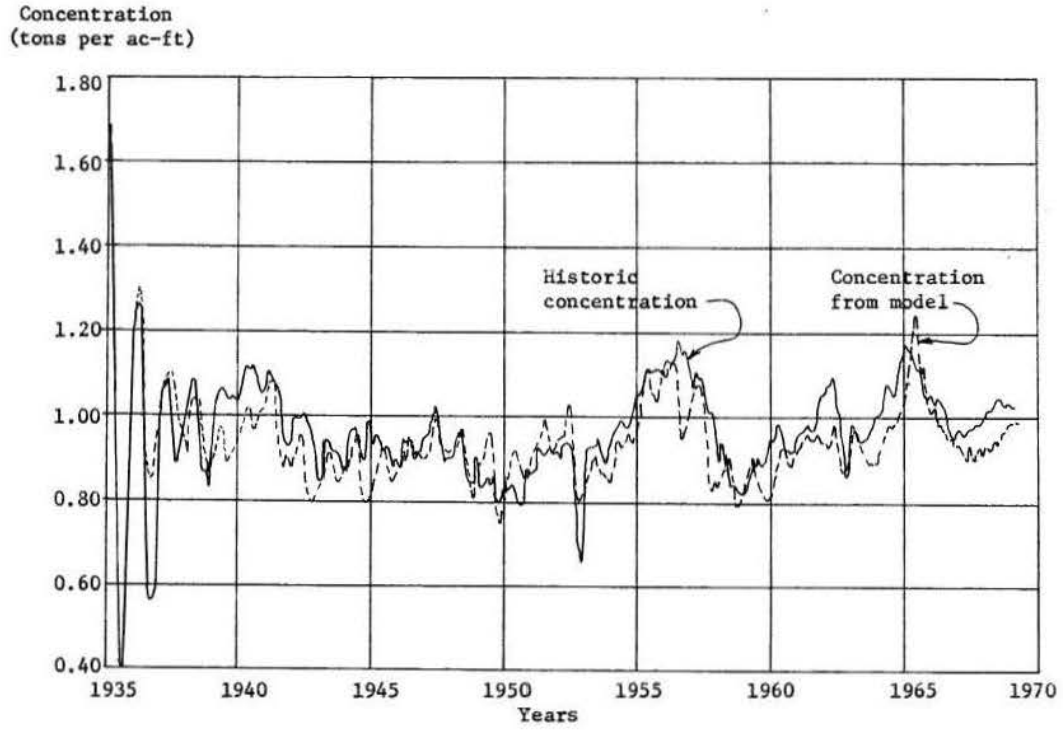

Fig. 7.3 Historic and estimated dissolved solids concentration of Lake Mead outflow.

Table 11

Fourier Analysis of the Salt Load
of the Colorado River near Grand Canyon

Period	Mean (10^3 T/month)	Variance	A	B	C	ϕ (deg.)	Percent variance explained a/
1945-1947	837	97700	- 308	- 78	318	194	51.7
1941-1950	878	161220	- 368	52	371	172	42.7
1948-1950	848	140380	- 395	139	418	161	62.2
1955-1956	611	50600	- 196	93	217	155	46.5
1961-1963	593	174750	- 128	45	136	161	5.3
1966-1968	627	34840	- 169	112	203	147	59.1
1941-1968	761	169720	- 286	67	294	167	25.5

a/ Values exceeding 61.6 are significant (67:76).

Table 12

Fourier Analysis of the Concentration of Dissolved Solids, C_s, below Hoover Dam

Period	Mean	Variance	A	B	C	ϕ (degrees)	Percent variance explained a/
1945-1947	0.923	0.0010	- .0168	.0121	.0207	144	21.4
1941-1950	0.918	0.0047	- .0172	.0264	.0315	128	10.6
1948-1950	0.856	0.0025	.0014	.0325	.0325	87	21.1
1955-1956	1.116	0.0017	- .0314	- .0259	.0407	219	48.7
1961-1963	.934	0.0010	- .0054	.0201	.0208	105	21.6
1966-1968	.959	0.0021	- .0054	.0043	.0069	142	1.1
1941-1968	.943	0.0076	- .0146	.0183	.0234	129	3.6

a/ Values exceeding 61.6 are significant (67:76).

The phase angle of the input and output series is interesting. For the inflowing salt load, the phase ranges from 147 to 194 degrees, or roughly six months. All the periods show this quite consistently. In contrast, the phase of the outflowing concentration series is highly variable, ranging from 87 to 219 degrees, or from three to seven months. This indicates a random mechanism which lags movements of water through the reservoir.

Equation 4.63 in Section 4.4 gave the concentration of salts in the outflow in terms of a constant load, flow, and time. Under steady-state conditions, the exponential term, exp (-t/T), approaches zero and concentration becomes equal to the ratio of load to flow. When this is calculated for the various periods in Table 13, the concentration values are all less than the historic ones. The reason for this is that the mixing model does not account for water loss by evaporation. From Fig. 5.4, the average monthly evaporation was about 70,000 acre-feet. When the concentration is adjusted by this factor, the values compare favorably with historic data. This comparison illustrates the applicability of a model based on the assumption of a completely mixed reservoir and steady-state conditions. Thus, for predicting the average concentration coming out of a reservoir, the ratio of the average salt load to the average flow adjusted for evaporation would work well.

The ratio of the amplitudes of input load and output concentration was tabulated in the column headed "Gain from data." The "Gain from model" was calculated from the system gain function, A_j , of Eq. 4.74 using the mean contents and detention time as tabulated.

Good agreement between the two gain values again indicates successful application of the model of the completely mixed reservoir. The gain for annual components can be predicted accurately if the system is close to steady-state behavior.

It is important to keep in perspective the order of magnitude of the quantities being investigated. The first step in the model resulted in a mean concentration value which was at most 10 percent in error when corrected for evaporation. The gain from input to output represents the change in amplitude of periodic fluctuations which are superimposed on the mean values. The size of this component of the output is insignificant when compared to the mean. For example, the 1941 to 1968 average concentration in the outflow was 0.94 tons/acre-feet. The amplitude of the yearly periodic component was only 0.0234 tons/acre-foot in that period. This is within the accuracy of the data itself. As the spectral analysis will show, the reservoir dampens out essentially all periodic components, leaving the output composed mainly of an average value with Markovian fluctuations added. Time lags and phase shifts of inputs are less well defined and appear greater by about three to four months than the theoretical values. Apparently, the time lag from the point of measured inflow to the outlet is highly variable. It undoubtedly changes with reservoir contents and rate of inflow. This is very likely and was pointed out in the discussion of reservoir circulation patterns.

The above analysis used the annual component of reservoir inputs and outputs to illustrate the gain function. Results of the complete spectrum of inputs, outputs, and the gain function will now be discussed.

The original data were first used to estimate spectra for inflowing and outflowing dissolved solids concentrations from 1935 to 1969. The input spectra, in Fig. 7.4, shows peaks at twelve and six-month periods, as well as some significant low-frequency variance. The 1935 to 1969 downstream dissolved solids spectrum in Fig. 7.5 shows peak variance in the frequency range below 0.05 cpm. A significant variance density at 0.083 cpm indicates strong annual periodicity in both series. However, when 1935 to 1940 data are removed, this component is no longer significant on the output as Fig. 7.7 illustrates. The periodicity in 1935 to 1940 data was very strong since the dampening effect of the reservoir was minor. The 1941 to 1968 dissolved solids spectrum in Fig. 7.7 is almost entirely composed of low frequency variance. The load spectrum of Fig. 7.6 shows periodicity in the

Table 13

Means, Amplitudes of Annual Periodic Components, Gain, and Phase for Selected Periods from 1935 to 1968

Period	Mean inflow (1,000 AF/mo)	Mean load (1,000 tons)	Mean contents (1,000 AF)	Detention time (months)	C_s from model (T/AF)	C_s from model adjusted for evaporation (T/AF)	Historic TDS (T/AF)
1945-1947	989	837	21,650	22	0.85	0.92	0.92
1941-1950	1,100	878	23,000	21	0.80	0.86	0.93
1948-1950	1,070	848	22,500	21	0.79	0.86	0.86
1955-1956	670	611	14,200	21	0.91	1.01	1.12
1961-1963	673	593	21,400	32	0.88	0.97	0.93
1966-1968	712	627	17,000	24	0.88	0.97	0.96
1941-1968	910	761	20,000	22	0.84	0.90	0.94

Period	Amplitude of load input	Amplitude of C_s Output	Gain from model ($\times 10^{-5}$)	Gain from data ($\times 10^{-5}$)	Input phase angle (degrees)	Output phase angle (degrees)	Phase shift from data (degrees)	Theoretical phase shift (degrees)
1945-1947	318	0.0207	8.3	6.5	194	144	310	85 or 445
1941-1950	371	0.0309	8.2	8.3	128	172	44 or 404	85 or 445
1948-1950	418	0.0325	6.1	7.8	161	87	286	85 or 445
1955-1956	217	0.0407	13.4	18.8	155	219	64 or 424	85 or 445
1961-1963	136	0.0208	8.9	15.3	161	105	304	87 or 447
1966-1968	203	0.0069	11.2	3.4	147	142	355	85 or 445
1941-1968	294	0.0234	9.5	18.6	167	129	322	85 or 445

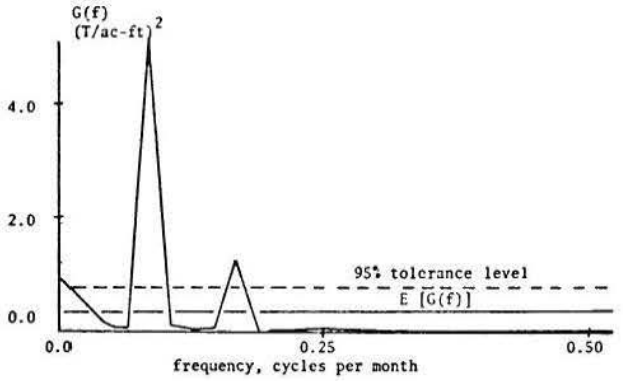

Fig. 7.4 Spectrum of dissolved solids of the Colorado River near Grand Canyon, 1935 to 1969.

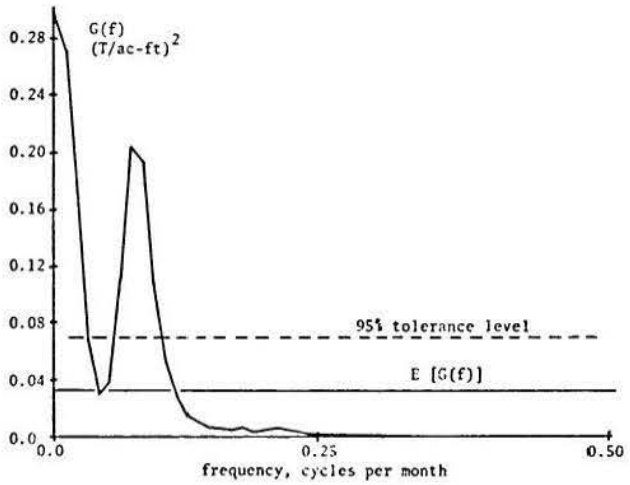

Fig. 7.5 Spectrum of dissolved solids of the Colorado River below Hoover Dam, 1935 to 1969.

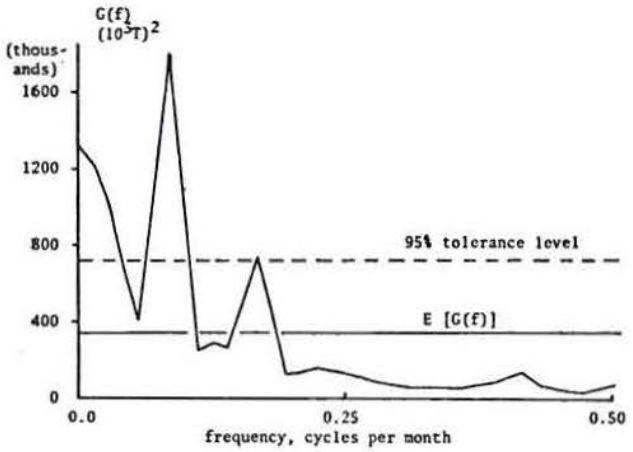

Fig. 7.6 Spectrum of salt load for the Colorado River near Grand Canyon.

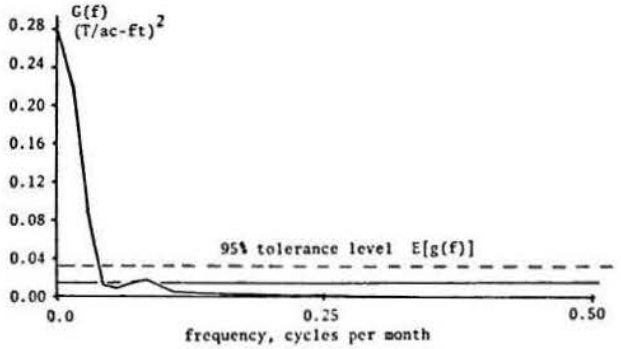

Fig. 7.7 Spectrum of dissolved solids of the Colorado River below Hoover Dam, 1941 to 1968.

data at twelve and six months, as well as considerable low frequency variance. These two spectra indicate the dampening effect of the reservoir on periodic inputs. Both six- and twelve-month cyclic patterns of load and concentration entering the system are almost completely obliviated in the dissolved solids output. The spectrum of Fig. 7.7 shows no trace of any six-month periodicity. A minor peak is displayed in the frequency range corresponding to an annual cycle. However, this peak is not statistically significant. It is also worthwhile to note the shift in density toward the extreme low-frequency end of the scale between Figs. 7.6 and 7.7. The smoothing effect of reservoir storage on fluctuations of salinity is evident.

The cross-correlogram of load and dissolved solids in Fig. 7.8 indicates an inverse relationship between load and concentration. This is as expected since the load indicates inflowing water to the system as well as concentration. Since concentration is nearly constant, a high load reflects a large water volume diluting the salt mass in the system. The maximum negative correlation occurs at about 17 or 18 months. However, the cross-correlation function is fairly smooth in this region, indicating longer and shorter lags are also important. Since both series are periodic, absolute values of the tolerance level are not meaningful. The negative correlation at about 17 months indicates a high inflowing salt load will be followed 17 months later by a low salinity concentration downstream. If a simple correlation between salt inflow and salinity outflow were made, only about 10 percent of the variance in the original series would be explained using the 17-month lag.

The system gain function, $|H(f)|$, is shown in Fig. 7.9. The theoretical gain computed from the model of a completely mixed reservoir with average values of flow and volume for 1941 to 1968 is also shown. This comparison illustrates good agreement between observed and predicted behavior of the reservoir. Despite the stratification and seasonal segregation of inflows, the system evidently mixes completely before outflows are released. The gain function reflects the changes observed in the spectra of inputs and outputs as well

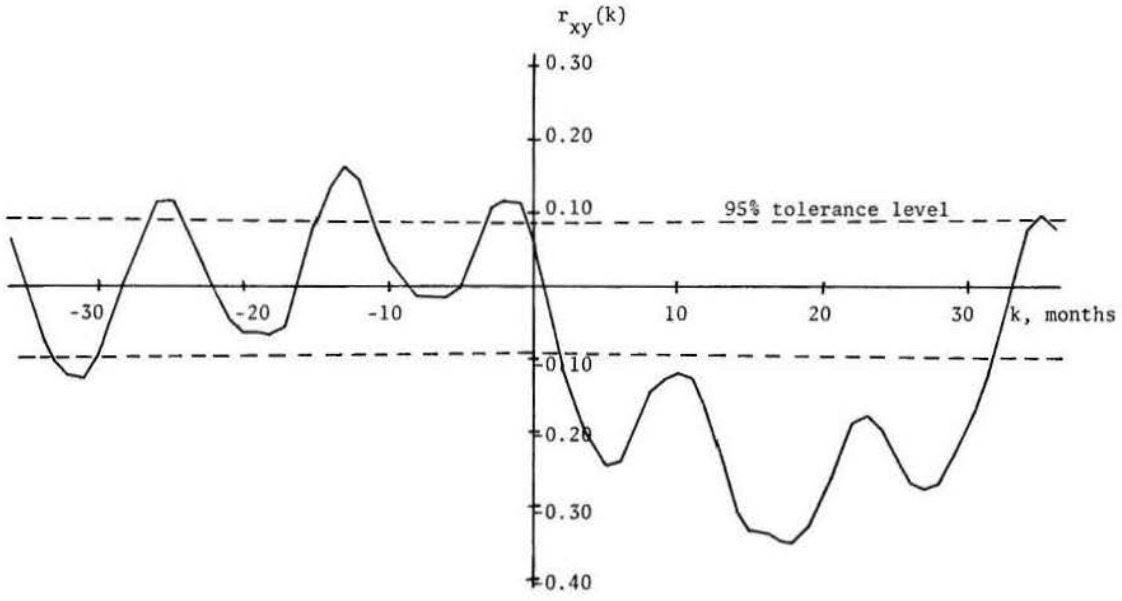

Fig. 7.8 Cross-correlation of inflowing salt load and outflowing dissolved solids, 1941 to 1968.

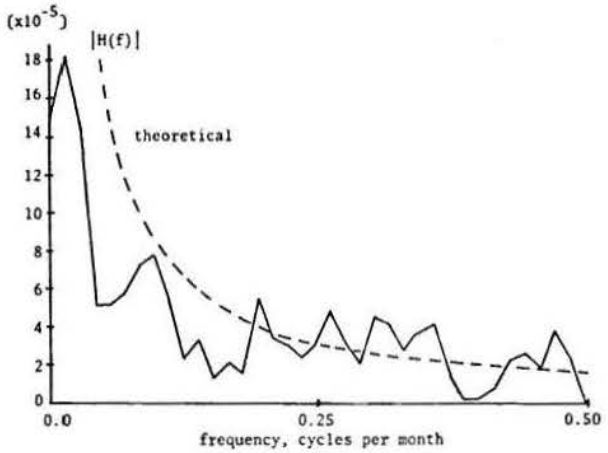

Fig. 7.9 Gain function of inflowing salt load and outflowing dissolved solids, 1941 to 1968.

as the results of Table 13. High frequency oscillations are dampened out whereas the low frequency components are passed with much less attenuation and impart a high dependence to the output sequence. The very small vaules of the gain function (on the order of 10^{-4}) indicate the extreme dampening of amplitudes of periodic components as inflows transverse the reservoir.

The phase function for 1941 to 1968 data in Fig. 7.10 does not show a smooth change with frequency. However, the average value, 3.16 radians, corresponds to an average lag of six or equivalently 18 months which is indicated by the cross-correlogram. For the system under study, phase analysis as discussed in Section 4.4 of Chapter IV does not appear applicable. This results from the flow and storage volume being periodic and changing over time which the model does not consider.

The analysis of load as the system input and dissolved solids as output was pursued as suggested by the mixing model structure of Section 4.4. Significant periodic components were removed from the 1941 to 1968 data. The load generally contained one or two significant harmonics whereas the concentration series was nearly aperiodic. The Fourier analysis was used to estimate the periodic components of each time series. The residual series of the difference between the data and the fitted function was standardized to have a mean of zero and unit variance. The spectra then have an expected value of the variance density equal to 2.0.

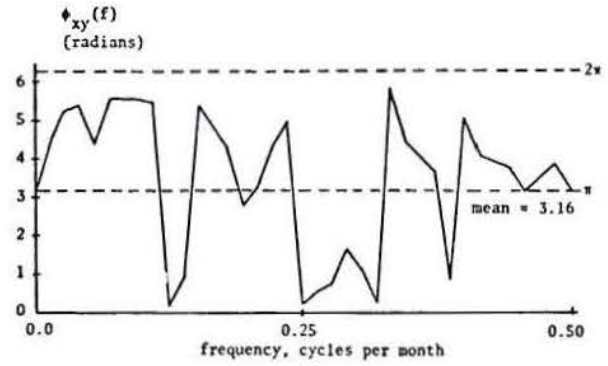

Fig. 7.10 Phase function of inflowing salt load and outflowing dissolved solids, 1941 to 1968.

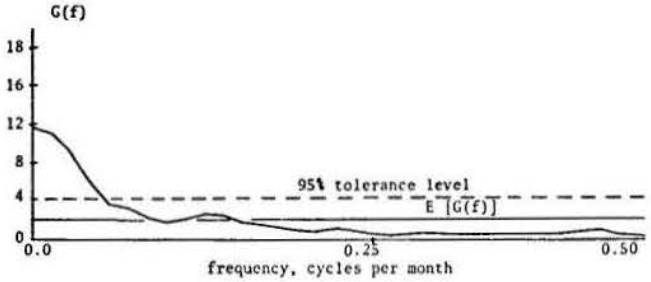

Fig. 7.11 Spectrum of residuals from the Fourier analysis of inflowing salt load, 1941 to 1968.

The spectra of the residuals from the Fourier analysis illustrated in Figs. 7.11 and 7.12 indicate no significant periodic components remain in either series as expected. Most of the variance occurs in frequencies with periods greater than two years. This shape is characteristic of a highly dependent Markovian type of process illustrated previously in Fig. 4.1. The gain function, Fig. 7.13, shows greatest attunuation at high frequencies and passes more variance at the low end of the spectrum. The value of the gain function is less than one at all frequencies. This indicates that periodic fluctuations of the input series are attenuated by the reservoir.

Correlograms of the residual load and dissolved solids series were plotted for both periods in Figs. 7.14 and 7.15. As suspected, a high serial correlation among consecutive points was found. The first-order Markov model apparently fits both processes well. The first serial correlation coefficient for the 1941 to 1968 salt load is 0.62. Thus, a first-order Markov model of this series would explain over 36 percent of the variance. For the output of 1941 to 1968, r_1 is 0.93 and a Markov model would explain over 81 percent of the variance in the residual series.

The cross-correlogram of Fourier residuals in Fig. 7.16 retains the general shape found in the original series. However, the minor lobes at twelve-month intervals have been removed. It appears that load inputs from 2 to 32 months affect the output concentration. This indicates a mixing process which extends over a period of at least two years.

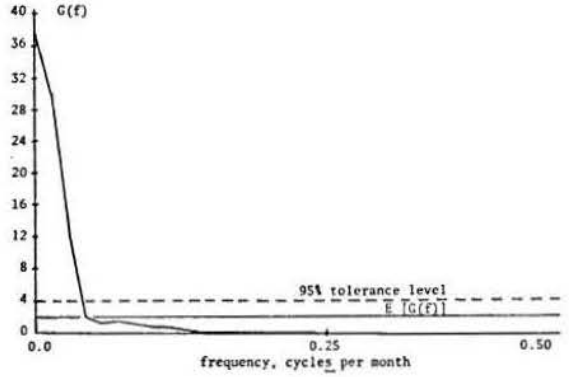

Fig. 7.12 Spectrum of residuals from the Fourier analysis of outflowing dissolved solids, 1941 to 1968.

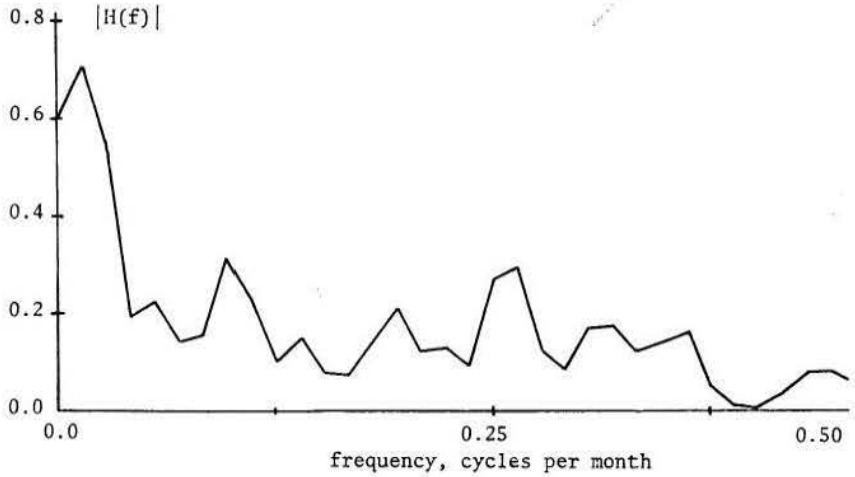

Fig. 7.13 Gain function of residuals from the Fourier analysis of inflowing salt load and outflowing dissolved solids, 1941 to 1968.

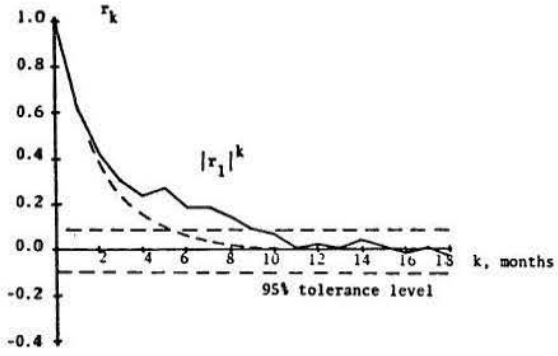

Fig. 7.14 Correlogram of residuals from Fourier analysis of inflowing salt load, 1941 to 1968.

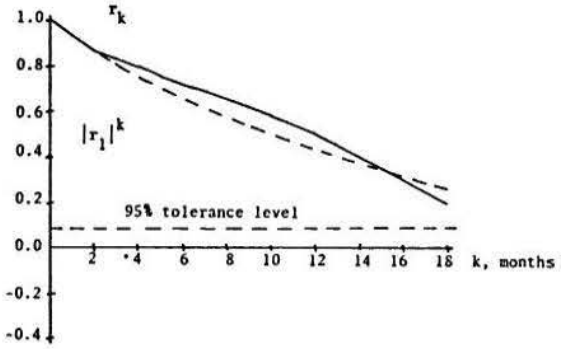

Fig. 7.15 Correlogram of residuals from Fourier analysis of outflowing dissolved solids, 1941 to 1968.

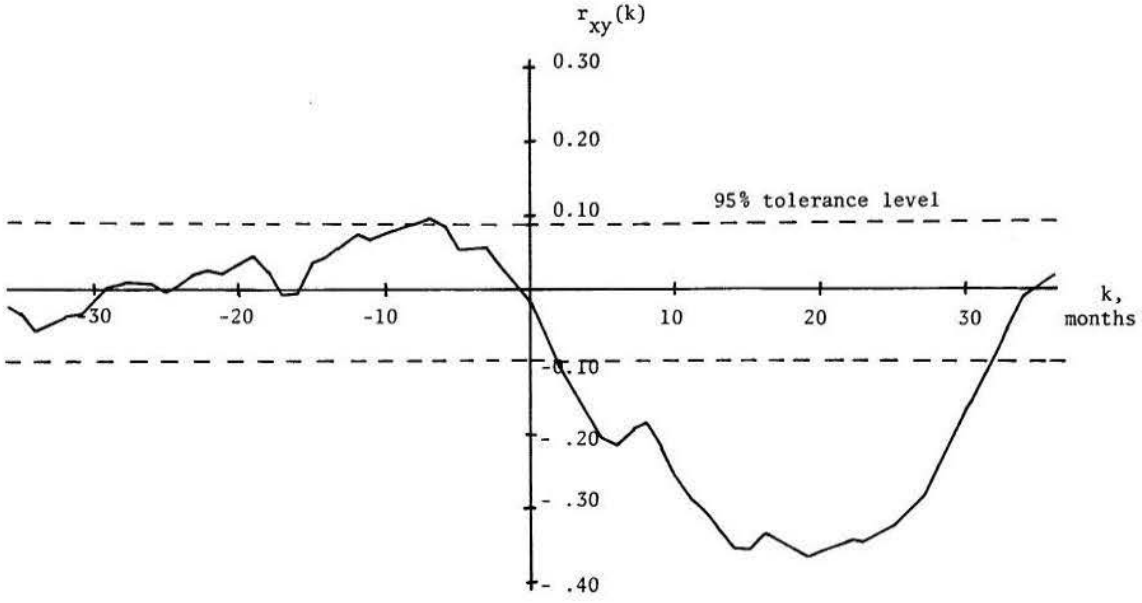

Fig. 7.16 Cross-correlogram of residuals from Fourier analysis of inflowing salt load and outflowing dissolved solids, 1941 to 1968.

The final time series analysis was to inspect the residuals from a first-order Markov model. They were calculated by

$$y_i = x_i - r_1 x_{i-1}. \qquad 7.9$$

Spectra of these residuals are plotted in Figs. 7.17 and 7.18. In both cases, no periodic components were found, indicating the residuals were completely random. Removal of first-order dependent component of the residual series reduced the large portion of variance previously associated with low frequencies. This shows that both the input and output time series represent processes with a strong dependence on past values. That is, a high value of load will tend to follow a previous high value. This memory property is more pronounced in the output series. The mixing process within the reservoir in largely responsible for this. Apparently "events" entering the reservoir are mixed or averaged together as the water moves to the outlet. Thus the concentration of the outflow in any one month will have properties which have been influenced by the quality from several months earlier and later. The gain function of Fig. 7.19 shows no particular pattern, indicating the random transfer of inputs through the system. Again, the gain value is less that one, indicating the dampening effect of the reservoir.

The cross-correlograms of Fig. 7.20 shows further the lack of any relationship between inputs and outputs. Both processes may now be considered independent. This is further confirmed by the coherence function of the Markov residuals in Fig. 7.21, which shows no significant correlation between the two series.

This analysis has explored the time series structure of the salt load as the input and the concentration of dissolved solids below the reservoir as the output. It has been shown that long-term records of both series can be well-represented by the common components. They are (1) a mean value, (2) a periodic variation about the mean, and (3) a random component which may exhibit Markovian dependence. The mean value of the output concentration is well-estimated by the ratio of salt load to the mean flow adjusted for evaporation. The unadjusted mean value is essentially the flow-weighted concentration of the inflow. Periodic components in the output are obtainable as dampened periodic components of the input load. The theoretical gain for specific frequencies as given by Eq. 4.74 gives a favorable estimate of the gain found from the data.

Both input and output series display linear dependence. The first-order Markov model was found to represent this well. The analysis of the final residual components for each series showed they were independent random processes which had no significant cross-correlation at any frequency or time lag.

7.4 Summary and Comparison of Methods

The discussion of the advantages and disadvantages of each approach of the precious section must be based upon the properties the model exhibits. For the objective of reproducing historic data, multiple regression analysis is superior. The highest correlations between predicted and observed data resulted from this method. However, a severe limitation on the general applicability of the resulting relationship exists. If the

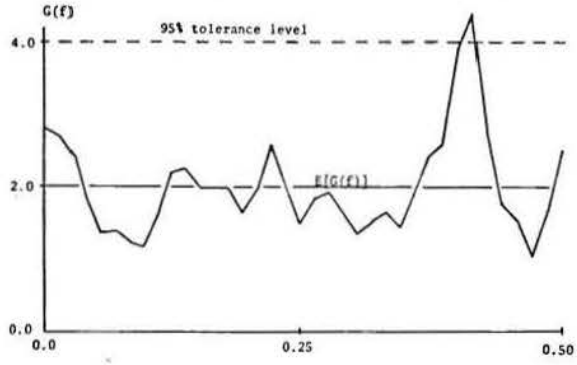

Fig. 7.17 Spectrum of residuals from Markov I model of inflowing salt load, 1941 to 1968.

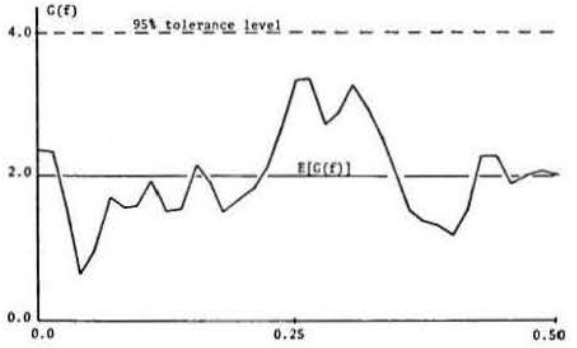

Fig. 7.18 Spectrum of residuals from Markov I model of outflowing dissolved solids, 1941 to 1968.

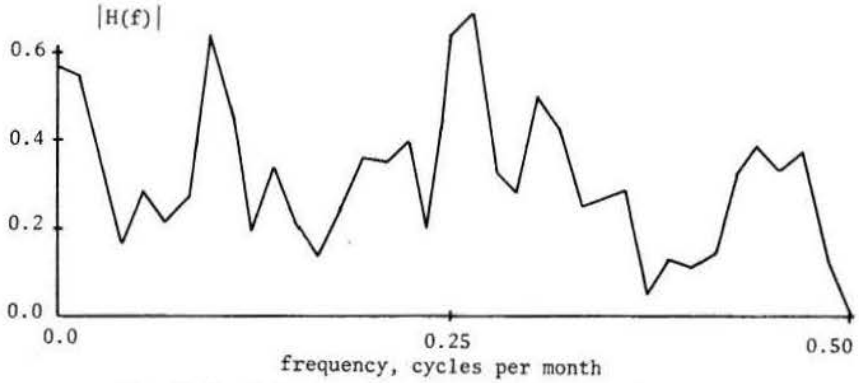

Fig. 7.19 Gain function of residuals from Markov I model of inflowing salt load and outflowing dissolved solids, 1941 to 1968.

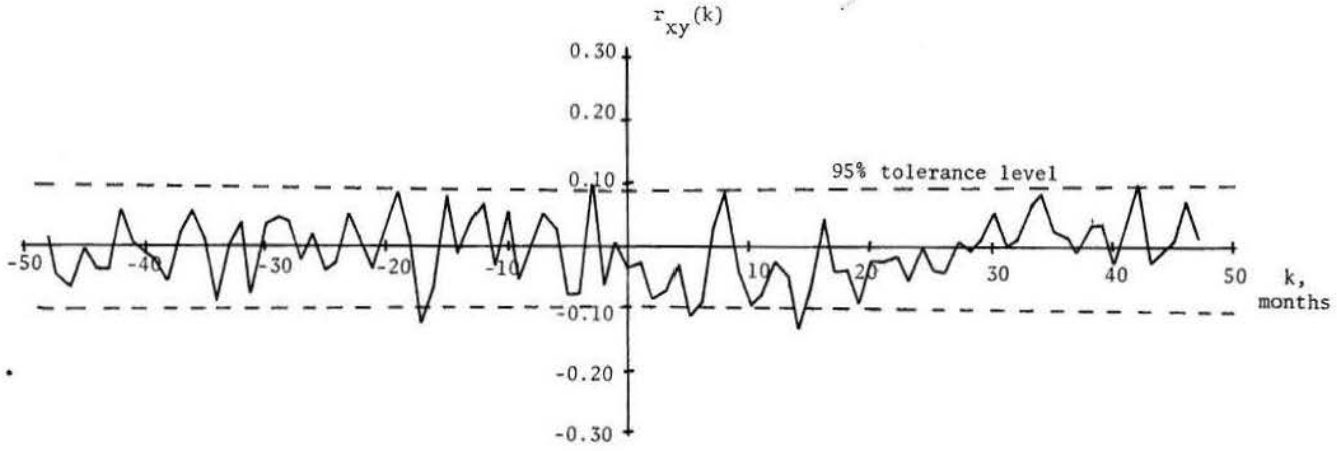

Fig. 7.20 Cross-correlogram of residuals from Markov I model of inflowing salt load and outflowing dissolved solids, 1941 to 1968.

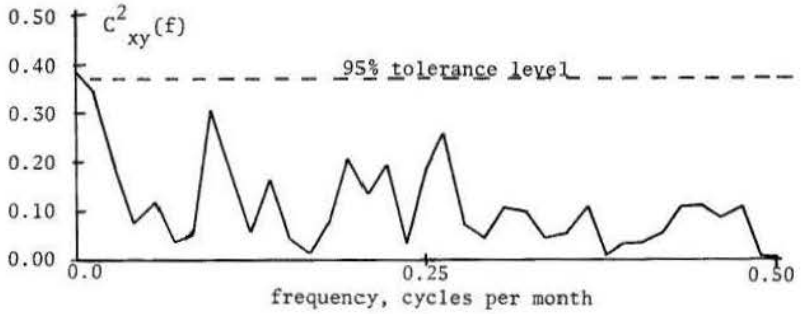

Fig. 7.21 Coherence function of residuals from Markov I model of inflowing salt load and outflowing dissolved solids, 1941 to 1968.

reservoir were operated differently, the model might not reflect outflow quality properly.

Another disadvantage of multiple regression is that it requires a fairly long historic record to reliably estimate the coefficients. For a new reservoir, or one where limited data had been collected, it would be risky to assume a multiple regression analysis would give a reliable model of the reservoir's behavior.

An advantage of the regression approach is its economy of calculation and computer storage requirements. For Eq. 7.18 it would be necessary to store and update only three variables to predict the concentration of the outflow. This advantage is especially valuable for modeling a long-term salinity trace using a short time step.

In summary, the regression approach is desireable for reservoirs such as Lake Mead which have an adequate data base for evaluating model coefficients. It is not a good technique for predicting behavior of reservoirs with a short period of data or those which will operate under conditions not included in the period of record.

The mixing model approach was found to work best when the mathematical structure was a simple as possible. It was shown that attempts to represent the detailed mixing and circulation processes gave poor results. The straightforward mass balance and dilution model produced superior correspondence to the historic data. This model also requires no parameter estimation and is directly applicable to a new reservoir where no data has been collected. It is also economical to operate since the updated tonnage in storage and monthly contents are the only quantities required. Changes in inflow patterns are easily accounted for, and assuming the system is completely mixed, outflow concentrations are accurately predicted. This model has the further advantage of maintaining continuity through the mass balance as well as tending to return to a stable condition when it over- or under-estimates the concentration.

The time series analysis of Section 7.3 illustrated the application of the completely mixed model formulation as given in Section 4.4. The steady-state estimate of outflow concentration adjusted for evaporation illustrated that even if the inflow, outflow and reservoir storage varied over time, the average properties were consistent with the model.

Spectral analysis was used to inspect the structure of the input and output time series. Spectra of inputs and outputs immediately identified the tremendous dampening effect of the reservoir and indicated high serial dependence of system output. The gain function verified this behavior. The gain function

based on the differential equation of the mass balance of salts was found to closely match the results from historical data. The analytical gain function can be used when inputs of known periodic components are anticipated. The output concentration can be immediately described. This study has shown that the gain analysis is valid even when the system inflow and volume are not constant as the model supposes. Inspection of the phase function from the historical data showed a high degree of variation among frequency components. The phase shift from inputs to outputs was not clearly defined and apparently fluctuated at random. The cross-correlogram did indicate an average lag of about 17 months from the time an input entered the reservoir until it was released.

After removal of periodic components, the autoregressive input and output characteristic became more clear. High serial correlation was found in all time series. The effect of the reservoir was to increase correlation between sequential outputs. For the 1941 to 1968 period, the first serial correlation coefficient was 0.62 for the input and 0.93 for the output. According to the theoretical correlation function of a moving average process in Eq. 4.83, r_1 would be about 0.94 for 17 terms. This coincides with the 17-month lag found between inputs and outputs from the cross-correlograms. However, since the theoretical correlation is based upon independent inputs this does not reflect the smoothing produced by the reservoir alone. Dependence in the input and output series followed the pattern of a Markov I model quite closely. Removal of serial dependence produced residual series which showed only random properties and were independent of each other. This was illustrated by their spectra, cross-correlogram and coherence function.

In summary, the time series analysis isolated the components of the input and output series. The mean of the outflowing concentration could be estimated from the flow-weighted average inflow concentration adjusted for evaporation. Periodicity was related to the gain function as developed in the analysis of cyclic input loads in Section 4.4. Serial correlation was added by the mixing mechanism of the reservoir which behaved like a moving-average process. The residual "noise" of the output concentration series accounted for less than 20 percent of the variance in the residuals from the Fourier analysis. For 1941 to 1968 data, this would be on the order of 0.0001 $(T/ac\ ft)^2$. Such variation could be due to inconsistencies in sampling and data collection procedures.

The multiple regression approach is most useful when data are available to estimate the regression coefficients. The other two approaches are generally applicable to any well-mixed reservoir and merit further discussion. The selection of either the finite-step mixing model, or the time series analysis based on the completely mixed reservoir depends on the nature of the problem being attacked and the relation of the reservoir to the problem. For a problem requiring an estimate of the long-term properties of outflow salinity with the inflow salt load specified, the steady-state values might be adequate. This could be simply an estimate of the mean concentration and its variance.

In another context, the problem might be to estimate a monthly outflow concentration for a reservoir which formed one subsystem of a large basin model. The properties of the inflow might not be specified until the basin simulation model had reached the point in its logic where quality had to be routed through the reservoir. In this case, the single time-step type of calculation would be best. As this brief discussion has shown, the choice of which model to use depends upon the needs of the modeler.

CHAPTER VIII

CONCLUSIONS AND SUGGESTIONS FOR FURTHER STUDY

8.1 Conclusions

This study has provided a comparison between several methods of modeling the complex process of reservoir mixing by simplified mathematical approaches. The behavior of the system was first explored by investigating mixing and circulation patterns from a limnological standpoint. Models were reviewed which attempted to reflect the processes governing quality movement within the reservoir. In general these models required extensive mathematical calculations (taking about a standard box of computer cards for the program), many parameters or coefficients, and several time series of meteorological data for the heat budget analysis. Although they could be used to predict the vertical distribution of water quality within a reservoir, they do not meet the model requirements laid out early in this study.

In the search for methods of representing the behavior of a complex system in a more compact fashion, the black-box, or input-output approach was reviewed. Along these lines, three methods of modeling the concentration of salinity in reservoir outflows were considered. In addition to the well-known multiple regression analysis, two mixing models were explored. One was based on a simple mass balance including inflowing salts, salt storage, reservoir volume, and outflowing salts. The tonnage in storage at any time was equal to the prior salt in storage plus any salt inflows minus the salt outflows. Concentration was estimated as the mass of salt in storage divided by the volume of water in storage.

The second model based on the assumption of a completely-mixed reservoir followed the prior work of Thomann (51). This model used relationships resulting from a differential equation which described the mass balance of salts in the system.

The three above approaches were applied to quality data from Lake Mead to compare their value for simulation use. Initially water and salt budgets were explored to account for system input, output, and storage. Although several uncertain sources of water and salts were encountered, bank storage and salt pickup were most elusive. Lack of adequate data prevented reliable modeling of both quantities. It was shown that bank storage could be modeled by a groundwater convolution model but the data contained too much error to judge its performance.

Regression analysis and the mixing model techniques all showed capability of reflecting the system's behavior. For the data sets pertaining to Lake Mead, the regression and mixing approaches provided the simplest method of modeling salinity of the outflows. Although both methods gave similar prediction results, the mixing model was judged superior since it was more general and could be applied to other reservoirs directly.

Results from the analysis of time series indicated the theoretical gain function described by Thomann (51) was valid even under conditions of time-varying inflow and storage. It was also shown that the time series could be decomposed into periodic, autoregressive, and independent random components. After removal of periodicity the output concentration showed very high serial dependence with r_1 of the first order Markov model equalling 0.93. Residuals from the deterministic components of inputs and outputs were random independent variables uncorrelated with each other.

Spectral analysis was used to verify the gain function as well as detect deterministic time series components. Cross correlograms between inputs and outputs indicated 17 to 18 months were required on the average for inputs to pass through the system. Although phase functions did not reveal any consistent pattern, the average phase for all frequencies reinforced the cross-correlogram results.

It should be noted that this study has utilized historic data to investiage methods which have been relatively untried. The analytical description of the concentration of outflowing salinity was based on the hypothetical behavior of an abstract system. As this study has shown, the theoretical model goes far towards duplicating the response of the real system.

The final model recommended for sequential time-step simulation is the simple mixing model. This model was judged superior to the others for simulation use as a result of its economy of calculation effort, accuracy of prediction, and general applicability.

8.2 Suggestions for Further Study

This study opens up several interesting areas of investigation related to reservoir water quality. One of the most obvious of these is an analysis of data from other reservoirs to find which conditions violate the assumption of complete mixing. Several reservoirs representing a variety of climates, a range of flow to storage ratios, and several patterns of the inflow time series should be analyzed similarly to Lake Mead. Results of such an investigation would give planners better information to judge the applicability of the mixing model under new conditions.

A second area of investigation which would be of great use in basin water quality studies is the relationships among specific ionic constituents as water is mixed in a reservoir. Perhaps multivariate techniques of principal components, factor analysis, or canonical analysis in the time domain, or cross-spectral analysis in the frequency domain would reveal relationships between the percentage distribution of ions in the inflow and in the release. Methods should be developed which the planner can use to estimate the ionic breakdown of total dissolved solids in the release. This type of study is very difficult due to the lack of consistent, long term water quality data above and below reservoirs.

Fairly simple mixing models which grossly reflect water movement and thermal stratification within the reservoir might be explored. Although a few such models were tried unsuccessfully in this study, the approach is a logical one to pursue. A compromise between the simple model of the completely mixed reservoir and the complex thermal stratification models might produce satisfactory results without extensive mathematical operations.

A final suggestion for further study is the exploration of the serial dependence in the outflow concentration time series. The increase in serial correlation of the Fourier analysis residuals from the inflow to the outflow is undoubtedly related to the detention and amount of mixing in the reservoir. It should be possible to relate r_1, the first serial correlation of the outflow concentration to r_1 of the inflow by means of certain reservoir characteristics. Similar to the gain and phase relationships, the analytical expression for linear dependence of the residuals should be found. This could be explored through the analysis of time series for several reservoirs.

REFERENCES

1. Anderson, E. R. and D. W. Pritchard. Physical Limnology of Lake Mead, Lake Mead Sedimentation Survey. Navy Electronics Laboratory Report 258, 1951.

2. Beard, L. R. and R. G. Willey. An Approach to Reservoir Temperature Analysis. Water Resources Research, Vol. 6, No. 5, 1970, pp. 1335-1345.

3. Benson, A. M. Spurious Correlation in Hydraulics and Hydrology. Jour. Hyd. Div., Am. Soc. Civil Engineers, Vol. 91, No. HY4, 1965, pp. 35-42.

4. Blackman, R. B. and J. W. Tukey. The Measurement of Power Spectra. Dover Publications Inc., New York, New York, 1958.

5. Bohan, J. P. and J. L. Grace, Jr. Mechanics of Stratified Flow Through Orifices. Jour. Hyd. Div., Am. Soc. Civil Engineers, Vol. 96, No. HY12, 1970, pp. 2401-2416.

6. Chayes, F. On Ratio Correlation in Petrography. The Journal of Geology, Vol. 57, No. 3, 1949, pp. 239-254.

7. Chemical Rubber Company. Handbook of Chemistry and Physics, 53rd Edition. Chemical Rubber Company Press, Cleveland, Ohio, 1972-1973.

8. Chow, V. T. and S. J. Kareliotis. Analysis of Stochastic Hydrologic Systems. Water Resources Research, Vol. 6, No. 6, 1970, pp. 1569-1582.

9. Clay, Jr., H. M. and E. G. Fruh. Management of Water Quality in Releases From Southwestern Impoundments. Water Resources Bulletin, Vol. 7, No. 1, 1971, pp. 137-147.

10. Cooper, Jr., H. H. and M. I. Rorabaugh. Ground Water Movements and Bank Storage Due to Flood Stages in Surface Streams. USGS Water Supply Paper 1536-J, U. S. Gov't. Print. Off., Washington, D. C., 1963, pp. 343-366.

11. Davis, J. R. and J. W. Wark. Private Communication of Unpublished Material.

12. Debler, W. R. Stratified Flow Into a Line Sink. Jour. Eng. Mechs. Div., Am. Soc. Civil Engineers, Vol. 85, No. EM3, 1959, pp. 57-65.

13. Demayo, A. The Computation and Interpretation of the Power Spectra of Water Quality Data. Technical Bulletin No. 16, Inland Waterways Branch, Dept. of Energy, Mines and Resources, Ottawa, Canada, 1969.

14. Department of Commerce. Climatological Data, Nevada, Annual Summaries. Weather Bureau, Asheville, North Carolina, n.d.

15. Dingman, S. L. and A. H. Johnson. Pollution Potential of Some New Hampshire Lakes. Water Resources Research, Vol. 7, No. 5, 1971, pp. 1208-1215.

16. Dixon, N. P., D. W. Hendricks, A. L. Huber and J. M. Bagley. Developing a Hydro-quality Simulation Model. Utah Water Research Laboratory and College of Engineering, Utah State Univ., Logan, Utah, Report PRWG67-1, 1970.

17. Elder, R. A. and W. O. Wunderlich. The Prediction of Withdrawal Layer Thickness in Density-Stratified Reservoirs. Water Resources Research Laboratory Report No. 4, Tennessee Valley Authority, Norris, Tennessee, 1969.

18. Environmental Protection Agency. The Mineral Quality Problem in the Colorado River Basin, Appendix A, Natural and Man-Made Conditions Affecting Mineral Quality. U. S. Environmental Protection Agency Regions VIII and IX, 1971.

19. Environmental Protection Agency. The Mineral Quality Problem in the Colorado River Basin, Appendix C, Salinity Control and Management Aspects, U. S. Environmental Protection Agency Regions VIII and IX, 1971.

20. Hall, F. R. and A. F. Moench. Application of the Convolution Equation to Stream-Aquifer Relationships. Water Resources Research, Vol. 8, No. 2, 1972, pp. 487-493.

21. Harbeck, Jr., G. E., M. A. Kohler, G. E. Kuberg and others. Water-Loss Investigations, Lake Mead Studies. USGS Professional Paper 298, 1958.

22. Hoffman, D. A., P. R. Tramutt and F. C. Heller. The Effect of Las Vegas Wash Effluent upon the Water Quality in Lake Mead. U. S. Dept. of Interior, Bureau of Reclamation Report REC ERC -71-11, 1971.

23. Hutchison, G. E. A Treatise on Limnology, Vol. I, Geography, Physics and Chemistry. John Wiley and Sons, Inc., New York, New York, 1957.

24. Jaske, R. T. A Three-Dimensional Study of Parameters Related to the Current Distribution in Lake Roosevelt. Battelle Memorial Institute, Pacific Northwest Laboratory, Richland, Washington, 1969.

25. Jenkins, G. M. and D. G. Watts. Spectral Analysis and Its Applications. Holden-Day, San Francisco, Calif., 1968.

26. Kartchner, A. D., N. P. Dixon and D. W. Hendricks. Modeling Diurnal Fluctuations in Stream Temperature and Dissolved Oxygen. Presented at 24th Annual Purdue Industrial Waste Conference, Utah Water Research Laboratory, College of Engineering, Utah State Univ., Logan, Utah, 1969.

27. King, D. L. Hydraulics of Stratified Flow, Second Progress Report, Selective Withdrawal From Reservoirs. U. S. Dept. of Interior, Bureau of Reclamation Report HYD-595, 1969.

28. Knisel, W. G. Response of Karst Aquifers to Recharge. Doctoral Thesis, Civil Engineering Dept., Colorado State Univ., 1971.

29. Koh, R. C. Viscous Stratified Flow Towards a Line Sink. Report KH-R-6, W. M. Keck Laboratory of Hydraulics and Water Resources, California Institute of Technology, 1964.

30. Kothandaraman, V. Analysis of Water Temperature Variations in a Large River. Jour. Hyd. Div., Am. Soc. Civil Engineers, Vol. 97, No. SA1, 1971, pp. 19-32.

31. Kriss, C. and D. P. Loucks. A Selected Annotated Bibliography on the Analysis of Water Resources Systems. Public. No. 35, Cornell Univ. Water Resources and Marine Center, Ithaca, New York, 1971.

32. Langbein, W. B. Water Budget, Section J. In Comprehensive Survey of Lake Mead, 1948-1949, by W. O. Smith, C. P. Vetter, G. B. Cummings and others, USGS Professional Paper 295, 1960.

33. Lara, J. M. and J. I. Sanders. The 1963-64 Lake Mead Survey. U. S. Dept. of Interior, Bureau of Reclamation Report REC-OCE-70-21, 1970.

34. Leifeste, D. K. and B. Popkin. Quality of Water and Stratification of Possum Kingdom, Whitney, Hubbard Creek, Proctor and Belton Reservoirs. Texas Water Development Board Report 85, 1968.

35. Matalas, N. C. Time Series Analysis. Water Resources Research, Vol. 3, No. 3, 1967, pp. 817-829.

36. Moench, A. F. and C. C. Kisiel. Application of the Convolution Relation to Estimating Recharge from an Ephemeral Stream. Water Resources Research, Vol. 6, No. 4, 1970, pp. 1087-94.

37. O'Donnell, T. Instantaneous Unit Hydrograph Derivation by Harmonic Analysis. International Association of Scientific Hydrology, Public. No. 51, 1960, pp. 546-557.

38. Orlob, G. T., and L. G. Selna. Temperature Variations in Deep Reservoirs. Jour. of Hyd. Div., Am. Soc. Civil Engineers, Vol. 96, No. HY2, 1970, pp. 391-410.

39. Pearson, K. On a Form of Spurious Correlation Which May Arise When Indices Are Used in the Measurement of Organs. Royal Society London Proc., Vol. 60, 1896-1897, pp. 489-502.

40. Phillippee, J. T. and J. M. Wiggert. Instantaneous Unit Hydrograph Response by Harmonic Analysis. Bulletin 15, Water Resources Research Center, Virginia Polytech. Inst., Blacksburg, Va., 1969.

41. Rechard, P. A. Determining Bank Storage of Lake Mead. Jour. Irr. and Drainage Div., Am. Soc. Civil Engineers, Vol. 91, No. IR1, 1965, pp. 141-157.

42. Reed, L. J. On the Correlation Between any Two Functions and Its Application to the General Case of Spurious Correlation. Jour. of the Washington Academy of Sciences, Vol. 11, No. 19, 1921, pp. 449-455.

43. Rodriguez-Iturbe, I. The Application of Cross-Spectral Analysis to Hydrologic Time Series. Colorado State Univ. Hydrology Paper No. 24, Ft. Collins, Colorado, 1967.

44. Rodriguez-Iturbe, I. and C. F. Nordin. Time Series Analysis of Water and Sediment Discharges. Bulletin of International Association of Scientific Hydrology, 1968, pp. 69-84.

45. Roesner, L. S., W. R. Norton, and G. T. Orlob. A Mathematical Model for Simulating the Temperature Structure of Stratified Reservoirs and Its Use in Reservoir Outlet Design. AISH-IASH International Symposium on Mathematical Models in Hydrology, Warsaw, Poland, 1971.

46. Roesner, L. A., and V. M. Yevjevich. Mathematical Models for Time Series of Monthly Precipitation and Monthly Runoff. Colorado State University Hydrology Paper No. 15, 1966.

47. Ryan, P. J., and D. R. F. Harleman. Prediction of the Annual Cycle of Temperature Changes in Stratified Lake or Reservoir: Mathematical Model and User's Manual. M. I. T. Hydrodynamics Lab. Technical Report No. 137, 1971.

48. Sharp, J. V. A. Analysis of Time Variant Behavior of Water Chemistry. Center for Water Resources Research, Desert Research Institute, Univ. of Nevada System, Reno, Preprint No. 71, Paper H-23, 51st Annual Meeting, Am. Geophys. Union, Wash., D. C., 1970.

49. Slawson, Jr., G. C. Water Quality in the Lower Colorado River and the Effect of Reservoirs. Unpublished Master's Thesis, Dept. of Hydrology and Water Resources, University of Arizona, 1972.

50. Systems Approach to Hydrology. Proceedings of the First Bilateral United States-Japan Seminar in Hydrology, Water Resources Publications, Ft. Collins, Colorado, 1971.

51. Thomann, R. V. Systems Analysis and Water Quality Management. Environmental Sciences Services Division, Environmental Research and Applications, Inc., 1972.

52. Thomann, R. V. Variability of Waste Treatment Plant Performance. Jour. Sanit. Eng. Div., Am. Soc. Civil Engineers, Vol. 96, No. SA3, 1970, pp. 819-837.

53. Thomann, R. V. Time-Series Analysis of Water Quality Data. Jour. Sanit. Eng. Div., Am. Soc. Civil Engineers, Vol. 93, No. SA1, 1967, pp. 103-125.

54. Thomas, H. E. First Fourteen Years of Lake Mead. USGS Circular 346, Washington, D. C., 1954.

55. Tilton, L. W., and J. K. Taylor. Accurate Representation of Reflectivity and Density of Distilled Water as a Function of Temperature. Jour. of Research, National Bureau of Standards, Vol. 18, 1937, pp. 205-214.

56. U. S. Dept. of the Interior. Lake Mead Density Currents Investigations. Vol. I & II, 1937-1940, Vol. III, 1940-1946.

57. U. S. Dept. of the Interior. Quality of Water, Colorado River Basin, Progress Report No. 4. U.S. Bureau of Reclamation, 1969.

58. U. S. Dept. of the Interior. Quality of Water, Colorado River Basin, Progress Report No. 5. U.S. Bureau of Reclamation, 1969.

59. Venetis, C. Finite Aquifers: Characteristic Responses and Applications. Jour. of Hydrology, Vol. 12, 1970, pp. 53-62.

60. Ward, J. C. Annual Variations of Stream Temperature. Jour. Sanit. Eng. Div., Am. Soc. Civil Engineers, Vol. 89, No. SA6, 1963, pp. 1-16.

61. Ward, J. C., and S. Karaki. Evaluation of Effect of Impoundment on Water Quality in Cheney Reservoir. Res. Rep. No. 25, Colorado State University, Ft. Collins, Colorado, 1969.

62. Wastler, T. A. Application of Spectral Analysis to Stream and Estuary Field Surveys. Public Health Service Publication No. 999WP-7, 1963.

63. Water Resources Engineers, Inc. Mathematical Models for the Prediction of Thermal Energy Changes in Impoundments. Final report to the FWPCA, Columbia River Thermal Effects Project, 1969.

64. Water Resources Engineers, Inc. Prediction of Thermal Energy Distribution in Streams and Reservoirs. Report prepared for Dept. of Fish and Game, State of California, 1968.

65. Wunderlich, W. O. The Dynamics of Density-Stratified Reservoirs. Reservoir Fisheries and Limnology, 1971, pp. 219-231.

66. Yevjevich, V. M. Probability and Statistics in Hydrology. Water Resources Publications, Fort Collins, Colorado, 1972.

67. Yevjevich, V. M. Stochastic Processes in Hydrology. Water Resources Publications, Fort Collins, Colorado, 1972.

68. Yevjevich, V. M. The Structure of Inputs and Outputs of Hydrologic Systems. United States-Japan Bi-Lateral Seminar in Hydrology, Honolulu, 1971, pp. 51-79.

69. Young, G. K. Comments on An Approach to Reservoir Temperature Analysis by L. R. Beard, and R. G. Willey. Water Resources Research, Vol. 7, No. 2, 1971, pp. 434-435.

KEY WORDS: Statistical techniques, reservoir, salinity, dissolved solids, mixing models.

ABSTRACT: The movement of dissolved solids (in the text also called "salinity") through a reservoir was investigated and modeled. It is shown that for a reservoir with a detention time greater than one year, the concentration of dissolved solids in the outflow can be modeled by a straightforward linear salt-mix model. A review of the thermal stratification pattern of a monomictic reservoir was made to provide an understanding of the mixing and movements of water in storage. Mathematical models which attempt to reflect this pattern are reviewed to ascertain their potential for use in a basin simulation model. Lake Mead was chosen as an example for comparing techniques of simplifying the relationship between quality of inflows, storage and outflows. Water and salt budgets were used to verify that inputs and outputs of water and salt had been accounted for during the 1935-1968 historic data period. Multiple re-

KEY WORDS: Statistical techniques, reservoir, salinity, dissolved solids, mixing models.

ABSTRACT: The movement of dissolved solids (in the text also called "salinity") through a reservoir was investigated and modeled. It is shown that for a reservoir with a detention time greater than one year, the concentration of dissolved solids in the outflow can be modeled by a straightforward linear salt-mix model. A review of the thermal stratification pattern of a monomictic reservoir was made to provide an understanding of the mixing and movements of water in storage. Mathematical models which attempt to reflect this pattern are reviewed to ascertain their potential for use in a basin simulation model. Lake Mead was chosen as an example for comparing techniques of simplifying the relationship between quality of inflows, storage and outflows. Water and salt budgets were used to verify that inputs and outputs of water and salt had been accounted for during the 1935-1968 historic data period. Multiple re-

KEY WORDS: Statistical techniques, reservoir, salinity, dissolved solids, mixing models.

ABSTRACT: The movement of dissolved solids (in the text also called "salinity") through a reservoir was investigated and modeled. It is shown that for a reservoir with a detention time greater than one year, the concentration of dissolved solids in the outflow can be modeled by a straightforward linear salt-mix model. A review of the thermal stratification pattern of a monomictic reservoir was made to provide an understanding of the mixing and movements of water in storage. Mathematical models which attempt to reflect this pattern are reviewed to ascertain their potential for use in a basin simulation model. Lake Mead was chosen as an example for comparing techniques of simplifying the relationship between quality of inflows, storage and outflows. Water and salt budgets were used to verify that inputs and outputs of water and salt had been accounted for during the 1935-1968 historic data period. Multiple re-

KEY WORDS: Statistical techniques, reservoir, salinity, dissolved solids, mixing models.

ABSTRACT: The movement of dissolved solids (in the text also called "salinity") through a reservoir was investigated and modeled. It is shown that for a reservoir with a detention time greater than one year, the concentration of dissolved solids in the outflow can be modeled by a straightforward linear salt-mix model. A review of the thermal stratification pattern of a monomictic reservoir was made to provide an understanding of the mixing and movements of water in storage. Mathematical models which attempt to reflect this pattern are reviewed to ascertain their potential for use in a basin simulation model. Lake Mead was chosen as an example for comparing techniques of simplifying the relationship between quality of inflows, storage and outflows. Water and salt budgets were used to verify that inputs and outputs of water and salt had been accounted for during the 1935-1968 historic data period. Multiple re-

gression analysis was used to model water movement into bank storage and to find a relationship between the salt concentration of the outflow and inflowing salt load and reservoir storage. Spectral analysis of the inflowing salt load and outflowing dissolved solids concentration was used to identify the smoothing effect of storage. Time series analysis methods were used to isolate periodic, time-dependent Markovian, and random components of inputs and outputs. For the objective of finding a model which reflects the system well, yet requires minimal numerical calculation, the simple mass balance approach is recommended.

John Hendrick
Techniques for Modeling Reservoir Salinity
Hydrology Paper #62
Colorado State University

gression analysis was used to model water movement into bank storage and to find a relationship between the salt concentration of the outflow and inflowing salt load and reservoir storage. Spectral analysis of the inflowing salt load and outflowing dissolved solids concentration was used to identify the smoothing effect of storage. Time series analysis methods were used to isolate periodic, time-dependent Markovian, and random components of inputs and outputs. For the objective of finding a model which reflects the system well, yet requires minimal numerical calculation, the simple mass balance approach is recommended.

John Hendrick
Techniques for Modeling Reservoir Salinity
Hydrology Paper #62
Colorado State University

gression analysis was used to model water movement into bank storage and to find a relationship between the salt concentration of the outflow and inflowing salt load and reservoir storage. Spectral analysis of the inflowing salt load and outflowing dissolved solids concentration was used to identify the smoothing effect of storage. Time series analysis methods were used to isolate periodic, time-dependent Markovian, and random components of inputs and outputs. For the objective of finding a model which reflects the system well, yet requires minimal numerical calculation, the simple mass balance approach is recommended.

John Hendrick
Techniques for Modeling Reservoir Salinity
Hydrology Paper #62
Colorado State University

gression analysis was used to model water movement into bank storage and to find a relationship between the salt concentration of the outflow and inflowing salt load and reservoir storage. Spectral analysis of the inflowing salt load and outflowing dissolved solids concentration was used to identify the smoothing effect of storage. Time series analysis methods were used to isolate periodic, time-dependent Markovian, and random components of inputs and outputs. For the objective of finding a model which reflects the system well, yet requires minimal numerical calculation, the simple mass balance approach is recommended.

John Hendrick
Techniques for Modeling Reservoir Salinity
Hydrology Paper #62
Colorado State University

LIST OF PREVIOUS 25 PAPERS

No. 37 Regional Discrimination of Change in Runoff, by Viboon Nimmanit and Hubert J. Morel-Seytoux, November 1969.

No. 38 Evaluation of the Effect of Impoundment on Water Quality in Cheney Reservoir, by J. C. Ward and S. Karaki, March 1970.

No. 39 The Kinematic Cascade as a Hydrologic Model, by David F. Kibler and David A. Woolhiser, February 1970.

No. 40 Application of Run-Lengths to Hydrologic Series, by Jaime Saldarriaga and Vujica Yevjevich, April 1970.

No. 41 Numerical Simulation of Dispersion in Groundwater Aquifers, by Donald Lee Reddell and Daniel K. Sunada, June 1970.

No. 42 Theoretical Probability Distribution for Flood Peaks, by Emir Zelenhasic, December 1970.

No. 43 Flood Routing Through Storm Drains, Part I, Solution of Problems of Unsteady Free Surface Flow in a Storm Drain, by V. Yevjevich and A. H. Barnes, November 1970.

No. 44 Flood Routing Through Storm Drains, Part II, Physical Facilities and Experiments, by V. Yevjevich and A. H. Barnes, November 1970.

No. 45 Flood Routing Through Storm Drains, Part III, Evaluation of Geometric and Hydraulic Parameters, by V. Yevjevich and A. H. Barnes, November 1970.

No. 46 Flood Routing Through Storm Drains, Part IV, Numerical Computer Methods of Solution, by V. Yevjevich and A. H. Barnes, November 1970.

No. 47 Mathematical Simulation of Infiltrating Watersheds, by Roger E. Smith and David A. Woolhiser, January 1971.

No. 48 Models for Subsurface Drainage, by W. E. Hedstrom, A. T. Corey and H. R. Duke, February 1971.

No. 49 Infiltration Affected by Flow of Air, by David B. McWhorter, May 1971.

No. 50 Probabilities of Observed Droughts, by Jaime Millan and Vujica Yevjevich, June 1971.

No. 51 Amplification Criterion of Gradually Varied, Single Peaked Waves, by John Peter Jolly and Vujica Yevjevich, December 1971.

No. 52 Stochastic Structure of Water Use Time Series, by Jose D. Salas-La Cruz and Vujica Yevjevich, June 1972.

No. 53 Agricultural Response to Hydrologic Drought, by V. J. Bidwell, July 1972.

No. 54 Loss of Information by Discretizing Hydrologic Series, by Mogens Dyhr-Nielsen, October 1972.

No. 55 Drought Impact on Regional Economy, by Jaime Millan, October 1972.

No. 56 Structural Analysis of Hydrologic Time Series, by Vujica Yevjevich, November 1972.

No. 57 Range Analysis for Storage Problems of Periodic-Stochastic Processes, by Jose Salas-La Cruz, November 1972.

No. 58 Applicability of Canonical Correlation in Hydrology, by Padoong Torranin, December 1972.

No. 59 Transposition of Storms, by Vijay Kumar Gupta, December 1972.

No. 60 Response of Karst Aquifers to Recharge, by Walter G. Knisel, December 1972.

No. 61 Drainage Design Based Upon Aeration, by Harold R. Duke, June 1973.